POLITECNICO DI TORINO

Dipartimento di Ingegneria Meccanica e Aerospaziale

Corso di Laurea Magistrale in Ingegneria Aerospaziale

Master's degree thesis

Impact of different subsystem architectures on aircraft engines in terms of Specific Fuel Consumption

SUPERVISOR:
Prof. Sabrina Corpino

CO-SUPERVISORS:
Prof. Marco Fioriti
Ing. Luca Boggero

CANDIDATE: Flavia Ferrari

22 Marzo 2018

"Reserve your right to think,
for even to think wrongly
is better than
not to think at all."
Hypatia

Acknowledgements

I first wish to thank my thesis advisors Prof.Sabrina Corpino and Prof.Marco Fioriti for their deep knowledge and support.
I express my thankfulness to Ing.Luca Boggero for his competence, patience and for the precious help he gave me throughout this thesis. A sincere thank goes to Ing.Francesca Tomasella for her insightful and kind suggestions.
I would also like to thank Ing.Matthias Strack and Ing.Florian Wolters from the German Aerospace Center (DLR) for their valuable collaboration during the thesis and to have expressed their deep interest on this work.

I wish to thank my parents who follow me on every path I undertake and to whom I dedicate my thesis. A special thank goes to my brother who has been my first supporter. With deep gratitude I thank my Grandfather who thought me that resolution can bring you wherever your dreams go.

I would love to thank my lifetime friends with whom I overwhelmed the distance from home. A special thank goes to Vittoria, for our unconditional and truly friendship, to Laura because we shared our lives and not just a house, to Beatrice who has almost become a sister. I would also like to name Berard who is always ready to help me, Mattia for his honesty and Andrea who always shares his deep culture with me.
Finally, I thank all those people who have filled my past two years with an hand, a call, a smile and helped me going trough my hard past months.

Sommario

La scopo di questa tesi è lo studio dell'impatto dei sottosistemi di bordo sul propulsore dell'aereo; più nel dettaglio, l'obiettivo è studiare come diverse architetture possono influenzare il Consumo Specifico, considerando potenza estratta all'albero e portata d'aria spillata al compressore.
Il Capitolo I contiene una descrizione di carattere generale sulla generazione e distribuzione della potenza su di un velivolo. In un aereo di architettura convenzionale la potenza è estratta e distribuita attraverso il sistema elettrico, idraulico e pneumatico. Al contrario, una configurazione innovativa, prevede di estrarre la potenza in forma elettrica alimentando tutte le utenze di bordo con questo sistema.
La prima sezione della tesi è dedicata al design dei sistemi, il cui risultato finale comprende sia la potenza sia il bleed richiesto dai sistemi in ogni fase del profilo di missione. Il design è svolto utilizzando il tool *Astrid* del Politecnico di Torino, la cui descrizione è presente nel Capitolo II. Inoltre, durante la tesi è stato migliorato il design preliminare di *Fuel boost pumps* e *Environmental Control System fans* al fine di calcolare il carico medio da essi richiesto. Entrambi gli studi si basano su un'accurata ricerca bibliografica e confronto di componenti reali.
Il Capitolo III è riservato alla descrizione dell'impatto dei sottosistemi secondari sul comportamento del motore; inoltre, all'interno del capitolo vengono descritti due modelli numerici presenti in letteratura, finalizzati al calcolo del Consumo Specifico. Un'ultima parte contiene la descrizione di due engine deck: il primo è stato sviluppato all'interno del progetto *Agile* (*Horizon 2020*) ed è relativo ad un motore più piccolo rispetto a quello considerato nella tesi. Il secondo engine deck, invece, è stato fornito da *Deutsches Zentrum für Luft und Raumfahrt e.V. (DLR)*, Institute of Propulsion Technology ed è realtivo ad un motore V2500.
Il Capitolo IV comprende il caso di studio: vengono definite quattro architetture, una convenzionale e tre innovative, prendendo come velivolo di riferimento un Airbus A320-200. Successivamente, viene calcolato il Consumo Specifico per le quattro configurazioni, inserendo come principali input la potenza e il bleed necessari nella condizione di crociera e calcolati nella sezione precedente della tesi. I due modelli analitici introdotti nel Capitolo III sono adottati sia per un CFM-56 che un V2500, entrambi motori installati su un A320. Infine, i risultati sono confrontati con quelli forniti dai due engine deck.

Summary

This work aims to study the influence of Secondary Power Systems on aircraft engines and to what extent different systems architectures can affect the Specific Fuel Consumption, taking into account only shaft-power and bleed air extraction.
As described in Chapter I, the following power generation and distribution systems equip a conventional aircraft: hydraulic, pneumatic and electric power systems. However in the aviation community the new trend is to unify as electric power all the on-board power generated.
The first part is devoted to the systems design in order to obtain shaft power off-takes and bleed air off-takes in every segment of mission profile. This stage is developed with a Politecnico di Torino in-house tool named *Astrid*, introduced in Chapter II. Furthermore two original preliminary design of the *Fuel boost pumps* and the *Environmental Control System fans* for a general aviation aircraft are provided. They both derives from a bibliography research over real components.
Chapter III describes the impact of on-board systems on the engine behaviour and analyses two already existent numerical approaches to compute the Specific Fuel Consumption. Then, two engine decks are introduced; the first one is designed within the *Agile Projecy* (*Horizon 2020*) project and it relates to a smaller engine than the one considered throughout the study. The latter is provided by the *Deutsches Zentrum für Luft und Raumfahrt e.V. (DLR)*, Institute of Propulsion Technology which refers to a V2500 engine.
Chapter IV contains the Case Study: one conventional and three innovative architectures have been chosen considering an Airbus A320-200 as the reference vehicle. Furthermore, SFC is computed for all four configurations. The main inputs for this phase are shaft power and bleed air off takes required in *cruise condition* which are available from the previous stage of this work. The two analytical models investigated in Chapter III are adopted for two engine models which both power the Airbus A320: CFM-56 and V2500. Hence, they are compared with the outputs provided by the engine decks.

Contents

List of Figures

List of Tables

Chapter 1

State of the art

This chapter provides a general overview of conventional and innovative configurations for the power of the on-board systems. The aim is to define the various power sources adopted on an aircraft also depicting new trends on the aviation industry.

1.1 Conventional architecture

In a conventional aircraft, the primary role of the engines is to provide the thrust needed for the flight; furthermore they must provide secondary power for non-propulsive subsystems. They are defined as those systems necessary to maintain certain level of performance, safety, controllability and comfort [22].

Different types of power sources extracted from the engines are commonly present: electrical, hydraulic, pneumatic and mechanical.

- *Electrical Power* loads avionics, lightening, in-flight entertainment, galleys and anti-ice protections for little surfaces. This kind of power is obtained from the main generator. It is very flexible and it does not require heavy infrastructure. The main drawback is that, at the state of the art, this source has lower power density than hydraulic one.
- *Hydraulic Power* supplies all Flight Controls and Landing Gear system actuators; it has a very high power density. Its first disadvantage concerns the weight and the lack of flexibility. Furthermore, if any leakage happens, the aircraft deals with very corrosive fluids [18].
- *Pneumatic Power* is taken as bleed air from engines' HP compressors. It provides power for Environmental Control System and supplies hot air for Wing Anti-Ice system. Its primary drawback is the low efficiency and the difficulty to find any existent leakage.
- *Mechanical Power* is driven from engines to the central hydraulic pumps and local pumps for all the engine accessories and to the main electrical generator. [39]

In figure 1.1 it is shown how the different systems are set in a conventional architecture.

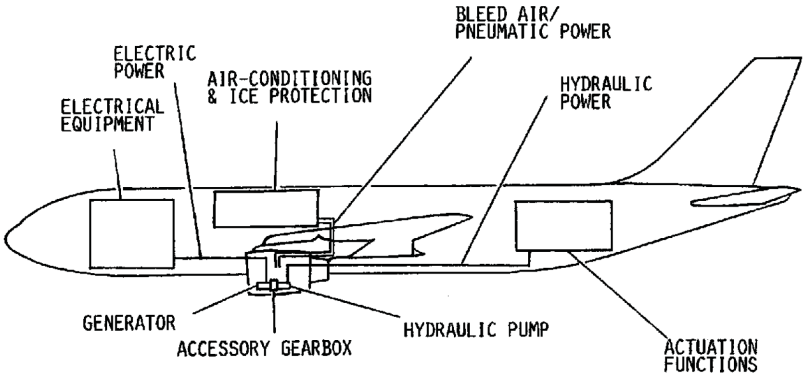

Figure 1.1: Secondary power system in a conventional civil aircraft [28]

At the state of art, power is extracted from gas turbine engines in two ways: by bleeding compressed air from one or more points on the engine's compressor and by extracting shaft power, through a system of gears from the engine's main shaft (fig.1.2). The gearbox is also necessary to rotate the main shaft and start the engine.

The described feature has been the universal standard for years. In figure 1.3 the four different power sources are schematically shown.

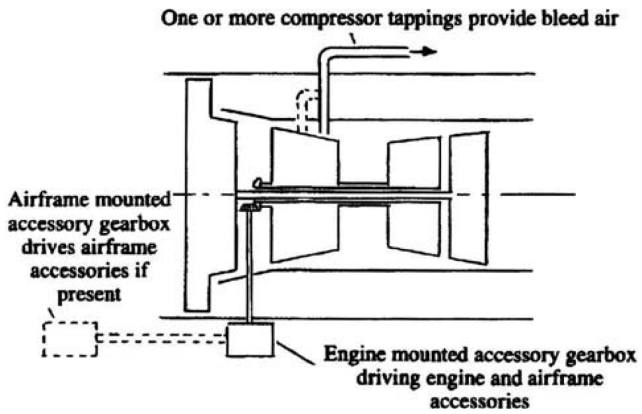

Figure 1.2: Power extraction on present engines [28]

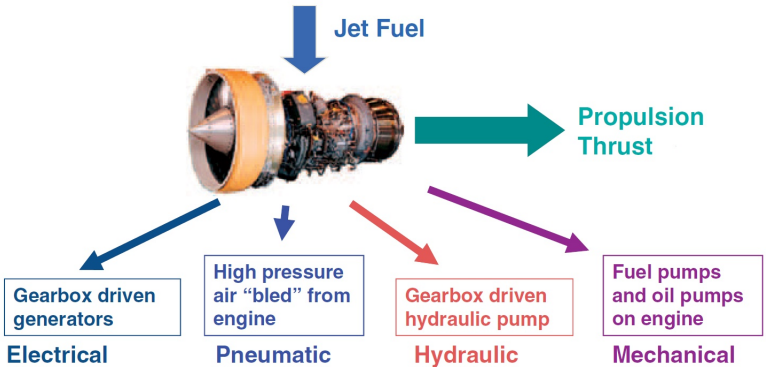

Figure 1.3: Scheme of the power sources in a conventional aircraft [39]

1.2 State of Art aircraft systems

In a standard civil aircraft, the following main on board systems are present

- **Avionic System** represents the series of electronic devices which ensure the pilot a comfortable navigation and communication within the aircraft and the ground.
- **Flight Control System** comprehends the actuators and surfaces necessary to provide aircraft controllability and manoeuvrability, along with different mission phases. Usually, the control surfaces are grouped in
  - primary control surfaces which are active throughout the whole flight and are responsible for pitch, roll and yaw control;
  - secondary power surfaces which work only in certain conditions. They consists of flaperons, slats and flap.
- **Landing Gear System** is responsible for the extraction and retraction of the landing gear, the steering and brake systems.
- **Fuel System** addresses to those components which feed the engine.
- **Environmental Control System** maintains an adequate ventilation in the cabin, along with temperature and humidity in a required range, to provide the maximum comfort for the passengers.
- **Ice Protection System** consists of all the item and architectures which prevent or eliminate ice formation on wing leading edge, nacelle leading edge, antennas and those surfaces which can ice up during the flight.
- **Other** such as lights, In flight entertainment (IFE), galleys, lavatories, etc.

In the following table are listed all the power systems considered throughout the thesis.

Environmental control system (ECS)
Electrical Power Systems (EPS)
Flight Control System
Fuel System
Hydraulic System
Ice and Rain protection
Wing Ice Protection (WIPS)
Nacelle Anti Ice
Landing Gear System
Pneumatic Power Systems
In-Flight Entertainment (IFE)
Galleys
Ovens
Lights
Engines

Table 1.1: Aircraft power systems

The Power generation and distribution systems are

- **Hydraulic System**
- **Pneumatic System**
- **Electric System**

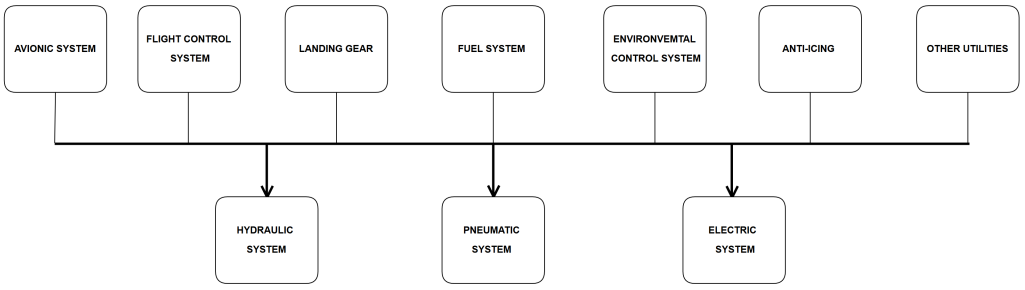

Figure 1.4: Utilities and power distribution systems.

The impact of each on board system on the other design subjects is extremely relevant, in term of overall weight, fuel consumption, available thrust reduction and other aspects such as aircraft stability, volumes, cost, handling qualities and RAMS.
This study is focused on the relationship between utilities, distribution systems and fuel consumption, in order to better understand which configuration could be the best for a consumption optimization.

In a conventional architecture shaft power is extracted from the engine's HP shaft through an engine-mounted gearbox (Accessory Gear Box) (GB in fig,1.5) and then it is transformed into electrical power by a generator (G in fig. 1.5); mechanical power is also converted to hydraulic power by engine driven pumps (P in fig. 1.5). On the other hand, hot pressurized air is extracted from the high stages of HP compressor using bleed system, which feed all the pneumatic utilities. In figure 1.5 this scheme is shown to better understand the great complexity required by the power conversion.
Besides, in an emergency situation, when both engine are off, the RAT (Ram Air Turbine) provides emergency power for the essential systems. The APU (Auxiliary Power Unit) assures the ground supply, not considering the ground facilities.

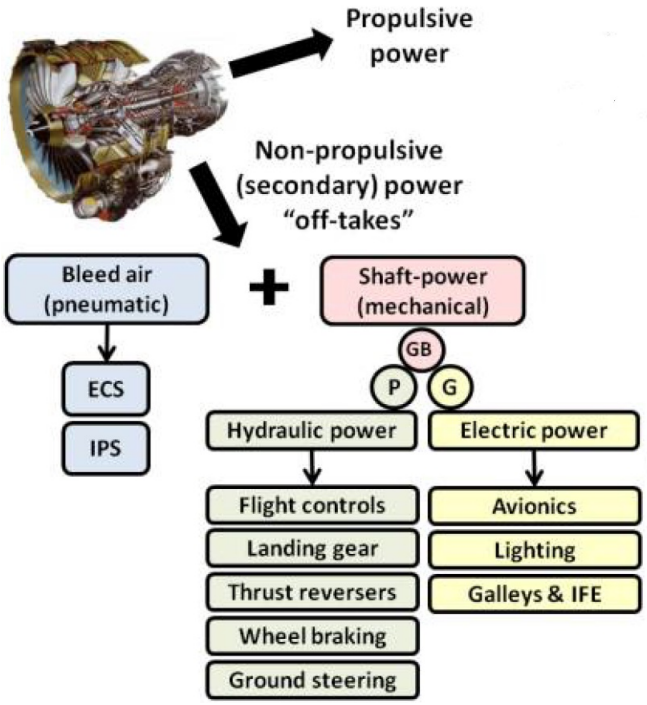

Figure 1.5: Non propulsive power distribution [32]

To provide an example, in the following diagram the percentages of the different power forms are shown for an Airbus A330; the graph illustrates that electrical, hydraulic and pneumatic power contributes with different rates to the overall power budget. Pneumatic distribution system contributes for more than 50%, while electrical and hydraulic ones represents almost constant and relatively smaller loads [24]. However, all three sources are necessary to size the power system: indeed, during the thesis, detailed power budgets will be presented, in order to better understand the contribution of the cited systems in different architectures.

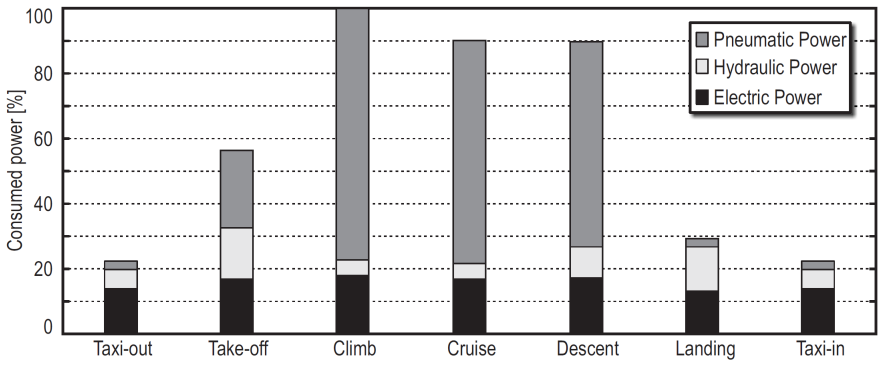

Figure 1.6: SPS demand for an Airbus A330 [15]

1.2.1 Issues related to the conventional architecture

The presence of the gearbox represents the main reason for the increasing dimensions of the nacelle. On the other hand, the first concerns in this field is the bleeding practice: the all over years studies indicates that the major responsible of the specific fuel consumption penalties is the bleed air flow [31]. According to these results, during the operations of a standard commercial transport aircraft, both altitude and engine thrust change in function of the fuel burn to achieve a maximum range. Thus, as the altitude increases, the engine thrust settings decreases and this lead to the increment of the SFC: the bleed air flow is quite constant during the lower-power settings and lower core flows [20].

The next most significant impact of the engine bleed is the pre cooler installation which brings two main drawbacks: its weight and the power plant complication. Indeed, the pre cooler function is to limit the temperature of the discharge air when the vehicle is in climbing phase. But at high altitude and cruise conditions, this is just a redundancy. Furthermore, during climbing itself, the engine encounters a fuel penalty for the fan bypass air, which is spent for the pre cooler. Another valuable consideration is about interfacing the bleed conducts with the decreasing dimensions of the compressor [20].
A similar problem addresses to the complexity for each system and the interaction between each other: interfacing different technologies reduces the whole system efficiency. The leakages which could eventually take place are difficult to detect and, in the event of an inadequate maintenance, the detrimental effects could spread all over the networks. Thus, ending with delays and grounded aircraft.[34]

Hydraulic power has represented (and still does) a real important technology on board the aircraft: indeed, it encountered a great development during the Second World War and continue to have a significant role on modern vehicles. This is mainly due to the delay of the electric technology which, for years, has been extremely less efficient than the hydraulic one. Moreover electric devices faced some difficulties to achieve an amount

of power density as large as the one provided through the hydraulic system.
Nowadays electric power is much more efficient than some decades ago and more enhancements are expected: for this reason, hydraulic system could be replaced with electric devices, which do not contemplate the risk linked to hydraulic fluids. At last, hydraulic equipments are way far heavier than electric actuators [28].

According to Torenbeek [37] in previous aircraft design literature, systems are considered as less important than the overall project. From early stages of the aviation age, each system have been designed in a modular structure and with few interconnection between each other. Thanks to the technology development and the increased research in this field, a different approach towards the design of the overall aircraft is gaining interest. Indeed, systems represent around 30% of Aircraft Empty Weight, Direct Operating Costs, Aircraft Development Costs and Direct Maintenance Costs [21]. Thus, a different overall aircraft design influences weight and net fuel consumption. [24] The main interest about the subsystems integration is related to mass and weight in this terms: the aim is to diminish weights, and reduce the over-sized systems in order to decrease the fuel consumption which is directly linked to the DOCS.

This thesis, will focus on two different, but still related, topic:

- the influence of Power Off Takes on Specific Fuel Consumption;
- how different subsystem architectures affect the Specific Fuel Consumption.

The following scheme represents how SPS affects the aircraft: the influence on the SFC is not as much investigated as the influence on costs. However, the fuel consumption is strictly related to them and even a slight decrease in SFC could be of great benefit in terms of aircraft operating costs.

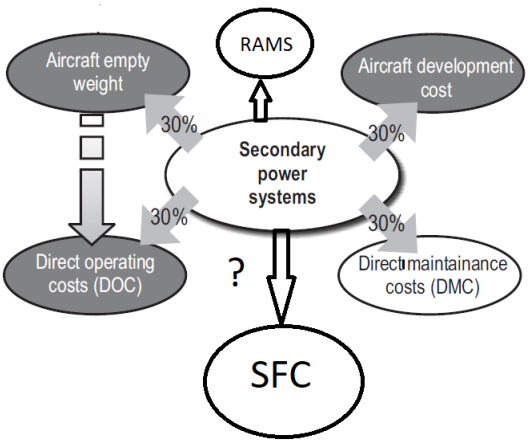

Figure 1.7: Systems integration [24]

The on board systems require different amount of power as well several forms of it; as previously mentioned, the extraction of various power sources creates inefficiencies. There are a lot drawbacks related to the secondary power systems: bleeding air generates both power and fuel waste. Moreover, hydraulic systems are often oversized because they feed those elements which works impulsively: for a small amount of time they require high level of power (e.g. when high lift devices are on) thus increasing mass and weight.

Similarly the volumes required by hydraulic cables throughout the aircraft are high. On the other hand, for what concerns the integration between subsystems and engine for the standard architecture, many disadvantages can be underlined [16]:

- complexity and weight increasing;
- costs increasing;
- the engine design generation of induced drag;
- specific Fuel Consumption growing;
- thrust reduction.

1.3 Innovative trends

In last decades, there has been a great interest over the More Electric and All Electric Aircraft concept; the oil crisis in the 1970s along with the increasing of the air transport demand, encouraged to a reconsideration of the technologies employed in the aviation field. The first goal was to improve the aircraft fuel efficiency: in more than 40 years, a lot of technological renovations have taken place, leading to a decrease in fuel consumption. Recently, also environmental regulations have brought the aerospace industry towards emissions and noise reduction. To meet very demanding requirements, the only solution is to evolve the architecture of both vehicle and engines. It is certainly true that the shift from conventional to innovative configurations introduces some critical problems, especially regarding the amount of power supplying gas turbine spool.
Besides, important developments concerning the fields of permanent magnet materials, semiconductor devices and electronics have been made. The bond between these two areas of interest lead to the possibility of innovative configurations of on board power generation and distribution.
The reappraisal of electrical power is an example: this source started to be adopted for functions traditionally powered by hydraulics and pneumatics. Another significant concept is the reduction of the nature of systems on the aircraft, each of them requiring redundancy and complexity. Furthermore, another aspect concerns the adoption of electrical technologies to extract power from engines.
All these considerations gave birth to the All Electric Aircraft (AEA), in which all the power systems are distributed in electrical form. In figure 1.8 a typical AEA is schematically shown [28].

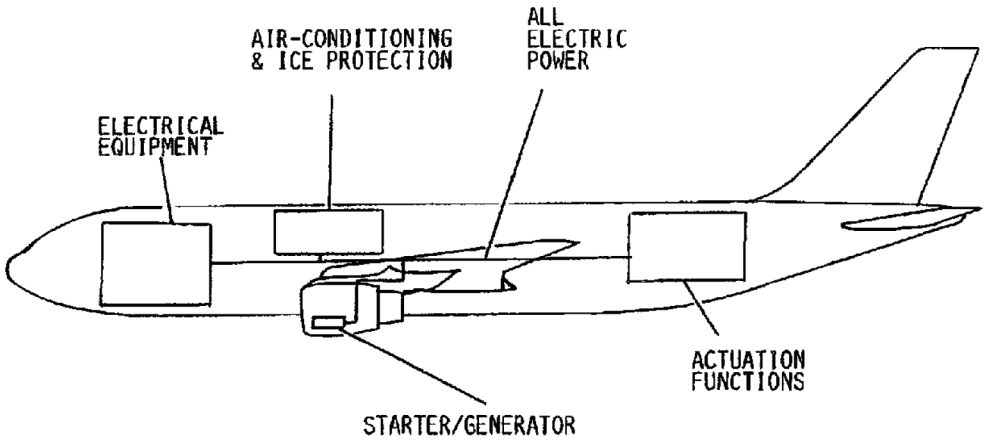

Figure 1.8: All electric aircfraft [28]

Clearly, if the overall architecture differs from the standard one, also the engine configuration need to be replaced. For this reason, since 1970s NASA Lewis Research Center focused the studies on this field, to the possibility of integration between an electrical generator and the main shaft of the conventional gas turbine engines [36].
In figure 1.9 an idea of the engine for an AEA is presented: this new configuration allows the gearbox removal, along with other weight and mechanical penalties.

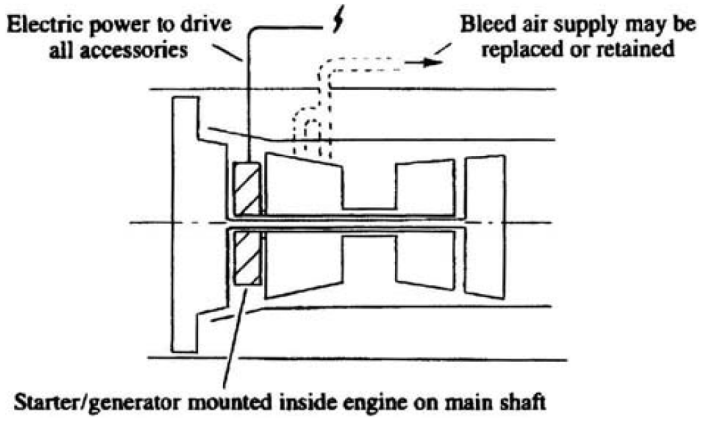

Figure 1.9: All electric engine scheme [28]

It is should be underlined that the innovative architecture consents to develop other possible configurations: as an example, the AEE could supply secondary power trough different sources, depending on the aircraft distribution systems. It could be necessary to dispense electric power to all the utilities, if each on board system is completely electric;

on the other hand, if the hydraulic system is retained, it should be supplied with hydraulic power, with electrically driven pumps, instead of engine driven ones. Pneumatic system could also be retained, thus the bleed extraction could be necessary.

The revolutionary design requires innovative solutions, such as high voltages electrical networks; on the other hand, the deletion of hydraulic pumps requires electrical actuators and, for future aircraft, the evolution of flight control surfaces.

1.4 More Electric Aircraft

Around the 1990s, the general awareness of the inevitable move to new aircraft system design, led to the adoption of electric power. However there was no a complete consensus on what extent the electric systems should be used. Especially, the enormous step between a conventional aircraft to an all All Electric one could not be made without intermediate configurations. Thus, the More Electric concept started to be diffused, replacing the AEA one.

More Electric Aircraft represent different typologies of vehicle, all with a common characteristic: *high level of integration between systems and engines, obtained extracting secondary power systems by a single electric source.* In MEA not all the on board systems are electrically powered, but most of them. Generally speaking, some hydraulic, pneumatic and mechanical power could be still present. Along with the general architecture, the More Electric Engine (MEE) requires some adaptations: while bigger generators are required to feed engine and other accessories, the Accessory Gearbox (AGB), oil system and conventional bearings could still be present [34].

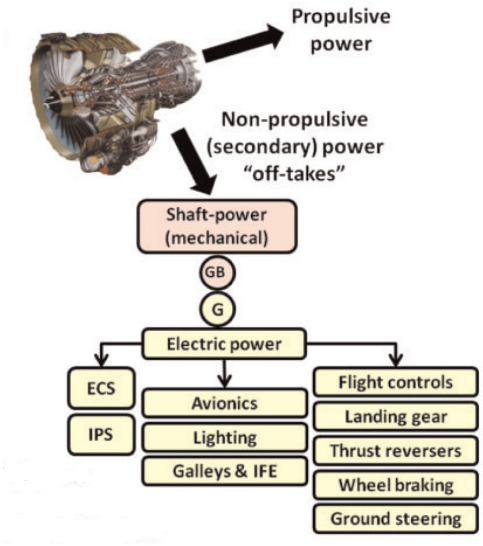

Figure 1.10: More Electric power off-takes system [32]

Nowadays, different technical developments have taken place both for the generation and distribution technologies as hybrid, bleed-less configuration, More Electric Engines, variable frequency generators, embedded digital systems or distributed systems architectures. Having said that, it is interesting to understand the trend of on-board energy power management.

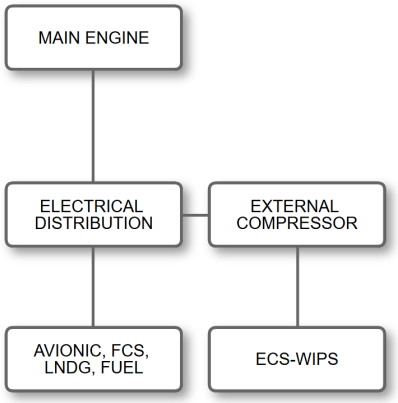

Figure 1.11: Trends to MAE

As previously cited, there are various possible More Electric Aircraft configurations: the principle behind all of them is the replacement of hydraulically and pneumatically supplied systems with electrically supplied ones. In figure 1.12 the basic idea is presented. The MEA structure should consist of the following equipments: clearly not all the possible configurations are equipped with all of them.

- Electric Wing Ice Protection
- Electric ECS
- Electric Engine Starting system
- Electric Power managing and control
- Electro-Mechanical actuators (EMA), Electro-Hydrostatic actuators (EHA) [38]
- Electric Braking
- Electric fuel pumps and oil pumps
- Electro-Mechanical thrust reversing actuation

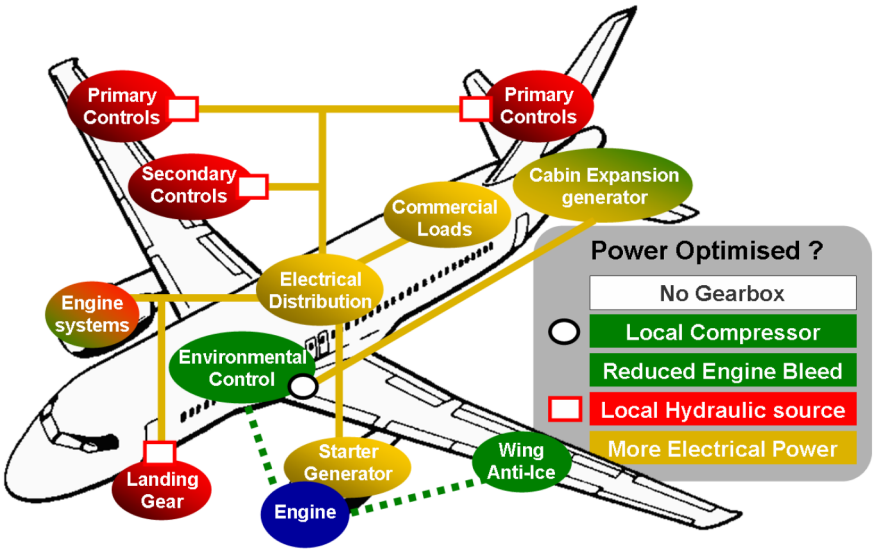

Figure 1.12: More Electric Architecture (example) [14]

The MEA concept relies on a more intense utilization of electric power, in order to optimize both the cycle cost and performance. Noticeably, the MEA requires a significantly higher load on electrical system, together with an higher quality power. To allow the installation it is obviously necessary a safe, reliable and autonomously control system. The main drawback about the MEA is the following: nowadays, electrical systems are still heavier than the conventional hydraulic or pneumatic systems. It is fair to assume that electrical devices will become lighter and smaller in the next years, because of the great improvements and incentives towards this technology. Furthermore, some studies evaluate that the all electric concept could bring to a reduction of the Overall Empty Weight; e.g. in [16] a configuration with EMAs and EHAs and without bleed-air system is given for an A330. The output consists OEW saving of a 0.5% and a fuel reduction of 4.5%.

1.4.1 Benefits

The replacement of hydraulic and pneumatic power distribution systems with a single electric one brings some benefits: in this chapter only a general overview of the advantages is provided [16]. However, the major interest throughout the study is to compute the Specific Fuel Consumption required by the power off-takes for Secondary Power Systems, and comparing different systems architectures.

- Reduction on the engine core size
- Improved systems integration and adoption of more efficient power units
- Mass reduction, especially if Variable Voltage Variable Frequency equipments are adopted

- Easier maintenance and control
- Improved performance of electric motors because the generators work supplying constant voltage to frequency ratio
- Reduction in Specific Fuel Consumption

Some of the technological innovation are briefly introduced here.

Hydraulic system removal

Hydraulic system inefficiencies have already been cited; the actual trend is to replace hydraulic actuation with electric actuators. The Electro-Hydrostatic Actuator (EHA) uses electronics and control techniques to provide more efficient flight control actuation. As previously mentioned, for most mission phases, actuators require very few power; anyway, the conventional components continually pressurise them. New techniques try to provide power only when surfaces need it. This requires the adoption of variable speed pumps.

The electromechanical actuator or EMA replaces the traditional hydraulic actuator with an electric motor and gearbox assembly which give an input to move the pump. Both EHAs and EMAs achieve a saving in energy. For example, although the weight of the EHA is twice the weight of the adjacent hydraulic actuator, the removal of one hydraulic system represents a very significant overall weight saving [38].

Power generation

The actual trend on electric power generation goes along with the tendency to supply all the Secondary Systems with Electric power.

The high voltage for the electric generation is an actual solution in order to increase the Power to Weight ratio. Indeed, high voltages lead to a smaller electric motors. Then, the Constant Speed Driver (which takes an input shaft rotating at a wide range of speeds and transform this power to an output shaft that rotates at a constant speed) becomes useless. Clearly this allows a weight saving.

New technologies comprise especially Permanent Magnet Generators along with high voltages up to 230 V AC Variable frequency or 540 V DC [39], and the further conversion to other frequencies. Innovative techniques also allow an electric engine starting.

Electric Wing Anti Ice

Conventional pneumatic wing anti ice consists of a hot air flow which is blown through the addressed surfaces. An innovative technology is the electro-thermal ice protection scheme: it consists of a series of heating resistance inserted on the interior of the exposed surfaces. The blankets can be heated with different intensity, whether for anti-ice or de-icing functions. This method is remarkably more efficient than the pneumatic system because no energy is exhausted. As a result, the required ice protection power usage is approximately half that of pneumatic systems [1].

Bleed less configuration

An example of a more electric architecture is the Bleed-less configuration where the pneumatic extraction from the engine compressor is replaced by an external compressor.

In this way, the outside air is delivered at the optimum pressure required by the subsystem; the main benefit relies on the fact that only shaft power is extracted from the spool and, consequently, a certain amount of fuel is saved. Moreover, the pressure of compressed air is fixed by the engine; often, on board utilities supplied by pneumatic system are designed to work at lower pressure level than the one extracted from the HP compressor. For this reason, in a conventional architecture, during the flight a lot of power is wasted. To face this problem, in a bleed-less configuration the function of providing thrust and providing power are separated.

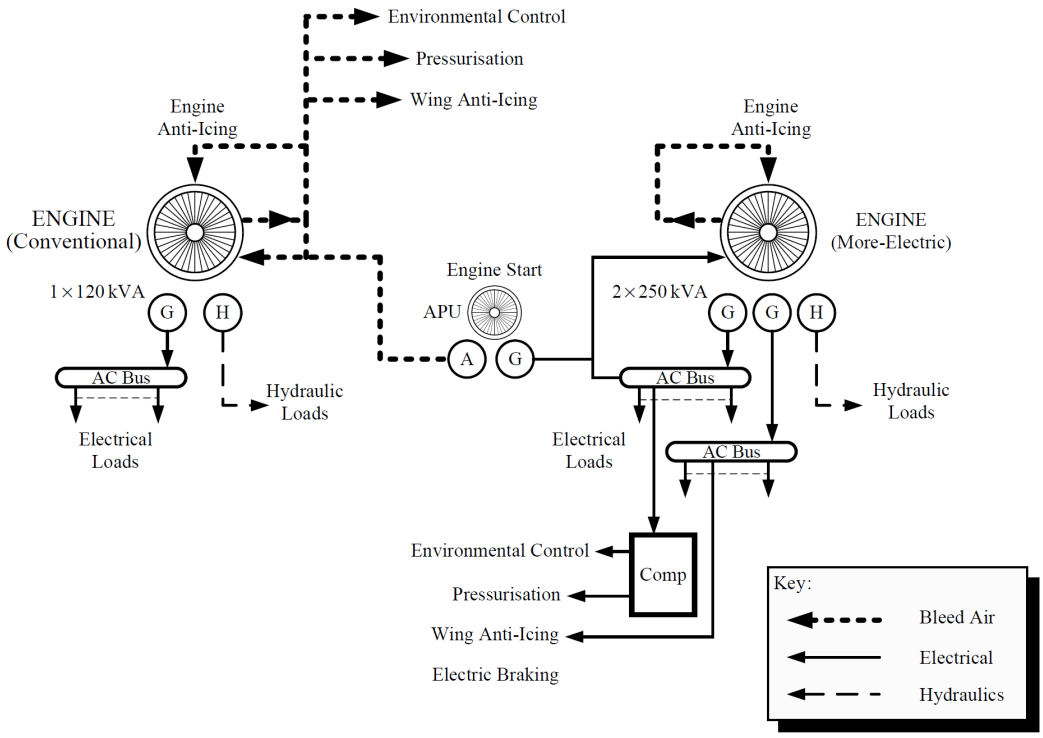

Figure 1.13: Comparison between a Conventional (left) and Innovative (right) electric scheme [31]

The BOEING 787 is the first aircraft which adopted the bleed-less configuration. This configuration has some discriminating factors from a conventional commercial aircraft: the most relevant relies on the deletion of pneumatic system and bleed manifold. The B787 innovative architecture brings some relevant benefits [1]: the saving in fuel consumption, the reduction in maintenance costs, improvement in the reliability for the high level of electronic devices to control the engine and the adoption of fewer parts. The overall weight is reduced, even if the ECS compressors are installed. The Environmental Control System must be supplied by electric sources: four electrically driven compressors are mounted to drive the ECS systems. The engine starter need to be electric and not

pneumatic.
Clearly, the increasing of electric supplied utilities requires the improvement of power system: for the B787 two 250 kVA generators are installed, with a 230 V AC distribution system, instead of the conventional 115 VAC. The generators are directly connected to the engine gearboxes and operate at variable frequency (360 to 800 Hz) proportional to the engine speed. It does not include the constant speed drive, which is the key component of an integrated drive generator (IDG) [1].

Instead the power sources for hydraulic system are engine driven (very similar to those mounted on a conventional architecture) and electric-motor driven pumps.
A difference between the hydraulic systems is represented by the pressure which sustains it: 5000 psi instead of the conventional 3000 psi. An higher pressure allow the adoption of smaller components. This choice gives the opportunity to reduce wires weight. Finally, the bleed less architectures is simpler with respect to the engine design: the removal of pneumatic systems enables the consequent elimination of the pre coolers, valves and all the pneumatic ducting.

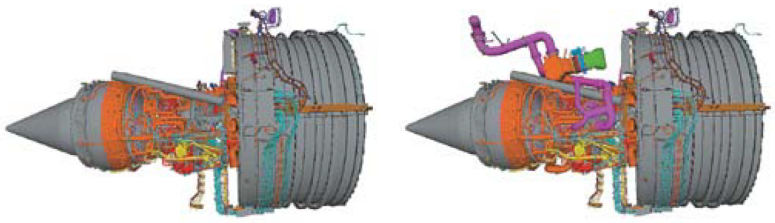

Figure 1.14: Comparison between the build up for a traditional (right) and bleed less engine (left)

Chapter 2

Systems design

This chapter aims to describe the approach adopted during the on-board system design. Furthermore a preliminary design of *fuel system* and *ECS recirculation fans* is provided.

2.1 Tool description

During the thesis the on board systems design has been accomplished with the aid of a Politecnico di Torino in-house tool, called Astrid. This tool allows the user to design conventional, More Electric and All Electric configurations [17]. An engineer can decide whether to proceed with a COMPLETE STUDY or a PARTIAL STUDY.

The complete study comprises the *conceptual design* and *on-board system design*; the conceptual design begins from the Top Level Requirements (TLARs) and concludes with the aircraft feasibility and the estimation of the design point.

The very first step of the design process is to the definition of the TLARs [17]

1. Mission requirements (mission profile, number of passengers, range ..);
2. Aircraft performances (speed, altitude...);
3. Propulsion system requirements (number of engine, SFC...)
4. Airplane geometry and materials
5. On board system requirements which depend on subsystem architecture.

In this works a *partial study* has been developed. The attention of the study is focused on the effects of different subsystems configuration on the Specific Fuel Consumption of the aircraft engines. Thus, the study over a reference commercial aircraft has been more useful. The work is therefore referred to a already existing vehicle (Airbus A320-200) (described in detail in *Chapter IV-Part I*).

1. A detailed mission profile is required.

- range
- altitude
- flight speed
- climb rate
- phase duration
- specific fuel consumption for each phase
- take off and landing speed
- maximum Mach speed

along with

2. vehicle geometry

- fuselage
- wings
- horizontal and vertical tail
- engines
- gravity center position
- empty weight

After these first boundary conditions are fixed, the second section the on board systems can be designed: AVIONIC, FLIGHT CONTROL, LANDING GEAR, ENVIRONMENTAL CONTROL, WING ICE PROTECTION, FUEL, HYDRAULIC, ELECTRIC. Once that all subsystems are designed, Astrid returns

- Weights of all systems [1]
- Shaft Power Off-takes for each mission segment
- Bleed Off-takes for each mission segment.

[1] Throughout the whole thesis, as will be expressed later, the systems masses are not taken into account

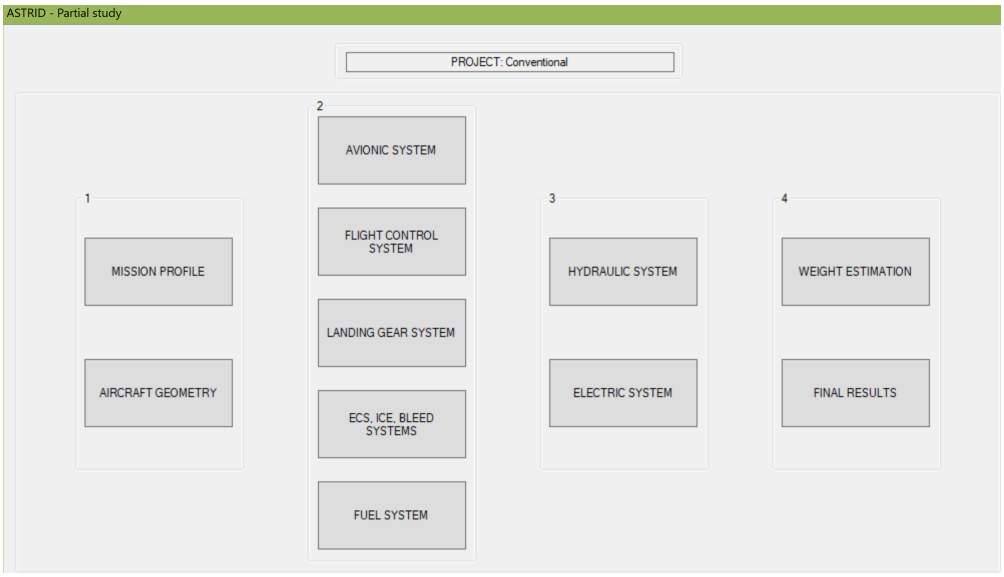

Figure 2.1: Astrid home page

The outputs considered during the study are *shaft power off-takes* and *bleed air off-takes*.

2.2 Fuel System

The aim of this section is to provide a plausible amount of power required by the fuel system which can be valuable for future researches during the aircraft conceptual design. Moreover, the analysis also aims to produce a comparison between the traditional and innovative technology for the fuel pumps: this can represent a reference for more accurate studies on the More Electric trend.

The starting point has been a research on the state of the art for what concerns the fuel boost pumps adopted over different vehicles; then, the focus has been on the A320, which is the reference vehicle. Moreover, some other vehicles have been compared in order to generalize the outputs.

2.2.1 General Design

The main purpose of the aircraft fuel system is to supply fuel to the engines in order to maintain the propulsion system active throughout all the mission phases. In a modern aircraft, fuel system main functions encompass not only the engine feed but also fuel pressurisation, fuel transfer and refuel/defuel, storage, fuel jettison. Moreover, the main components are

- *fuel transfer pumps*,
- *fuel boost pumps*,

- *fuel transfer valves*,
- *Non-Return valves*
- *fuel quantity sensors*
- *storage tanks*
- *fuel lines*

All these devices need to be designed following the Chapter 14 of CFR (Code of Federal regulation) [6].
Even if all the requirements and constraints contained in FAR regulation are restrictive, different possible solutions exist for different aircraft and engines mounted on them.

The complexity behind the fuel system makes difficult to generalise its design, even if for a preliminary stage. However, the aim of this section is to find the amount of power required by the boost pumps (sometimes called Engine Feed pumps), once the fuel flow is known.

The boost pumps are those pumps whose function is to provide fuel from the tank to the engine, in order to prevent aeration [31]: for example, in case of air into the line, this could cause the detrimental situation of "flame out" and the complete loss of power. Once the fuel enters the engine, the dedicate main gear fuel pumps compress and heat the fuel to be ignited in the combustion chamber.

Fuel boost pumps are usually electrically driven: it can be found, that electric power is function of

- fuel flow rate
- delivery pressure

and the interesting issue is about the proportion between these three physical quantities and to what extent they affect each others.

The most significant reference values for which it is necessary to draw a general estimation is the *delivery pressure*. Indeed, each engine works with specific requirements and conditions as well as the main gear fuel pumps. However, in a preliminary phase, designers need an average size value of the required power for every single system.

From the literature and according to [2] the boots pump need to maintain the fuel pressure in range between 20 psig and 40 psig which mean 1.37 bar to 2.7 bar.

Assuming that, for this constrain, each pump delivers the fuel at a slightly higher pressure, in order to overcome the losses through the entire lines. The power varies as a function of the fuel flow rate and the pressure at which the fuel is delivered.

The fuel flow rate needed in a single mission phases can be expressed in equation 2.1

$$\dot{m} = SFC * P_{phase} + SFC_{APU} * P_{APU} \tag{2.1}$$

$$\dot{m}_{engine} = SFC[lb/lbfhr] * P_{TO}[lb] = [lb/hr] \tag{2.2}$$

Where

- SFC is the specific fuel consumption for the single phase;
- P is the thrust produced.

Clearly, in every different mission segment, the engine receives a proper amount of fuel; on the other hand, not all the feed pumps can work at different flow rates.

- **Fixed Frequency pumps**: these pumps boost the fuel at a fixed flow rate, which, for most of flight segments, exceeds the one required. The amount of fuel not entering the engine is recirculated through a system of conduits and pumps which collect the fuel and force it in the tank again.
- **Variable Frequency pumps**: these have been developed to be mounted on those aircraft which are supplied by variable frequency generators . There are different models and motor types available to meet the possible demands. The principle that led toward the introduction of these pumps is the need of less power absorption along with a low level of total harmonic distortion. To satisfy this purpose, the variable frequency pumps are able to blow the fuel at different ranges, depending on the the mission phase. By this way, fuel recirculation is far less significant if compared to fixed frequency pumps.

To compute the fluid power required by a pump equations 2.3 have been adopted

$$P = \frac{[m^3]}{[s]} * [Pa] \tag{2.3}$$

$$P_{real} = P/\eta = [W] \tag{2.4}$$

Where

$$\eta = \eta_{fluid}\eta_{electric} = 0.8 \tag{2.5}$$

is the efficiency considered. It is the product between the fluid efficiency and the one related to electric motor.

It is necessary to define the relation between the fluid power and the electrical one. The basic principle is that a fixed frequency electric motors rotate, most of the time, at a different speed than the required one. For this reason to find the electric power required by a single boost pump, a k factor is adopted.

$$P_{electric} = k * P_{fluid} \tag{2.6}$$

where

$$\begin{cases} k = 1.6, & Q > 1600 l/h \\ k = -0.0002 * Q + 5.403, & 1600 < Q < 18000 \\ k = -0.0192 * Q + 35.621 & \end{cases}$$

Previous equations are based on a detalied bibliography research. For an higher fuel flow rate required, the power transmission factor tends to decrease. As previously said, the boost pump need to maintain the fuel pressure in range between 20 and 40 psig.
To a very preliminary design stage, the following assumptions have been considered

1. delivery pressure is 2.2 bar;
2. the tank is pressurized a 1 bar;
3. the losses are less that 1 bar;
4. one pump feed one engine at time.

Assumptions 1 and 2

The value of 2.2 bar is an average one between some real delivery pressure values of a fuel boost pumps found in literature, especially referring to [2] from Eaton Company. To a detailed study, every single configuration should be studied; anyway, the choice of 2.2 bar as a delivery pressure instead of the maximum one found in the literature is based on the fact that each fuel tank is kept a 1 bar. Given that, even if for some case studies, the inlet pressure require by the engine is slightly more than 2.2 bar, the fuel system is still capable to feed it.

Assumptions 3

- $\Phi = 0.038\,\mathrm{m}$: tube diameter [7]
- $v = \frac{Q}{\Phi} = \frac{m^3/s}{\mathrm{m}^2} = \mathrm{m/s}$ fuel speed;
- $Re = \frac{v*d}{\nu} = \frac{\mathrm{m/sm}}{\mathrm{m/s}} =$ Reynolds number

The tubes adopted for the fuel systems are usually of NBR (nitrile-butadiene rubber) with a roughness of $\epsilon = 0.3\mu m$, from which the relative roughness $\frac{\epsilon}{D} = 7.89 * 10^{-6}$. From this value, it necessary to refer the Moody diagram and obtain the friction fractor, which is almost constant for the range of Reynolds considered $\rightarrow \zeta \simeq 0.04$

Equation 2.7 has been adopted to estimate the pressure drops along the line.

$$\Delta p_{line} = \zeta \frac{L}{\Phi} \rho \frac{v^2}{2} = \mathrm{bar} \tag{2.7}$$

where

- $\zeta \simeq 0.04$;
- L m is the tubes length;
- $v = \mathrm{m/s}$ is the fuel velocity;
- $\rho = 0.789\,\mathrm{kg/m^3}$ is the fuel density.

2.2.2 Pressure drops due to the bank manoueuvres

Then, the losses due to the bank manoeuvres can be computed taking into account a max roll angle of 35 °C.

The specific weight of fuel (JET AP Avitur)is $\gamma = 7693[N/m^3]$. The load factor is

$$n = 1/\cos\beta = 1.2208 \tag{2.8}$$

Considering a the fluid height within the tank, the bank manoeuvre losses can be computed as follow

$$\Delta p_{bank} = \Delta h1 * \gamma * n = [bar] \tag{2.9}$$

Adding the two terms from equations 2.9 and 2.7 the total pressure gap that a pump encounters is found as

$$\Delta p_{line} + \Delta p_{bank} = \Delta p_{tot} \tag{2.10}$$

Assumption 4

The last assumption is that one single pump can feed one engine at time. The Code of Federal Regulation [6] does not suggest a clear requirement on this issue. Anyway, the main purpose of this preliminary study is to define the power required during the flight by the boost pumps.

A typical performance curves of a pump is shown in figure 2.2 which describes the relation between the fuel flow rate and the delivery pressure: this diagram is useful for the designer to chose the more suitable pump for the engine and aircraft under study. In this stage, the purpose is to make an esteem an average power consumed by the fuel systems: for this reason, the pressure at which a pump works is fixed at 2.2 bar while the variable becomes the fuel flow rate. Referring to equation 2.3 the trend of electric power against the flow rate at a fixed delivery pressure is shown in figure 2.3.

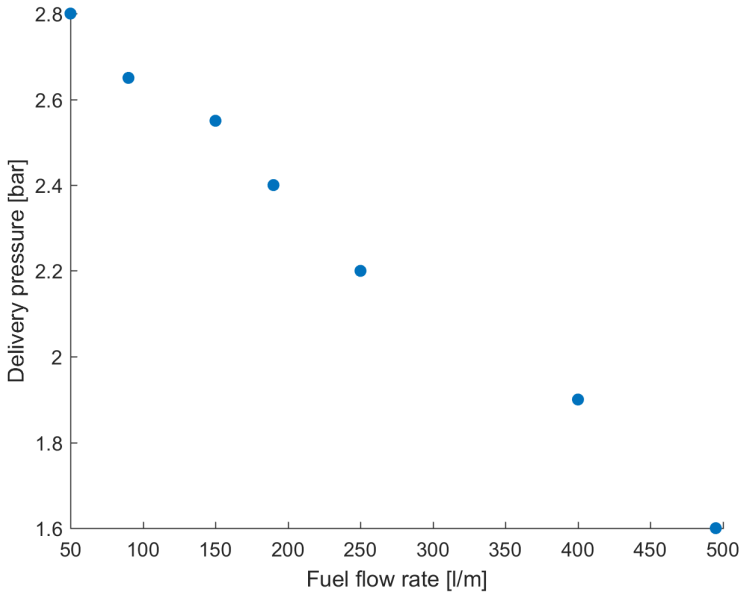

Figure 2.2: Performance curve built with values of Eaton Corporation boost pumps[5]

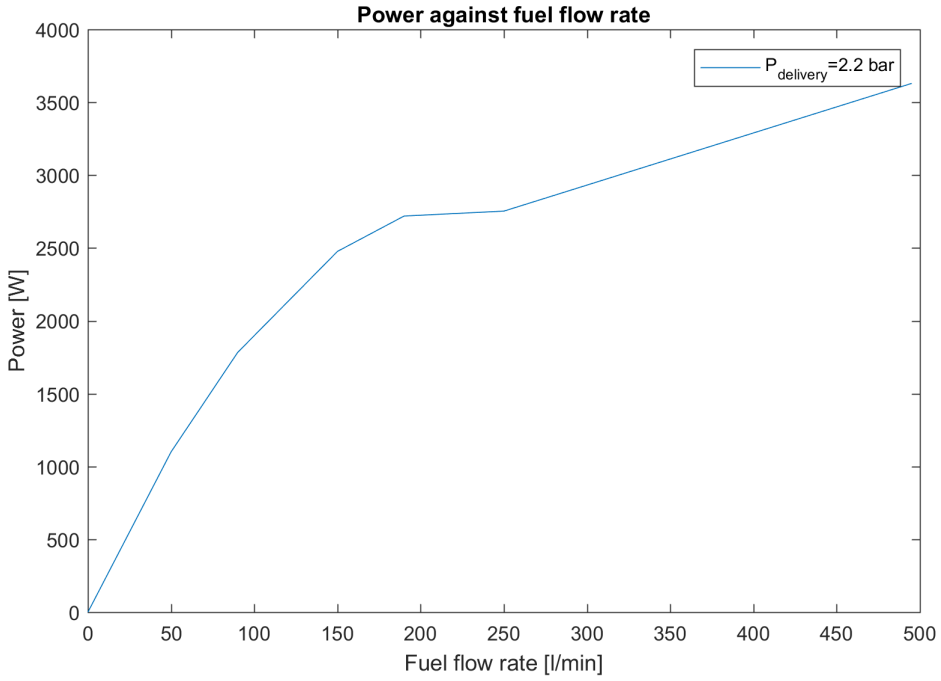

Figure 2.3: Electric Power for a single pump

Some comments can be drawn from the previous diagram: the electric power increases as the fuel flow rate raises, but non with the same rate. This is due to the power factor "kp" previously defined.

A low order model has been constructed in order to relate the fuel flow rate to the electric power by a single fuel pump.

$$\underbrace{P}_{W} = a \underbrace{Q^2}_{l/min} + b \underbrace{Q}_{l/min} + c \tag{2.11}$$

$$\underbrace{P}_{W} = -0.014 \underbrace{Q^2}_{l/min} + 13.09 \underbrace{Q}_{l/min} + 639.88 \tag{2.12}$$

The most valuable process in order to provide a relation which can describe the behaviour of a general civil transport aircraft, is focused on studying different existing examples and comparing the results.

1. Airbus A320
2. Airbus A340
3. Airbus A380

2.2.3 A320 (180 passengers)

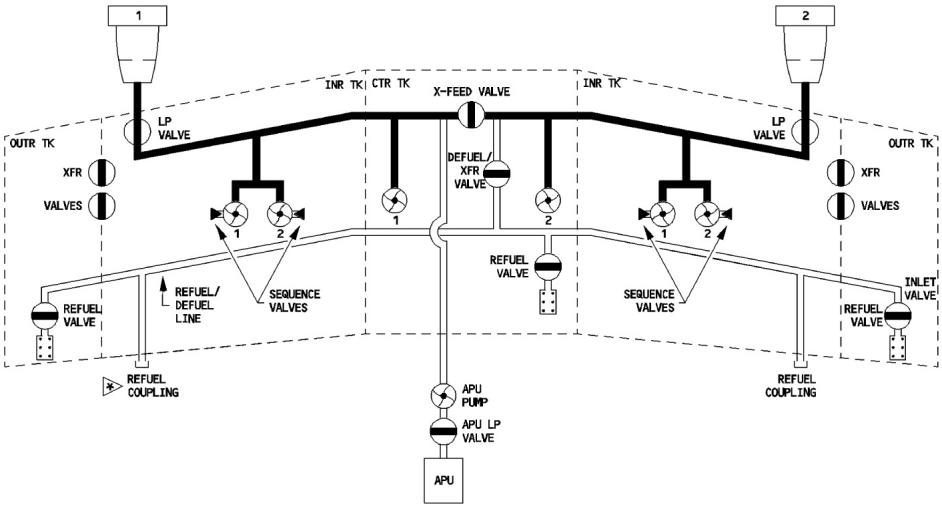

Figure 2.4: Fuel systems scheme of an A320 [8]

For our case study the following data are available.

$$\dot{m}_{engineTO} = SFC_{TO}[lb/lbfhr] * P_{TO}[lb] = 0.34 * 27000 = 9180[lb/hr] = 4163.978[kg/h]$$

$$\dot{m}_{engineCRUISE} = SFC_{TO}[lb/lbfhr] * P_{TO}[lb] = 0.545 * 5000 = 2725[lb/hr] = 1236[kg/h]$$

$$\dot{m}_{APU} = SFC_{APU}[kg/kWh] * P_{APU}[kW] = 0.486 * 447.4 = 217[kg/hr]$$

$$\dot{m}_{TO} = 4163 + 217 = 4380[kg/hr]$$

$$\dot{m}_{CRUISE} = 1236 + 217 = 1453[kg/hr]$$

$$\dot{m}_{max} = 4380kg/h = 92.99l/min \tag{2.13}$$

$$\dot{m}_{min} = 1453kg/h = 30.84l/min \tag{2.14}$$

$$\dot{m}_{mean} = 2916kg/h = 61.9l/min \tag{2.15}$$

For an A320 during take off, 4 wing tank pumps are on, while, during cruise 6 pumps remain on, until the central tank is empty.

It is necessary to underline that the A320 fuel pumps work at a fixed fuel flow rate which is the maximum one. With 92.99 l/min it can be found

$$P_{to} = 6.8kW \tag{2.16}$$

$$P_{cruise} = 10.3kW \tag{2.17}$$

2.2.4 A340 (350 passengers)

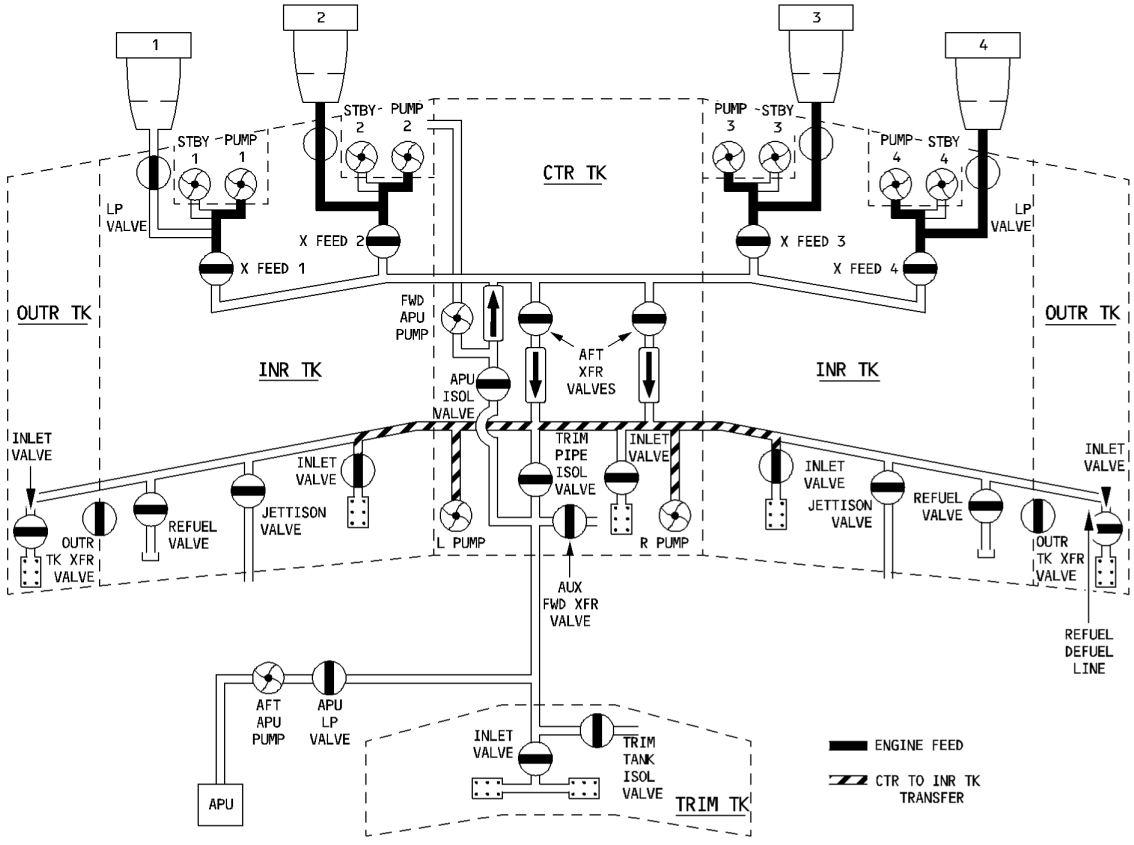

Figure 2.5: Fuel systems scheme of an A340 [9]

A340 is powered by 4 engine (CFM 56 C like). It has 4 fuel pumps on while 4 are in stand by. Also the central tank are on throughout the flight. Engine thrust is about 34000 lbf in take off [4] , which along with 2.1

$$P_{A340_{to}} = 9.12kW \tag{2.18}$$

$$P_{A340_{cruise}} = 13.68kW \tag{2.19}$$

Both the A320 and A340 are equipped with fixed frequency pumps, which always work at the same maximum fuel flow rate. As the central tank pumps are off while the take-off manoeuvre, during cruise condition, all pumps requires a larger amount of power.
Taking into account the future innovative trends, it could be assumed that they are equipped with variable frequency generators in order to find the power saving. It is assumed that, during cruise, the fuel flow rate can be one half or even one third than the fuel flow in take-off segment (2.13). With these new values the power is now computed, in order to find the influence of a More Electric component on the vehicles.

A320 variable frequency

$$P_{to} = 6.8kW \tag{2.20}$$

$$P_{cruise} = 6.1W \tag{2.21}$$

A340 variable frequency

$$P_{A340_{to}} = 9.12kW \tag{2.22}$$

$$P_{A340_{cruise}} = 7.5kW \tag{2.23}$$

In table 2.1 it is reported the comparison between fixed frequency pumps mounted in conventional aircraft and variable frequency pumps, which will be possibly set on More Electric Aircraft.

Model	**Conventional [kW]**	**More Electric [kW]**	**Ratio**
A320	10.3	6.1	0.59
A340	13.68	7.5	0.55

Table 2.1: Comparison between the power required during cruise condition by the fixed frequency boost pumps and variable frequency boost pumps

Previous results highlight the possible advantages derived from the adoption of innovative fuel feed pumps, in terms of power saving in cruise condition. This will also affect the sizing stage of this components which are oversized in order to meet the requirements of few mission stages.

2.2.5 A380 (up to 850 passengers)

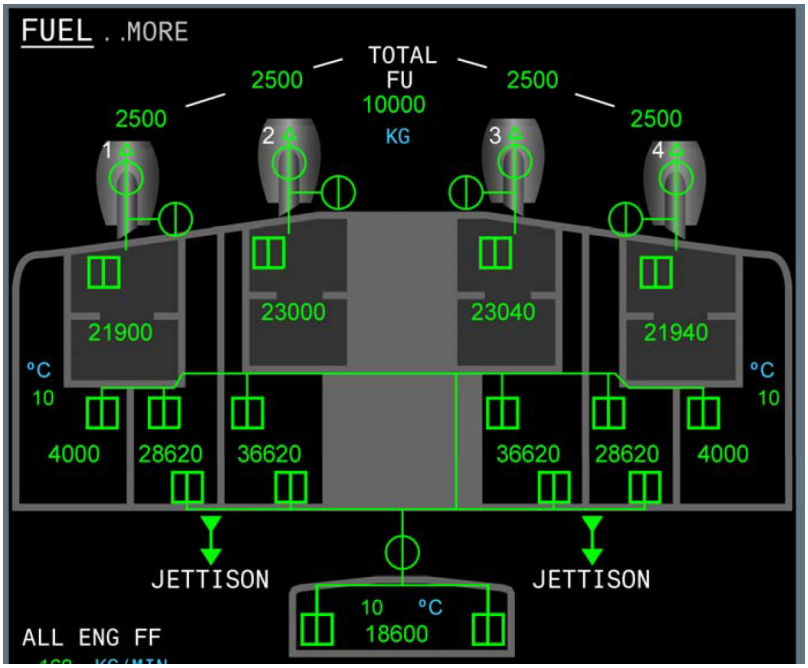

Figure 2.6: Fuel systems scheme of an A380 [3]

For an A380, which is powered by four engines (Trent 900) the fuel system is equipped with 8 main pumps, where 4 of them are in stand by. Taking into account [4] the T.O. thrust is 77 000 lbf and considering eq. 2.1, during the take off a maximum fuel flow rate (250 l/min) is supplied by each of 4 pumps, while 6 pumps are on during cruise, at minimum flow rate (100 l/min) [3]

$$P_{to} = 18kW \tag{2.24}$$

$$P_{cruise} = 10.8kW \tag{2.25}$$

2.2.6 Trim tanks

Another important issue is related to the trim tanks, which can be present on an aircraft. The trim tank transfer system control the vehicle Center of Gravity.

For an A380 the Center of Gravity control transfers only from the trim tank to the left or right wing tank. This operation happens before landing [3], when the fuel is transferred until all the trim tank is empty.

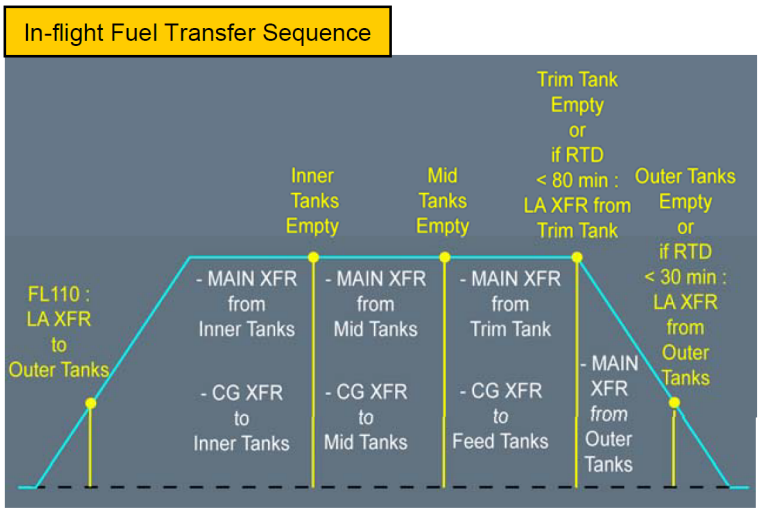

Figure 2.7: Tranfer sequence of an A380 [3]

USABLE FUEL (Fuel Specific Density: 0.785 kg/l)								
		Outer Tanks (each)	Feed Tanks 1/4 (each)	Mid Tanks (each)	Inner Tanks (each)	Feed Tanks 2/3 (each)	Trim Tank	Total
VOLUME	(liters)	10 520	27 960	36 460	46 140	29 340	23 700	324 540
	(US gallons)	2 780	7 390	9 630	12 190	7 750	6 260	85 740
WEIGHT	(kg)	8 260	21 950	28 620	36 220	23 030	18 600	254 760
	(lbs)	18 200	48 390	63 100	79 850	50 780	41 020	561 660

Figure 2.8: Fuel tanks capacity for an A380 [3]

For an A380 the fuel transfer occurs in this sequence [3]

- Inner tanks to feed tanks, until empty;
- mid tanks to feed tanks, until empty;
- trim tanks to feed tanks, until empty;
- outer tanks to feed tanks.

Moreover fig. 2.7 represents that the trim tank transfer begins before landing, in the last segment of cruise condition (1/3 of it).

Given that an A380 is a long range aircraft, whose average cruise flight duration could be 7.5 hours.

Applying the same computational model, the two fuel transfer pumps from trim tank to feed tanks can have an influence of

$$P_{trim} = 0.2 * P_{TO} \tag{2.26}$$

when they are active.

2.2.7 Conclusion

This flow chart contains the main logical process which leads to the estimation if the power required by the engine feed system.

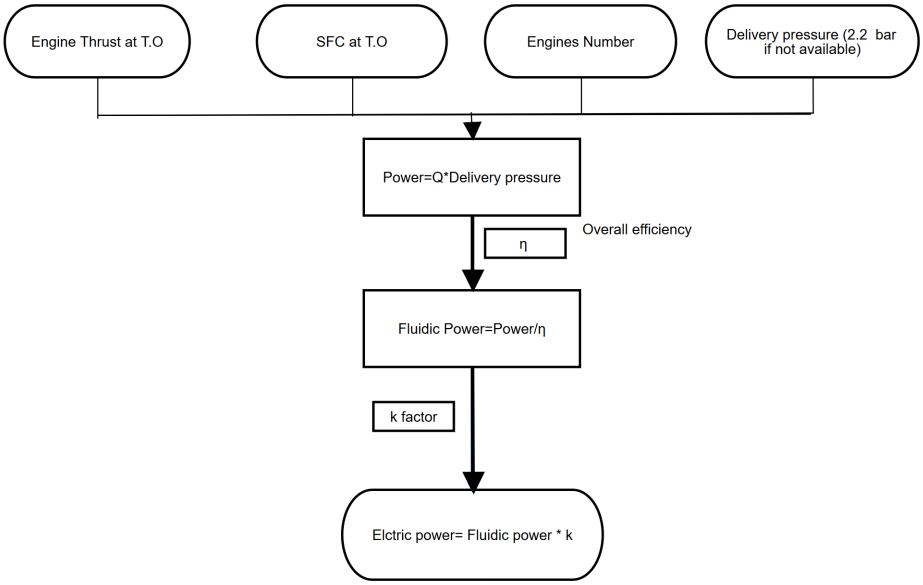

To give a general equation which can be applied for the conceptual study of an aircraft the following input are necessary

1. Engine thrust at Take-Off [2]
2. Specific fuel consumption at Take-Off
3. Number of engines
4. Delivery pressure (if not available $P = 2.2bar$)

$$P = \frac{[m^3]}{[s]} * [Pa] \tag{2.27}$$

$$\downarrow$$

$$P_{real} = P/\eta = P/0.8 = [W] \tag{2.28}$$

$$\downarrow$$

[2]Otherwise the user could also insert the fuel flow rate, if available.

$$P_{electric} = k * P_{fluid} \tag{2.29}$$

where

$$\begin{cases} k = 1.6, & Q > 1600 l/h \\ k = -0.0002 * Q + 5.403, & 1600 < Q < 18000 \\ k = -0.0192 * Q + 35.621 \end{cases}$$

Fixed frequency pumps

$$\boxed{P_{CRUISE} = 1.5 * P_{TO}}$$

Variable frequency

$$\boxed{P_{CRUISE} = (0.6 - 0.8) * P_{TO}}$$

The previous relations

which is a mean value between the results of the previous case studies (according to 2.1 and 2.24).

The range between $0.6 - 0.8$ is addressed to the presence of the trim pumps.

Even if the previous analysis is based on the four assumptions it is useful for two main reasons

1. during the conceptual design, the outcomes of section **Conclusions** can be adopted for reference values which will be optimized during the following stages;
2. fuel boost pumps represent an example of how a high level of integration between subsystems (engines, fuel systems and electric system) can lead to beneficial effects for the aircraft.

2.3 Environmental Control System: fans

The aim of this analysis is to find the electrical power required by the ventilation and recirculation fans on board the aircraft. This amount of power is actually independent from Environmental Control System architecture.

The starting point of the study has been the Code of Federal Regulations, especially **25.831 (a)**, [6] which express the following regulations:

- "Section 25.831 (a) specifies that the ventilation system must be designed to provide a minimum of 0.55 pounds of fresh air per minute per person (10 cubic feet per minute ofair at 8,000 feet pressure altitude and at cabin temperature of 75° F.) for normal operations. If the airplane incorporates a recirculation system, the required fresh air may be mixed with filtered, recirculated air. A larger amount of fresh air

may be required due to secondary considerations, such as equipment cooling, window or windshield defogging, control of smoke or toxic fumes, or smoke evacuation. Increased fresh air flow may also be needed in some instances to compensate for high ambient temperatures and humidity". [6]

- "Takeoff with the air conditioning or bleed air system "off" may be an acceptable procedure provided the ventilation system continues to provide an acceptable environment in the passenger cabin and cockpit for the brief period when the ventilation system is not operating normally" [6].

If 10 cfm per minute is the minimum volume of fresh air per occupant which the system must provide, the volume flow rate for all the occupant should be

$$\underbrace{10cfm}_{volume/person} * \underbrace{n}_{passenger} \tag{2.30}$$

Equation 2.30 contains the first parameter of this study: *the passengers number.*

Civil aircraft cabins are usually separated into different zones (e.g. First and Economy class) which simplify the control over heating and cooling operations. The zones number depends on the the vehicle type. For example, a short- and medium range aircraft like the Airbus A320 is consists of two different cabin zones while a larger long-range A330/A340 series have up to six [11].

The external air is mixed with recirculated air in a mixing unit. The recirculation process increases humidity and purity; indeed it also comprehends air filtration through some HEPA filters (High Efficiency Particulate Air).

The ratio between bleed and recirculated air is around $60-40\%$; however, in the next aircraft generation the forecasts assumes that this value will increase. By this way, the bleed air can diminish. As an example, the the A380-800 consumes 60% less bleed air than the B747-400. [11]

2.3.1 Fan types

This subsection provides an overview of the fans kind which equip a general aviation aircraft.

- **Cabin**. For what concerns the cabin, the number of fans can varies from 2 to 6 for larger models; 2 fans are usually for ventilation and than 2 fans have are adopted for the recirculation system.
- **Avionic**.The avionic ventilation system is almost the same for each aircraft, because the avionic bays are designed within a standard. They consist of a blower fan which pulls the air from the cabin to the bay. On the other side, an extraction fan which drives the air overboard or through the cargo compartment.

- **Cargo**. Cargo compartments fans receives the air from the cabin and avionic stages. Usually vehicles are equipped with an aft and one forward compartment. Each aircraft has a different cargo volume, which means, also, that the airflow required increases with it.
- **Galleys-Lavatories**. An interesting issue is related to the galley and lavatories, especially for the more modern and larger vehicles. Indeed, to spare the volume on board the aircraft, the aviation companies trend is to build lavatories and galleys close to each other, in order to leave more space for additional seats. By this way, the ventilation system is influenced, too. Especially, even if a configuration is equipped with 5-6 lavatories and galleys, the extraction fans are no more than 2 or 3; they, indeed, are mounted in the tail or in the forward side of the vehicle.

When air enters the cabin it then follows different path: it goes trough the galleys and lavatories, which eject overboard. The other air percentage is induced to avionic bays where the blower fans drag the air into the avionic compartment and the extraction fans pull it overboard or to the cargo. Finally, other air from cabin directly goes to the cargo zone. Fig. 2.9 shows a simplified standard air cycle for a conventional civil aircraft, although the fans number varies with vehicle configuration.

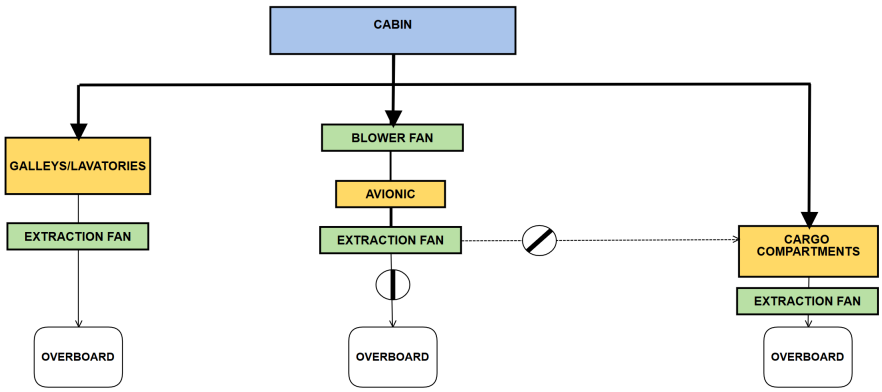

Figure 2.9: Air flow path

To maintain the pressurization of the cabin, the air flow which is extracted overboard need to be less than the air flow entering the cabin.

$$\dot{m}_{in} > \dot{m}_{overboard} \tag{2.31}$$

$$\dot{m}_{cabin} > \dot{m}_{extract.fans(galleys,lavatories,cargo)} \tag{2.32}$$

In order to find the amount of power required by the ECS, the ventilation fans produced by *2017 Safran Ventilation Systems* have been analysed [12]. The analysis results are, then, provided here.

The Electric power of a single fan is function of

- Working pressure
- Air flow rate
- Electric supply type

Then starting from real available products, the following equation describes the relation between three variables

$$P = \frac{[m^3]}{[s]} * [Pa] \tag{2.33}$$

$$P_{real} = P/\eta = [W] \tag{2.34}$$

where

1. $\eta_{ff} = 0.65$ [1];
2. $\eta_{vf} = 0.7$[2]

The power required by a fan is proportional to air flow rate and working pressure, as expressed in figure 2.10 and figure 2.11

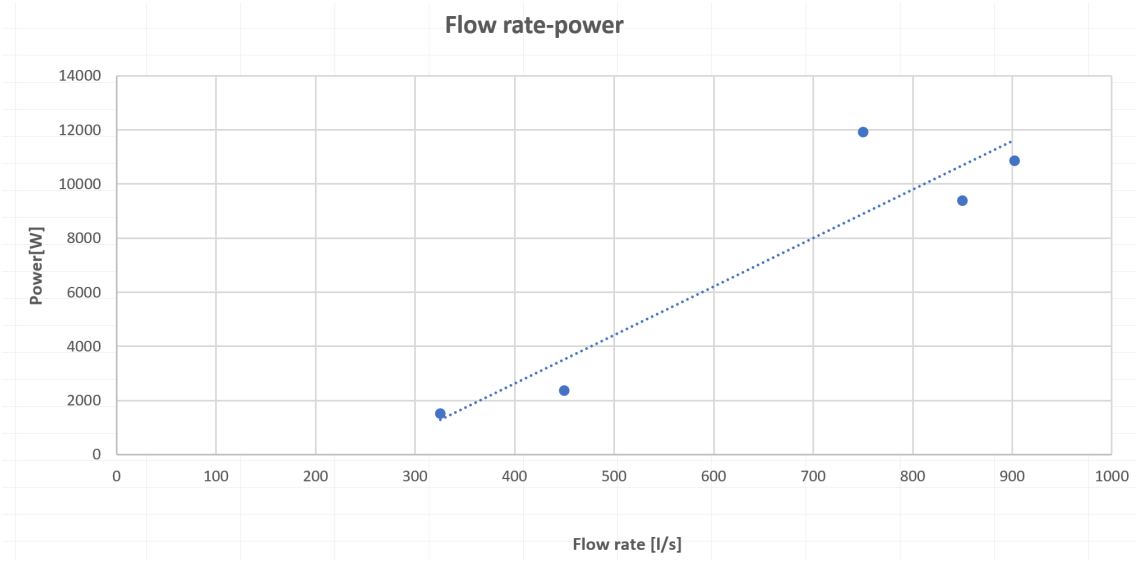

Figure 2.10: Relation between power and flow rate for cabin fans

[1]Fixed frequency

[2]Variable frequency

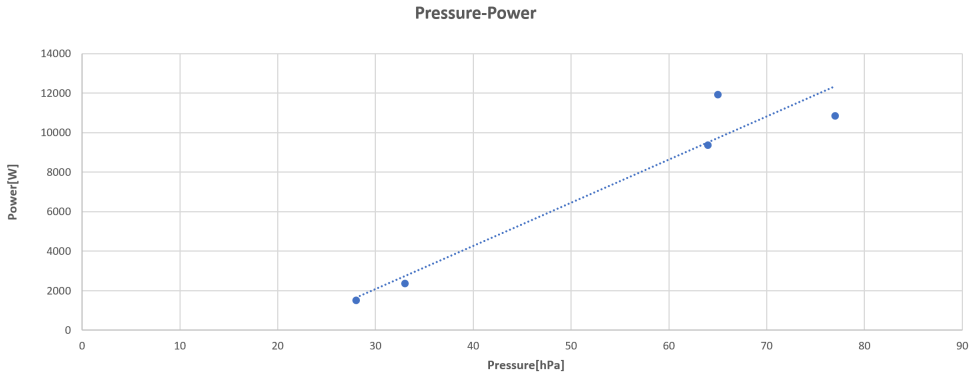

Figure 2.11: Relation between power and working pressure for cabin fans

The flow rate varies as a function of the in cabin air required, which from eq. 2.30 is first related to the number of passengers. On the other hand, the working pressure depends on the fan use.
Extraction fans address the air overboard: they work around 2000 Pa.
Blowing fan work on board the vehicle (usually in the avionic compartment) hence the pressure is almost twofold the previous cited.
Cabin recirculation fans work in a range of 6000 Pa to 8000 Pa

A320- 180 passengers
For the specific case study of Airbus A320

- 2 fans in cabin (A320 Air Cond Flight Operating Manual 1.21.10 P2 [8]);
- 1 fan for each cargo compartment (2 cargo c.) (Air Cond Flight Operating Manual 1.21.40 P2 [8]);
- 1 fan for each galley and lavatory (taking into account 2 galleys and 3 lavatories) (A320 Air Cond Flight Operating Manual 1.21.30 P9 [8] and Aircraft Characteristics Airport and Maintenance Planning [13]) ;
- 2 fans for avionic bay (2 bays): 1 blower fan and 1 extraction fan (Air Cond Flight Operating Manual 1.30 P3 [8]);
- 1 Ground cooling unit, to ensure an adequate temperature when the outside one is too high (Air Cond Flight Operating Manual 1.21.30 P8 [8]) ;
- 1 venturi tube for the battery (Air Cond Flight Operating Manual 1.21.30 P9 [8]).

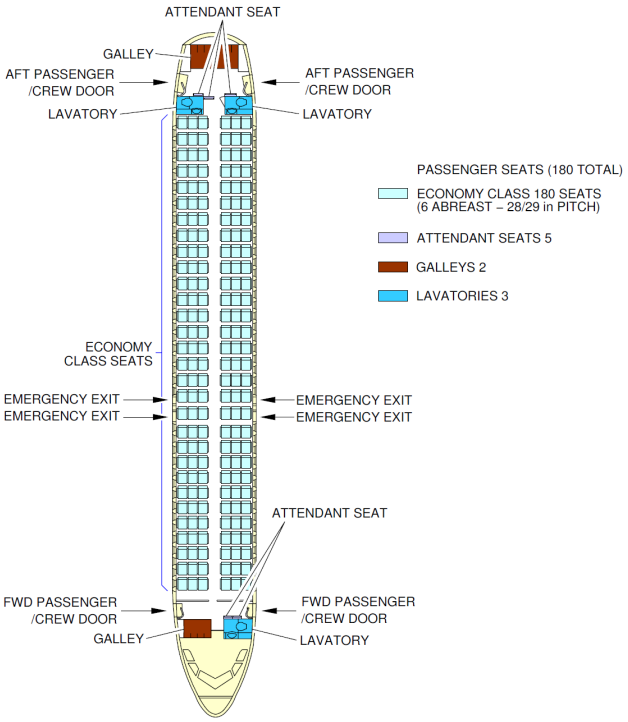

Figure 2.12: A320 configuration [13]

With formula 2.31 and 2.30, inlet air is 849 l/s a preliminary estimation of the power required by the ECS is contained in this table [4].

. .

[4]The flow rate values refers to the Safran products available on the website [12]. While the power are estimated through eq.2.33

[5]Fan number is assumed from the configuration reported in [13] and [8]

	l/s	FAN NUMBER [5]	l/s	POWER[W]	
INLET AIR	849				
Cabin	450	2	900	4567	
Galley/Lav	150	2	300	750	
Cargo	150	2	300	750	
Avionic	116	2	232	596	
	509	2		8144	
				14809	TOT
		10	832	8740	AVIONIC
		FAN N.(tot)	AIR OUT	6069.230769	TOT-AVIONIC

Table 2.2: ECS power required for an A320

A350-350 passengers Adopting formula 2.31 and 2.30, inlet air is 1651 l/s. Following the same procedure for the A350 with configuration in figure [13]

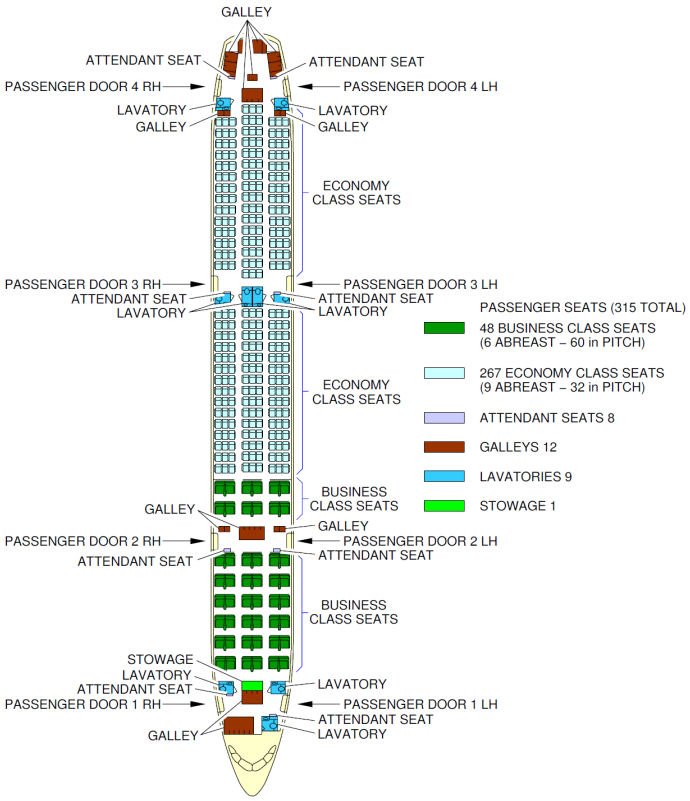

Figure 2.13: A350 configuration [13]

[5]Fan number is assumed from the configuration reported in [13] and [8]

	l/s	FAN NUMBER [6]	l/s	POWER[W]	
INLET AIR	1651				
Cabin	450	5	2250	12375	
	325	1	325	1516	
Galley/Lav	371	3	1113	8254	
Cargo	150	3	450	750	
Avionic	116	2		375	
	509	2		596	
				32011	TOT
		16	1563	8144	AVIONIC
		FAN N.(tot)	AIR OUT	23867	TOT-AVIONIC

Table 2.3: ECS power required for an A350

A380-750 passengers

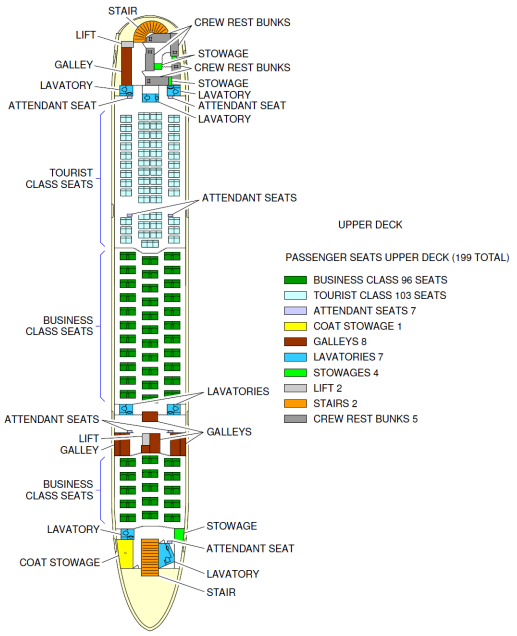

Figure 2.14: A380 standard configuration (upper deck)[13]

[6]Fan number is assumed from the configuration reported in [13] and assuming that for an average of 115 people, one fan is necessary for lavatory and galleys compartment.

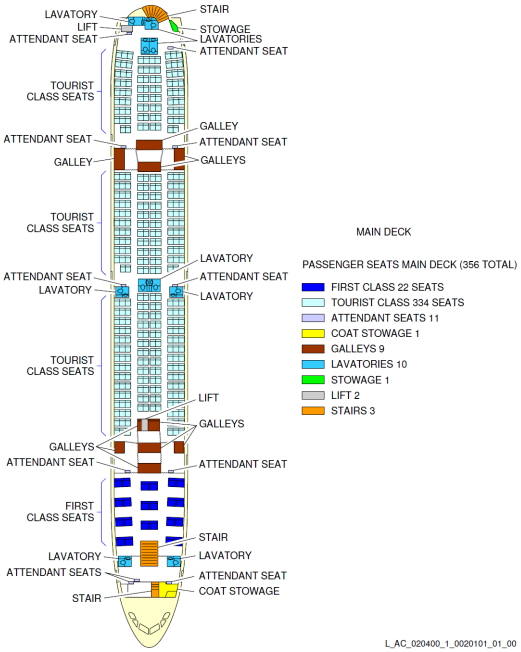

Figure 2.15: A380 standard configuration (main deck) [13]

	l/s	FAN NUMBER [6]	l/s	POWER[W]	
INLET AIR	3775				
Cabin	450	9	4050	20556	
Galley/Lav	300	6	1800	15600	
Cargo	150	8	1200	3000	
Avionic	116	2	232	596	
	509	2		8144	
				47896.57	TOT
		27	3232	8740.571	AVIONIC
		FAN N.(tot)	AIR OUT	39156	TOT-AVIONIC

Table 2.4: ECS power required for an A380

Conclusion on ECS fan

- The fans required by the avionic system are 2 for each bay. On average, an aircraft is equipped with 2 avionic bay. Moreover, as the avionic devices do not significantly

[6] Fan number is assumed from the configuration reported in [13] and assuming that for an average of 115 people, one fan is necessary for lavatory and galleys compartment.

change between modern aircraft a general result is that around *8 kW* are required for the avionic ventilation.

- An interesting relation stands between the number of passengers and the numbers of fans. Assuming a standard of 4 fans for avionic, the remaining can be related to the passengers number. It can be found that *1 fan is need for 30/32 passengers.*
- The number of galleys/lavatory fans is *1 fan for 115 passengers.*
- During cruise and landing, galleys and lavatories are not active along with their fans. Hence, the power required by the ECS decreases with respect to the one required in cruise. The decrement is significantly higher for larger aircraft.
  The following table contains the ratio between the required ECS power during take-off (and landing) and cruise condition, where all utilities are active.

Model	N.Passengers	Power ratio
A320	180	0.94
A350	350	0.74
A380	750	0.67

Table 2.5: Comparison between different mission phases

- Even if the fan number can be fixed as 1 for 30 passengers, the power does not increase only with the passenger number, because it also depends on the power required by single fan. Moreover with the technological innovation, it can be assumed that the components will be more efficient, thanks to the speed control of fans. Table 2.6 contains a comparison between the increment of passenger number (with respect to an A320), and the relative increment of the power.
  The ratio between the power of the vehicle and the one of an A320, does not coincide with the ratio between the passenger numbers.

	A350	A380
$\frac{N.pass}{N.pass_{A320}}$	1.99	4.16
$\frac{Power}{Power_{A320}}$	3.49	5.8
$\frac{Power}{Passenger}$	1.79	1.40

Table 2.6: Trend among passengers number and power required.

N passenger	Power required[W]
180	6069.231
350	23867.32
750	39156

Table 2.7: Passenger number and power (estimated values).

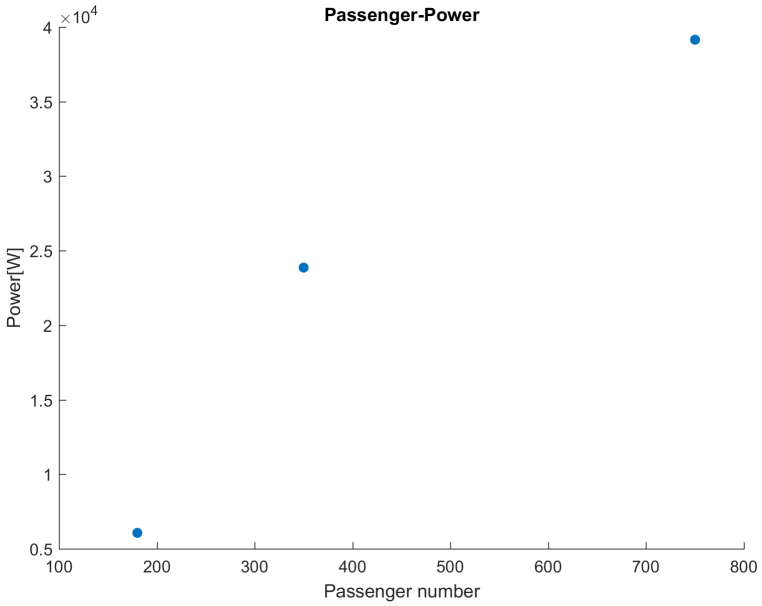

Figure 2.16: A320, A3850 A380 estimated values

Finally, for a preliminary design, a first degree polynomial can be adopted, in order to relate the passenger number with the Power required by ECS fans.

$$\underbrace{ECS_{power}}_{W} = 54.49 * n_{passenger} - 221 + \underbrace{8000}_{W} \tag{2.35}$$

This equations expresses that the power for the ECS fans is function of number of passenger but, also, a constant values of 8000 W for the avionic ventilation need to be added.

Chapter 3

Engine-subsytem integration

Aerospace industry is moving towards innovative aircraft configurations, different solution in any field, to reduce fuel consumption, emissions and costs. In this contest the more electric architecture has been proposed as an opportunity for aircraft design changes. As previously cited, most works have focused their attention towards the new technologies to adopt. Furthermore, in literature, many works are related to the benefits in terms of costs, which a MEA could bring. However, of high interest is the integration between subsystems and engine: indeed secondary power utilities have an impact on engine performances. Clearly, the change in the loads introduces consequent differences on propulsive system, especially for two reasons.

The first is that a MEA/AEA architecture requires distinct distribution systems forms (e.g. replacing hydraulic actuators with electric ones) which could mean a weight or a drag increment (e.g. external compressor).

The second very interesting reason, which is the topic of this thesis, is related both to the increment of electric power an the removal of bleed system. These two fundamental issues need to be studied along with each other in order to fully understand which are the benefits and the drawbacks of new architectures. The aim of this chapter is to describe how power off takes and bleed air off takes can affect the engine.

3.1 General overview

Shaft power and bleed air off takes have detrimental effects on engine performances, in terms of thrust and specific fuel consumption. The SP (seconday power) extraction brings an increase of 1-4 % in fuel consumption [33]. Even if studies on this field started around 1970's, this is a really actual topic because there is not a definitive solution to obtain optimized future aircraft. About engine-subsystems integration, various possibilities can be found because there is a difference between designing an optimum single component and an optimum integrated upper level system. The overall goal should be to understand which is the most suitable compromise between on boards systems and thrust production.

According to the last decades trends, it is likely that, in future, aircraft will face an higher demand in terms of secondary power to satisfy passengers comfort requirements.

The effect of electrical power offtake can have a significant repercussion on the engine. The next figure shows two operational scenarios that can have distintc effects on the engine operations. Consider the first scenario shown, which is typical during the taxi, hold and descent phases of flight. During these phases, the aircraft does not require large amounts of thrust and hence the power setting of the engine is low. However, the on-board systems still require electrical power. This is indicated proportionately in the next figure. It is clear that the effect of the electrically powered systems during this phase is significant since they require a high proportion of engine power during that phase. Hence the electrically powered systems can have a significant impact on the control of the engine during that phase segment.

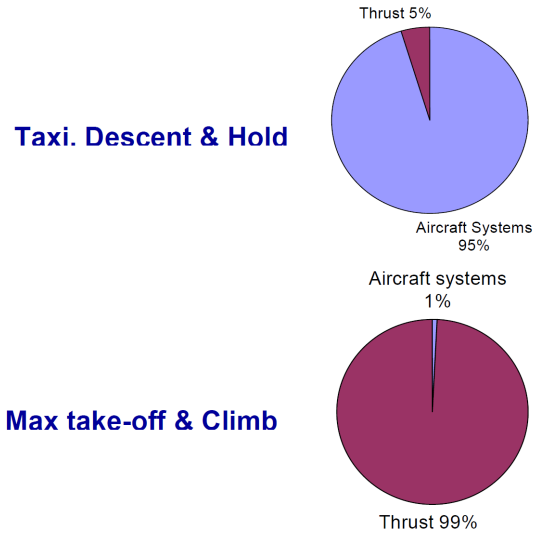

Figure 3.1: Thrust to power percentage for different mission phases [27]

In order to understand the following studies, it is necessary to describe how power is extracted from the engine.

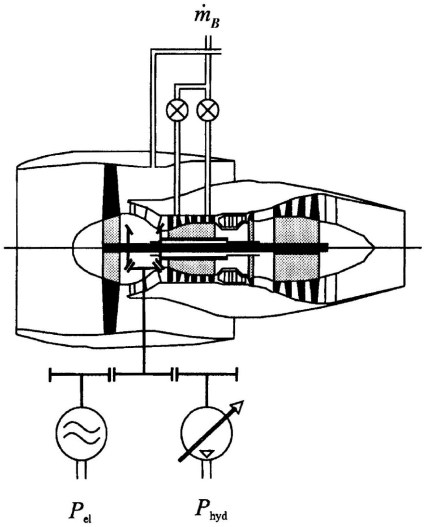

Figure 3.2: Secondary power and bleed air extraction [35]

In figure 3.2 is presented the basic principle of the off-takes within the engine

- Power is extracted from the high pressure or low pressure shaft.
- An internal gearbox is needed to couple the engine shaft to the radial driveshaft: this is located between the low and high pressure compressors [35]. On two shafts engine, power is extracted from the internal gearbox from the high pressure shaft. In some cases, power can be taken from both shafts: this is actually a choice that influences the acessory gearbox location.
- The radial driveshafts drive and external Accessory Geargbox (AGB): they expands through the entire engine from the front air duct to the rear one. They runs at high speed because they are designed as small as possible, in order to limit the flow separation [35].
- The Accessory Gearbox consists of a curve casing, where several accessories are mounted on [35]. The drive in the casing is provided by a spur gears, while idle gears are adopted between them.
- Accessories are the generators e.g. Variable Speed Constant Frequency (VSCF) generators, Integrated Drive Genertors (IDG), hydraulic pumps, and high or low pressure compressor [35].
- Bleed air is extracted from the the compressor: the stages at which air is bled can change from one engine to another.

3.1.1 Shaft Power and Bleed Air off-takes: how they affect the engine

A closer look to the thermodynamic aspect of the engine operating principle reveals some relevant issues about the shaft power off-takes. Indeed, when power is extracted from the

shaft, it inevitably reduces the spool rotational speed; moreover the mass flow will drop and, consequently the thrust of the overall engine. On the other hand, the majority of commercial aircraft are equipped with FADEC (Full Authority Digital Engine Control) whose function is to regulate the shaft speed.

In in order to achieve that

- fuel flow is increased;
- Turbine Entry Temperature rises.

Clearly, the previous effects generates very high pressure throughout the turbine stages, bringing the engine to the dangerous situation of the surge; then the pressure ratio increases as well as the turbine and compressor speed. By this way, the FADEC can restore the equilibrium near the trhust level required [23].

Figure 3.3 highlights that, when power is extracted, turbine is more stressed because it rotates at lower speed but need to deliver more work; the only way to obtain this situation is by increasing the TET.

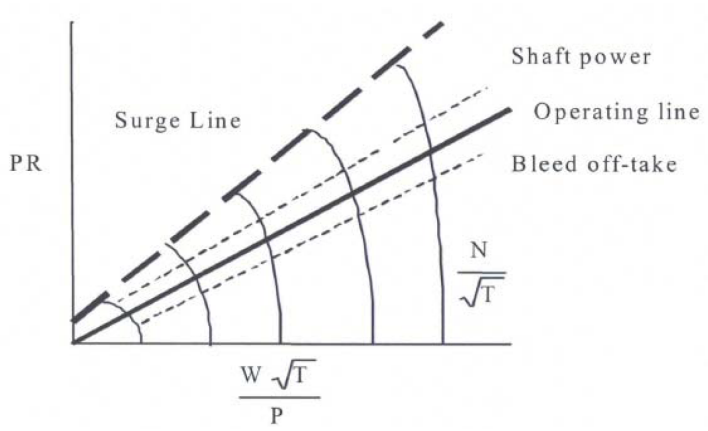

Figure 3.3: Secondary power and bleed air extraction [16]

Bleeding practice, on the other hand, increase the stability margin.

Usually, shaft power is extracted from the High Pressure shaft: when the speed is reduced , the mass flow passing trough the turbine and compressor decreases. But this also produces a decrement of the mass flow trough the LP compressor and turbine.

If shaft power is extracted from the LP shaft, the main consequence is again the speed reduction; along with that, the fan undergoes a significant decrease of its speed. The HP shaft is not subjected to speed drop: it, otherwise increases the rpm and the mass flow trough the LP turbine and compressor. The drawback lays on the fact that, decreasing rotational speed (especially of the LP shaft which runs slower) means a considerable decrease of single component efficiencies [23].

To maintain engine stability the designer could downmatch the compressor, thus increasing the turbine area or he could rise the surge margin [23]; the last solution means more compressor stages.

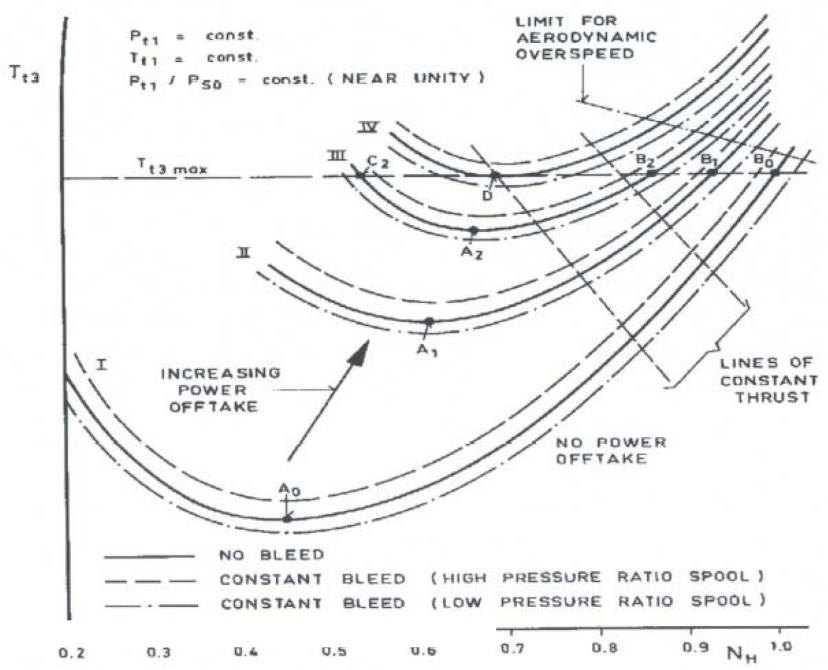

Figure 3.4: TET against power extraction [16]

In figure 3.4 TET is depicted as a function of

- Ratio between power off takes and total power on the engine core
- Bleed air

The diagram provides an interesting map of the TET behaviour: it increases along with the ratio between shaft power and core power; also the bleed air off takes have an influence on TET. Taking into account an extraction from the HP spool (as it usually happens) the TET slightly rises if compared to the bleedless configuration.

According to [23] and [35] the secondary power extraction is a very current issue, especially for low thrust ratings engines: for a fixed power off take, the detrimental effects grow while the power produced by the core decreases. Low thrust ratings mean an higher specific fuel consumption, because the ratio P/T is higher than the one at low thrust rating engine. This will be explained in the following section.

3.1.2 SFC equations

The influence of subsystems architectures on the performance of the propulsion system is addressed to the increment of fuel flow rate that the subsystems require.

It can be described with the following equations [18]

$$\dot{m}_{fuel} = T_{req} * SFC \tag{3.1}$$

$$\Delta\dot{m}_{fuel} = T_{req} * \Delta SFC + \Delta T_{req} * SFC \tag{3.2}$$

$$\Delta\dot{m}_{fuel} = T_{req} * (\Delta SFC_{shaft} + \Delta SFC_{bleed}) + (\Delta D_0 + \Delta D_i) * SFC \tag{3.3}$$

Where

- T_{req} is the required thrust;
- SFC represent the specific fuel consumption in a fixed flight condition;
- ΔSFC_{shaft} is the increment in the SFC due to the Shaft Power Off Takes:
- ΔSFC_{bleed} is the increment in SFC due to the Bleed air extraction;
- ΔD_0 is the increments at zero lift drag;
- ΔD_i is the induced drag increment.

Equation 3.3 underlines that secondary power systems affect the engine performances both directly and indirectly: to take into account the detrimental direct effects it is possible to calculates the power required by the shaft power extraction and the bleed air extraction. The following step is to find the relation

$$\Delta SFC_{shaft} = f(P_{shaft}) \tag{3.4}$$

$$\Delta SFC_{bleed} = f(\dot{m}_{bleed}) \tag{3.5}$$

This is actually the aim of the thesis.

On the other hand some subsystems also affect the engine (especially the fuel flow rate) because they add drag to the aircraft. More in detail

1. ΔD_0 takes into accounts the effect of external additions or modifications to the vehicle frame;
2. ΔD_i represents the lift-independent component: accounts for the increased lift required to offset the new mass and the fuel increment.

$$\Delta\dot{m}_{fuel} = \Delta\dot{m}_{shaft} + \Delta\dot{m}_{bleeed} + \Delta\dot{m}_{drag} + \Delta\dot{m}_{weight} \tag{3.6}$$

These two last increments present in equation (3.6) are not considered during the thesis, but they could be interesting field for future researches.

The real challenge in aviation is the introduction of more efficient systems, which could be the more electric ones. The replacement of hydraulic or pneumatic systems with electrical ones brings some advantages. But the real benefits and drawbacks of these configurations, when applied to an engine, are not fully investigated. In order to increase the knowledge in this field, during the thesis different SFC implementation models have been applied to the same study case, and then compared with each others.

3.2 SFC computation: model 1

The SFC model presented by Scholz [35] aims to compute the fuel consumption due to the power off-takes. It gives comparisons between some real engine data and then it deals with the simulations given by the TURBOMATCH engine simulation model, based on calibrated world engine data [35]. Finally, it provides generic equation for the SFC. The main results is represented by the k_p factor, which relates the fuel consumption increment due to the power off takes, to the Power/Thrust ratio. It does not take into account the bleed air off-takes.

3.2.1 SFC clean engine

The SFC is often provided by the constructor in take-off and cruise conditions. This is a variable parameter which increase with Mach. However, equation 3.7, [37], [25]

$$SFC = \frac{0.697\sqrt{\frac{T(h)}{t_0}\left(\phi - \vartheta - \chi/\eta_{compr}\right)}}{\sqrt{5\eta_{nozzle}(1+\eta_{fan}\eta_{turb}BPR) * \left(G + 0.2M^2 BPR\frac{\eta_{compr}}{\eta_{fan}\eta_{turb}}\right)} - M(1+BPR)} \tag{3.7}$$

Where

$$G = (\phi - \chi/\eta_{compr})\left(1 - \frac{1.01}{\eta_{gg}^{\gamma-1/\gamma}(\chi+\vartheta)\left(1 - \frac{\chi}{\phi\eta_{compr}\eta_{turb}}\right)}\right)$$

$$\theta = 1 + \frac{\gamma - 1}{2} M^2;$$

$$\phi = \frac{T_{TE}}{T(h)};$$

$$\chi = \vartheta \left(OAPR^{\frac{\gamma-1}{\gamma}} - 1 \right);$$

$$\eta_{gg} = 1 - \frac{0.7 M^2 (1 - \eta_{inlet})}{1 + 0.2 M^2}$$

Turbine Entry Temperature

$$T_{TE} = \frac{-8000 K kN}{T_{TO}} + 1520 K \tag{3.8}$$

$$OAPR = 2.66810^{-5} 1/kN T_{TO} + 3.517 BPR + 0.05566$$

$$\eta_{compr} = \frac{-2kN}{2kN + T_{TO}} - \frac{0.1171}{0.1171 + BPR} - M * 0.0541 + 0.9407$$

$$\eta_{turb} = \frac{-3.403kN}{3.403kN + T_{TO}} + 1.048 - M * 0.1553$$

$$\eta_{inlet} = 1 - (1.3 + 0.25 BPR) \frac{\Delta p}{p}$$

$$\eta_{fan} = \frac{-5.978kN}{5.978kN + T_{TO}} - M * 0.1479 - \frac{0.1335}{0.1335 + BPR} + 1.055$$

$$\eta_{nozzle} = \frac{-2.032kN}{2.032kN + T_{TO}} + 1.008 - M * 0.009868$$

- $T(h)$ [K] is the temperature at the altitude considered ;
- $T_0 = 288K$ is the temperature at sea level;
- M is the Mach number;
- BPR is the by pass ratio;
- η_{gg} gas generator efficiency;
- η_{compr} compressor efficiency;
- η_{turb} turbine efficiency;
- η_{inlet} inlet efficiency;
- η_{fan} fan efficiency;
- η_{nozzle} nozzle efficiency;

- $OAPR$ overall pressure ratio;
- $T_{TO}[N]$ is the take-off thrust of one engine;
- $\Delta p/p = 0.02$ is the inlet pressure loss;
- $\gamma = 1.4$ is the ratio of specific heats;

Formula 3.7 represents one of the various models to compute the SFC of a Clean engine, considering neither shaft power off-takes nor bleed air extraction, but this is still a really accurate algorithm to obtain the SFC.

Once the SFC has been computed, it is necessary to obtain the relation between the SFC due to the power off-takes and the SFC of the previously calculated SFC. Referring to this study, the fuel mass flow rate necessary to drive secondary power systems is

$$\underbrace{\dot{m}_{shaft}}_{kg/s} = \underbrace{SFC_{shaft}}_{kg/Ws} * \underbrace{P}_{W} \tag{3.9}$$

where the Power specific fuel consumption is the one required by the SPS (secondary Power Systems) and P represents the amount in power-off takes. On the other hand, the fuel flow of a jet engine $\dot{m}$ base on thrust produced is

$$\underbrace{\dot{m}}_{kg/s} = \underbrace{SFC}_{kg/Ns} * \underbrace{T}_{N} \tag{3.10}$$

Clearly the extraction of secondary power generates an increment on the SFC and on the fuel flow rate, which can be written as

$$\dot{m}_{shaft} = \Delta SFC * T \tag{3.11}$$

which, composed with 3.9 becomes

$$\Delta SFC * T = SFC_{shaft} * P \tag{3.12}$$

$$\frac{\Delta SFC}{SFC} * T = \frac{SFC_{shaft}}{SFC} * P \tag{3.13}$$

During the study it was observed that ΔSFC is proportional to P/T ratio: this means that the amount of shaft power off-takes influences in different ways the various engines. Clearly, the problem is to find the relation

$$\frac{\Delta SFC}{SFC} = f(\frac{P}{T}) \tag{3.14}$$

$$\frac{\Delta SFC}{SFC} = k_p \frac{P}{T} \tag{3.15}$$

where k_p is defined ad the shaft power factor

$$\underbrace{k_P}_{N/W} = \underbrace{\frac{SFC_{Shaft}}{SFC}}_{\frac{kg/WS}{kg/Ns}} \tag{3.16}$$

One the k_p factor is known, it will be able to compute the fuel consumption due to the shaft power off takes

$$\dot{m}_{shaft} = k_p * SFC * P \tag{3.17}$$

The work presented in [35], based on the previous assumptions, is then developed with simulations on the engine. The tool TURBOMATCH allows investigations on the effecs of power off-takes, taking into account several factors: the Turbine Entry Temperature, spool velocities, stall and surge margins. Indeed, the overall influence of the off-takes are quite complex to define and cannot be generalized.

Limits of this model

1. The first lack of Scholz analytical process is ascribed to the absence of Bleed air off-takes;
2. it relates the increment in SFC to the P/T ratio, whose relation is found to be linearly proportional. However, a most accurate thermodynamic analysis should be necessary in order to express real influence of the off-takes on TET.
3. It addresses to a cruise condition.

3.3 SFC computation: model 2

The main limit of Scholz investigation is that it does not contemplate the bleed air off-takes. For this reason, during the thesis, it was necessary to adopt another more accurate model which takes into account the the bleed air extraction.

The work presented in [23] contains a thermodynamic analysis whose aim is to relate the size of the offtakes to the core power through a set of equations. These equations contains the design parameters, known in the early stages of engine design. Their predictions are, then, compared to the outcomes found from an in-house tool, capable of simulating the engine behaviour. The analytical expressions have been validated against the numerical simulations conducted with Turbomatch tool by Cranfield University [30]. The output of the validation test has been that the equations derived are in good agreement with the numerical simulation. The comparison between experimental datas and analytical ones are beyond the scope of the thesis; for sake of clarity the validation is described in chapter V of [23].

The most relevant observation is that the main driving factor of the SFC increment is the ratio between the magnitude of those penalties and the core power. Moreover, as the analytical expressions deeply investigate both engine behaviour and its design, the derived equations can be adopted even if the design parameters changes. Throughout the thesis, some of the equations (which will be expressed in this section) have been adopted to our case study.

The basic principles on which the analysis is constructed, are described in subsection **Engine Fundamentals**.

3.3.1 Engine Fundamentals

The total engine efficiency is given by equation 3.18 as the product of core, transmission and propulsive efficiencies.

$$\eta_0 = \eta_{core} * \eta_{pr}\eta_{tr} \tag{3.18}$$

To better understand the work, the previous cited efficiencies are described in figure 3.5

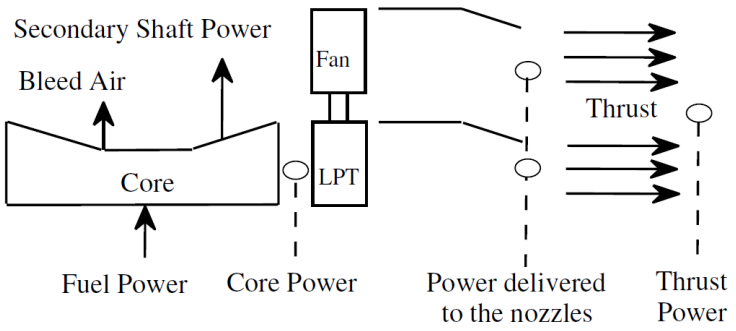

Figure 3.5: Schematic representation of the engine components and the fuel flow [23]

This figure shows the power conversions which take place in a turbofan engine. The fuel flow enters the core and it is burned in the the combustion chamber. The first power conversion is, then, the translation of fuel power to hot-gas thermal power.

Meanwhile, a lower amount of power is extracted from the core in the form of bleed air and shaft power off-takes. This means that not all the fuel power is available at the exit of the engine core.

- The **core efficiency** represents the ratio between the core power at the exit of it and the power provided by the fuel. It depends on
  - Engine overall pressure ratio
  - Turbine Entry Temperature
  - Isentropic Efficiencies

  - Pressure losses of single components.

- The **transmission efficiency** can be expressed by [23]

$$\eta_{tr} = \frac{1 + BPR}{1 + BPR/(\eta_{fan} * \eta_{lpt})} \tag{3.19}$$

  Once the hot gas power exits the core, it goes trough the LP turbine, fan and bypass duct, and then it is transmitted to bypass nozzle. So this efficiency represents the fraction of power delivered trough the nozzle and the power produced by the core. The transmission efficiency depends on

  - bypass ratio
  - LP turbine efficiency
  - fan efficiency

- **Propulsive efficiency** is related to the power which reaches the nozzle and is converted to thrust, thanks to the expansion of the air into the external ambient. It can be expressed as

$$\eta_{pr} = \frac{1}{1 + ST/(2V_0)} \tag{3.20}$$

  [29] representing the fraction between the thrust power produced against the power that the nozzle delivers.

In the following figures the behaviour of the efficiencies are shown.

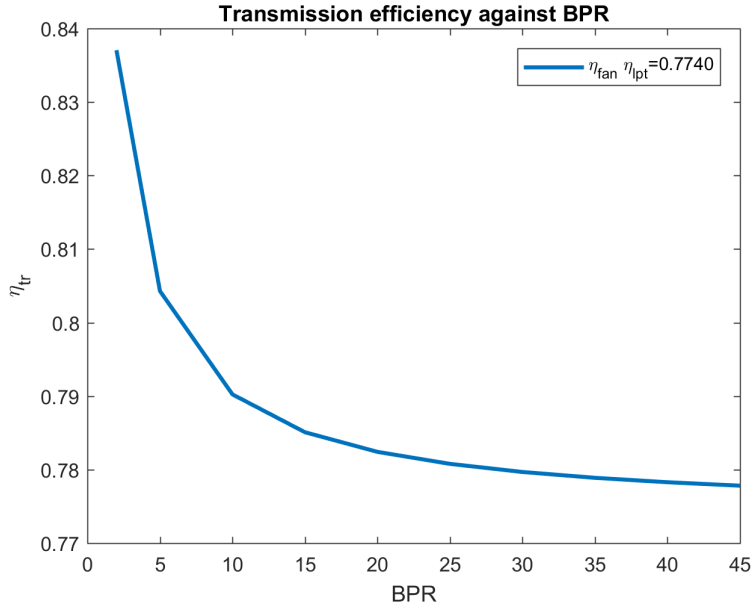

Figure 3.6: Transmission efficiency against BPR for fixed $\eta_{fan}\eta_{lpt}$ product

The graph underlines that, for a given product of $\eta_{fan}\eta_{lpt}$ the transmission efficiency decrease with increasing BPR, tending to $\eta_{fan}\eta_{lpt}$ value.

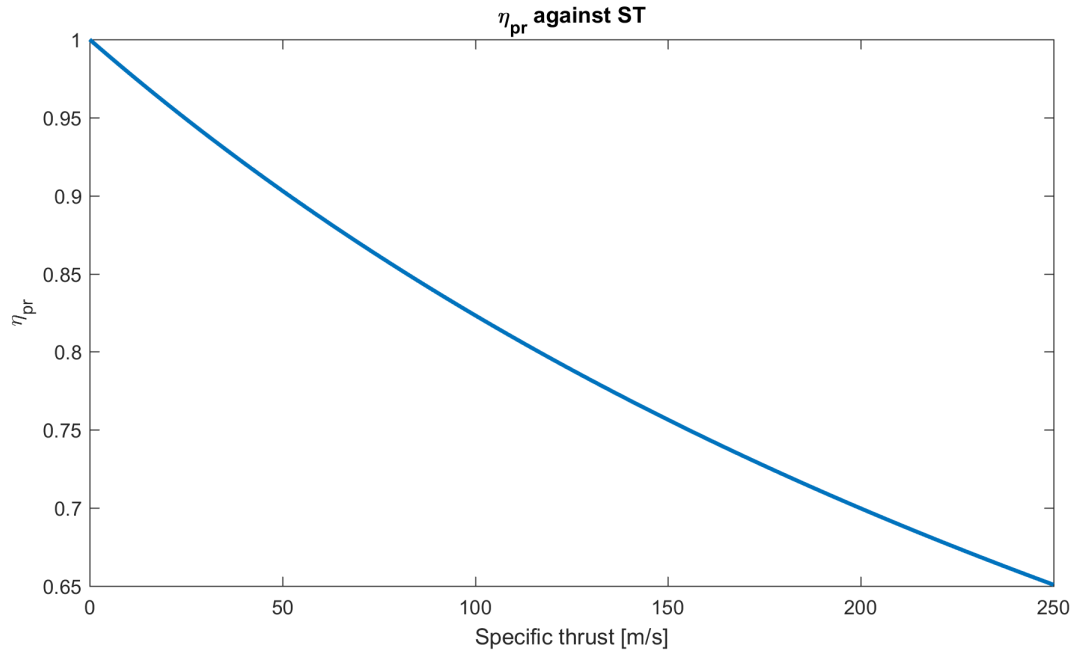

Figure 3.7: Propulsive efficiency against specific thrust

Propulsive efficiency falls when Specific Thrust increases, while tending to 1 when ST moves to 0.

The definition of these three efficiencies are of great interest to comprehend the work: indeed, the assessment on the effects of secondary power systems extraction derives from the variations of the single efficiencies.

It is necessary to underline the fixed design parameters which remain constant throughout the analysis: it, indeed, refers to the design point

$$CONSTANT = \begin{cases} TET \\ OAPR \\ \eta \end{cases}$$

Another important assumption is that *no installation penalties are considered.*

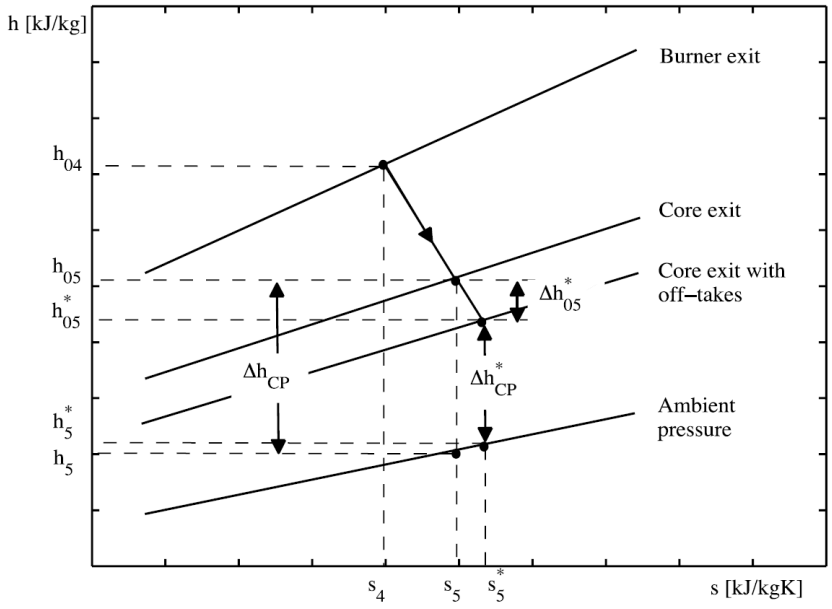

Figure 3.8: Enthalpy-entropy diagram [23]

Figure 3.8 represent an Enthalpy-entropy diagram at the engine core exit before and after the extraction of power off-takes. The required power by the systems let the pressure ratio to increase, thus, the pressure at the exit of the core will decrease of a ΔT and hence, the core will undertake a drop in enthalpy (Δh_{cp}). So the enthalpy finally produced by the core after the extraction of power off takes is described as

$$\Delta h^*_{cp} = \Delta h_{cp} - \Delta h^*_{05} - (h^*_5 - h_5) \tag{3.21}$$

whereΔh^*_{05} represents the enthalpy drop due to the power off-takes. Then, the power available once the power are extracted is found as

$$P^*_{cp} = P_{cp} - P_{shaft} \tag{3.22}$$

$$P^*_{cp} = P_{cp} - m_c * \Delta h^*_{05} \tag{3.23}$$

where m_c is the core flow.

With some more algebra, the power drop is expressed as a drop of the core efficiency

$$\frac{\eta^*_{core}}{\eta_{core}} = 1 - \frac{P_{shaft}}{P_{cp}} \tag{3.24}$$

and the power produced by the core is obtained as

$$P_{cp} = \frac{\overbrace{Thrust}^{kN}\overbrace{V_{flight}}^{m/s}}{\eta_{tr} * \eta_{pr}} \tag{3.25}$$

The decrease in core efficiency due to the shaft power off takes, is then computed as

$$\frac{\eta^*_{core}}{\eta_{core}} = 1 - \frac{P_{shaft}\eta_{tr}\eta_{pr}}{TV_0} \tag{3.26}$$

$$= 1 - \frac{2 * P_{shaft} * (BPR + 1)}{T * [BPR/(\eta_{fan}\eta_{lpt}) + 1] * (2V_0 + ST)} \tag{3.27}$$

In order to find the detrimental effects caused by the bleed air, the assumption adopted in [23] is that the extraction happens in the High Pressure compressor where the enthalpy increment is Δh_b.

Beginning from the power balance in the high pressure spool

$$\Delta h_{hpt^*} = \Delta h_{hpc} + \frac{\dot{m}_b}{\dot{m}_c - \dot{m}_b} * \Delta_{hb} = \Delta h_{hpc} + \frac{\beta}{1-\beta}\Delta_{hb} \tag{3.28}$$

where $\beta = \frac{\dot{m}_b}{\dot{m}_{core}}$ is the ratio between the bleed air and the core mass flow.
With some algebra, the fall of the enthalpy becomes

$$\Delta h^*_{cp} = \Delta h_{cp} - \frac{\beta}{1-\beta}\Delta_{hb} \tag{3.29}$$

Finally, the power after the extraction of the bleed air becomes

$$P^* = (1-\beta)P_{cp} - \dot{m}_{bleed}\Delta_{hb} \tag{3.30}$$

$$\beta = \frac{\dot{m}_{bleed}}{\dot{m}_{core}} = \frac{\dot{m}_{bleed} * ST * (1 + BPR)}{T} \tag{3.31}$$

The decrease of core efficiency due to the bleed off takes is

$$\frac{\eta^*_{core}}{\eta_{core}} = 1 - \frac{2\dot{m}_{bleed}\Delta_{hb}(1 + BPR)}{(1-\beta)T[BPR/(\eta_{fan}\eta_{lpt}) + 1](2 * V_0 + ST)} \tag{3.32}$$

While the overall efficiency of a clean engine is

$$\eta_0 = \eta_{core}\eta_{tr}\eta_{pr} \tag{3.33}$$

the efficiency after the extraction is defined with η^*_0.

The aim is to find the decrement of the efficiency which means the increment of the SFC. The analysis is done maintaining the BPR constant; this means that, from eq. 3.19,

the transmission efficiency remains constant, while the total engine mass flow will rise in order to keep the thrust constant. On the other hand, the Specific Thrust will fall.

The decrease on the overall efficiency is expressed by

$$\frac{\eta_0^*}{\eta_0} = -\frac{V_0}{ST} + \frac{V_0}{ST} * \sqrt{1 + \frac{2ST}{V_0}\frac{\eta_{core}^*}{\eta_{core}}\left(1 + \frac{ST}{2V_0}\right)} \tag{3.34}$$

Finally, the SFC increment is calculated as

$$\frac{\Delta SFC}{SFC}\% = \left(\frac{\eta_0^{*\,-1}}{\eta_0} - 1\right) * 100 \tag{3.35}$$

From a thermodynamic point of view, the equation derived in [23] are useful to draw some conclusions with respect to the effects of secondary power over the engine

1. From eq. 3.18 the core efficiency is reduced by the power off takes because they they are not useful to produce thrust;
2. equation 3.32 underlines that the core efficiency is not only function of the off-takes; indeed, the real dependency is between the core efficiency and the ratio between the power off takes and the power produced by the core. For a fixed amount of power extracted, the efficiency decreases as the power produced by the core decreases.
3. the core power demand is related to the need of a certain thrust.

3.4 SFC computation: engine deck 1

The other available method to compute the increment in SFC due to the shaft power off-takes is to use an engine deck which, as it is defined, does not deal with derived equations (as done with model 2). On the other hand, an engine deck is a complex simulation software based on one single specifications. It computes thermodynamic analysis knowing the real entropy, enthalpy diagrams, the temperatures involved, the pressure ratio, the inlet and exhaust pressures. Clearly, also the geometric dimensions, by pass ratio, overall pressure ratio.

Once the engine deck is available, the engine behaviour is almost completely known and some variables can be changed, depending on the required analysis.

The first engine deck has been developed within the HORIZON 2020 AGILE project [10] and it is based on a smaller engine than the CFM 56. The following characteristics are available

- $T = 12\,\text{kN}$, thrust at a single mission segment;
- $SFC_{c.e} = 14.1223\,\text{g/kN} * \text{s}$, SFC on the clean engine
- $h = 11\,000\,\text{m}$, flight altitude
- $M = 0.78$, Mach considered
- $P = 6\,\text{bar}$, air bleed pressure

Starting from these values, 42 different combinations of bleed air and power off takes are created.

- Bleed air changes from $0 < [kg/s] < 0.8$ with 0.1 kg/s steps
- Power Off-takes varies $0 < [kW] < 100$ with 20 kW steps

Within the outcomes are

1. Specific fuel consumption $[g/kNs]$
2. Fuel flow $[kg/s]$.

Description	
Altitude	m
Mach Number	
Overboard Bleed	kg/s
Power Offtake	kW
Net Thrust	kN
Sp. Fuel Consumption	g/(kN*s)
Fuel Flow	kg/s
Air Bleed pressure	kN

Table 3.1: Input data

3.5 SFC computation: engine deck 2

The engine deck provided by the *Deutsches Zentrum für Luft und Raumfahrt e.V. (DLR)*, Institute of Propulsion Technology, has been realized trough an in-house performance tool named *GTlab*. The engine deck is referred to a V2500 like engine, which powers an A320.

Shaft power	[W]
Bleed air	[kg/s]
Altitude	[m]
Mach	
Cruise Thrust	[N]
Fuel flow	[kg/s]
Δ fuel flow	[kg/s]
SFC	[g/kNs]
ΔSFC	
$\Delta SFC/SFC(\%)$	
TET	[K]
BPR	
OAPR	

Table 3.2: DLR outputs scheme

The inputs of this computation (along with the real thermodynamic values) are

- $T = 22\,\text{kN}$, thrust at a single mission segment;
- $SFC_{c.e} = 16.445\,\text{g/kN} * \text{s}$, SFC of the clean engine
- $h = 10\,000\,\text{m}$, flight altitude
- $M = 0.8$, Mach considered.
- $BPR = 5.24$, Fan bypass ratio

The output provided are

1. Specific fuel consumption $[g/kNs]$
2. Fuel flow $[kg/s]$.

Chapter 4

Case study

The outcomes of the developed study are contained in this chapter. Part I represents the main Top Level Requirements (TLRs) of the reference vehicle and the system design stage conducted for the vehicle. The four architectures are, then, described. Finally, the values obtained for *shaft power off-takes* and *bleed air off-takes* are reported.
Part II, on the other hand, aims to describe the effects that each architecture brings to the Specific Fuel Consumption, for what concerns the shaft power and bleed air extraction.

Part I

Shaft power and bleed air off-takes: outcomes

4.1 Reference Vehicle

The Reference vehicle is the Airbus A320-200. The top level requirements [8], [26] are reported here.

Range[km]	4800
Passenger number	180
MTOW [kg]	73500
Landing weight [kg]	61000
Lenght [m]	37.57
Height [m]	12.17
wing area $[m^2]$	122.6
wing span [m]	34.1
V cruise $[m/s]$	233
Mach cruise	0.8
cruise altitude [m]	11000
T.O. distance [m]	1960
Landing distance[m]	1650
Propulsion	CFM 56-B/V2500

Table 4.1: Input data

The mission profile adopted *for all four architecture* is depicted in fig. 4.2

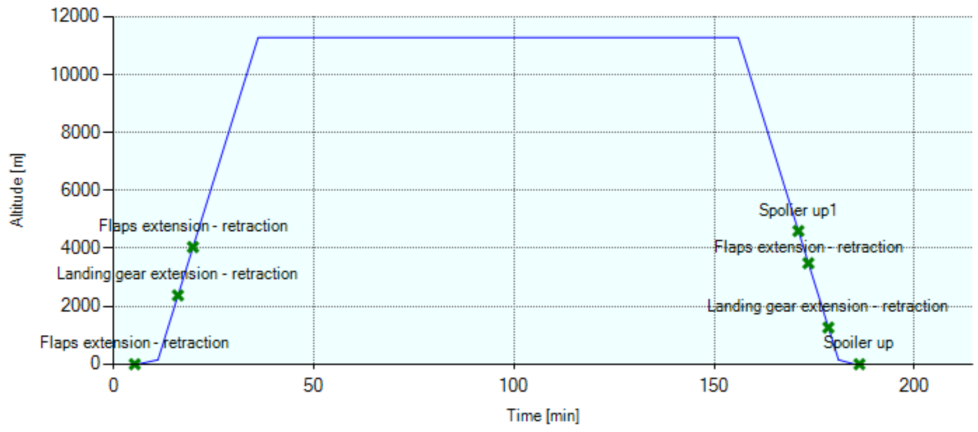

Figure 4.1: Mission profile adopted

	Min	h start m	h end m	Speed m/s	Climb rate m/s	SFC lb/lb/h
Taxi	5	0	0	2.7778	0	0.4
T.O 1	1	0	0	79.1667	0	0.3404
Flaps ext.	20	-	-	-	-	-
T.O. 2	1	0	152.4	0	0.508	0.3404
Climb	45	152.4	11277.6	0	4.1204	0.3404
LNDG retr.	20	-	-	-	-	-
Flaps retr.	35	-	-	-	-	-
Cruise	120	11277.6	11277.6	233.3333	0	0.5454
Desc.	35	11277.6	152.4	0	-5.2977	0.5454
Spolier up1	60	-	-	-	-	-
LNDG ext.	90	-	-	-	-	-
Flaps ext.	70	-	-	-	-	-
LND 1.	4	152.4	0	-0.635	-0.635	0.545
LND	5	0	0	77.7778	0	0.545
Spoiler up	25	-	-	-	-	-
Taxi	5	0	0	2.7778	0	0.4

Table 4.2: Mission Profile specifications

The complete mission phases are expressed in following table.

Taxi out	Main Phase
Take off (run)	Main Phase
Flaps extension	Sub phase
Take off (manoeuvre)	Main Phase
Climb	Main Phase
Landing gear retraction	Sub phase
Flaps retraction	Sub phase
Subsonic cruise	Main Phase
Descent	Main Phase
Spolier up1	Sub phase
Landing gear extension	Sub phase
Flaps extension	Sub phase
Landing (manoeuvre)	Main Phase
Landing (run)	Main Phase
Spoiler up	Sub phase
Taxi in	Main Phase

Table 4.3: Segment phases

4.2 Systems

The on board systems are designed with the tool Astrid. This stage ends with the power budget for every system, which describes the active devices during a single flight segment.

The mission profile and the definition of the active components during each segment is maintained constant for all four architectures. The difference is on the distribution power chosen between them.

4.2.1 Avionic system

The avionic system corresponds to the one mounted on typical commercial aircraft [8], [26]. It consists of the *Navigation*, *Flight Control*, *Communication and Audio*, *Identification and Surveillance* and *Flight Management* functions.

Then, the devices which accomplish those functions are chosen within a database provided by Astrid. For each component the following characteristic are taken into account

- Function
- Weight
- Volume
- Absorbed power
- Installation constraints, design features
- Number of equipment, number of redundancy.

	[kW]
Taxi out	4.756
Take off(run)	4.678
Flaps extension	4.656
Take off (manoeuvre)	4.1365
Climb	5.0675
Landing gear retraction	4.836
Flaps retraction	4.8425
Subsonic Cruise	4.844
Descent	4.756
Flaps extension	4.756
Landing gear extension	4.756
Landing(manoeuvre)	4.756
Landing (run)	4.756
Spoiler up	4.756
Taxi in	4.756

Table 4.4: Avionic System power budget

4.2.2 Flight Control System

Flight control system design is achieved by different steps.

- definition of the surfaces mounted on the vehicle:
- surfaces sizing: surface area, mean chord, local wing chord at the point where the surface is positioned, maximum excursion angle, max flight speed, excursion time [26], reported in table 4.5.

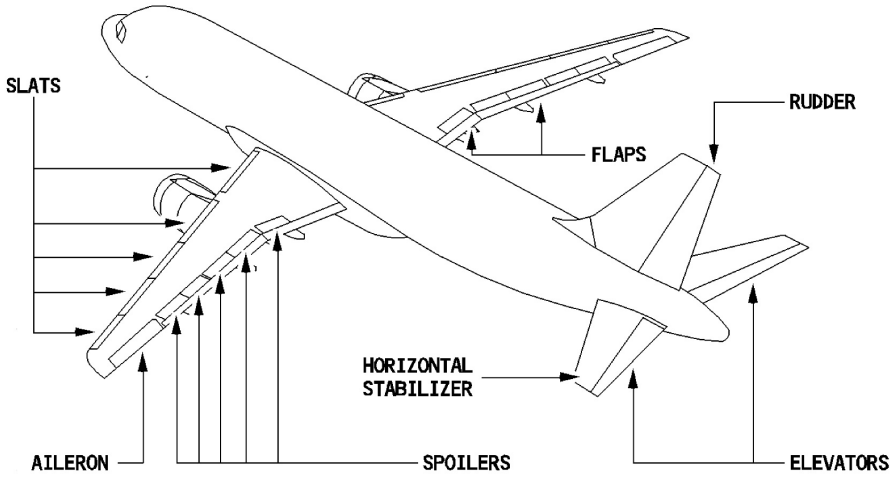

Figure 4.2: Reference flight control system [8]

Astrid provides the *stall moment* and the *hinge coefficient*.
For a primary surface or high lift device tool computes the max hinge moment; on the other hand, for the speedbrakes it computes the max aerodynamic moment. The actuators sizing phase requires

- choice between hydraulic and electric power supply;
- feed pressure: 3000 psi of 5000 psi (if hydraulic) or electric voltage;
- actuators number and redundancies;
- choice between rotative, crew drive system (drive unit or motor actuator) or linear cylinder.

Primary surfaces and spoilers are moved by cylinder linear actuators, while high lift devices are moved by rotary actuators. For innovative configurations, EHAs is adopted for primar surfaces and spoilers, while EMAs replace rotative actuators

The output are *Weight* and *Required power* for the mobile surface actuation.

Primary surfaces (ailerons, elevators and rudder) are always on function. Flaps and slats work almost impulsively during take off and descent. Spoilers are active during landing. In table 4.5 are reported the dimensions for each control surface.

	Area	Mean c.	Chord	Max δ	Max α	Vel	Time
	m^2	[m]	[m]	[deg]	[deg]	$[m/s]$	[s]
L.E Slat 1	1.3	-	0.4	27.0	7.0	138.9	0.5
L.E (2-4)	5.1	-	0.4	27.0	7.0	138.9	0.5
Hor. Stab.	5.2	2.4	2.0	13.5	4.0	138.9	0.5
Internal Flap	5.3	-	0.4	25.0	7.0	97.2	5.0
External Flap	5.3	-	0.4	25.0	7.0	97.2	5.0
Aileron	1.4	2.0	0.4	25.0	7.0	138.9	0.5
Elevator	5.2	2.4	0.8	30.0	7.0	138.9	0.5
Rudder	7.1	3.2	1.5	25.0	7.0	138.9	0.5
Spoiler	1.1	-	0.8	40.0	7.0	55.6	0.5

Table 4.5: Flight control surfaces characteristic

	Mom.	Hinge c.
	[Nm]	
L.E. Slat 1	5675.08	-
L.E. Slat 2	22700.31	-
Horizontal Stabilzer	40986.52	0.34
Int.Flap	11910.34	-
Ext. Flap	11299.55	-
Aileron	2100	0.33
Elevator	3800	0.08
Rudder	8200	0.06
Spoiler	2102.3	-

Table 4.6: Flight control surfaces outputs

The equipment are 1 rudder, 1 elevator (for wing), 1 aileron (for wing), 5 leading edge slats (for wing), 5 spoiler (for wing), 1 internal and 1 external flap (for wing).

	Cat.	Type	P [W]	P[psi]	Stall F [N]
L.E. slats 1	Hydr.	Rotary	2575.11	3000.00	71883.00
L.E. slats (2-4)	Hydr.	Rotary	10300.43	3000.00	71883.00
Hor.Stab	Hydr.	Linear motion	4659.00	3000.00	
Int. Flap	Hydr.	Rotary	500.28	3000.00	71883.00
Ext. Flap	Hydr.	Rotary	474.62	3000.00	71883.00
Aileron	Hydr.	Cyl. (lin.)	441.04	3000.00	5250.00
Elevator	Hydr.	Cyl. (lin.)	959.15	3000.00	5367.23
Rudder	Hydr.	Cyl. (lin.)	1148.11	3000.00	3644.44
Spoiler	Hydr.	Cyl. (lin.)	1413.69	3000.00	5938.70

Table 4.7: Flight control actuators specifications

4.2.3 Landing Gear System

The tricycle Landing Gear architecture consists of two central and one forward struts. The systems which need to be designed are

- Extraction/retraction
- Steering
- Braking.

The extraction/retraction system is present both on main gear and nose gear; the steering system is only mounted on the nose one, while braking system works on the two wheels of the main gear.

Extraction system. Every strut is equipped with the extraction system. The design has been achieved trough the following step:

- estimation of single strut weight
- excursion angle
- excursion duration
- distance between the strut C.G. and hinge axis

Finally *actuation speed*, *Stall force* and *Moment* as $M = W * g * arm$ are computed thus the *hydraulic power* required is obtained.

The forward extraction system is equipped with *one* strut, while the central is equipped with *two* of them.

		t	W	CG arm	Vel	F	Moment
	[°]	[s]	[kg]	[m]	[rad/s]	[N]	[Nm]
For.	85	8	450	2.35	0.19	4414	10374
Cent2	85	8	1000	2.36	0.19	9810	23151

Actuators	n act	Mom.	Cat.	Type		Speed	Power
	.		[Nm]			[rad/s]	[W]
For.	-	10374.07	Hydr	Cyl.(lin.)	-	0.19	924.47
Cent.	-	23151.60	Hydr	Cyl.(lin.)	-	0.19	2063.12

Table 4.8: Extraction system data.

Steering system. The steering system equips only the nose landing gear. The design process is the following

- Maximum static gear load, assuming a reasonable distance between the two landing gears and the distance with the gravity centre.

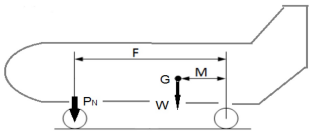

Figure 4.3: Reference dimension required

- Wheel radius, wheel radius under load, friction coefficient, steering angular speed are assumed.

Finally *Steering moment* and *Steering Power* are computed.

Max Load	Radius	Radius under load	Frict. coeff.	Angular speed	Moment	Power
[N]	[m]	[m]		$[rad/s]$	[Nm]	[W]
9740.51	0.9	0.8	0.8	0.18	31518.4	5673.3

Table 4.9: Forward steering system data

Braking system. The braking system is mounted only on the main landing gear. The following steps are necessary in order to define the required power

- definition of the power supply: hydraulic (and the alimentation pressure) or electric (in this case also the voltage is required);
- the vehicle with a landing aircraft mass of 63 000 kg covers the landing distance of 1650 m with a speed of 79 m/s. This allow to provide the maximum braking force 115 000 N.

The breaking power is finally computed: 10 900.8 W. In the power budget the steering is active only during the taxi phases, the retraction system works only before the climb and after the descent. Braking system is active only during the landing (run) manoeuvre.

	[kW]
Taxi out	5.67
Take off(run)	5.67
Flps extension	5.67
Take off (manoeuvre)	5.67
Climb	5.67
Landing gear retraction	5.67
Flaps retraction	5.67
Subsonic Cruise	0
Descent	0
Flaps extension	0
Landing gear extension	5.67
Landing(manoeuvre)	0
Landing (run)	22.37
Spoiler up	5.67
Taxi in	5.67

Table 4.10: Landing gear system results

4.2.4 Fuel system

The estimation of the power required by the fuel system begins from the definition of engine position, fuel tank position and capacity, the maximum fuel flow, fuel quantity and fuel control unit pressure.

Then for each tank, pumps can accomplish different functions: fuel transfer from outer to inner tank, engine feed and APU feed.

For this case of study, outer pumps are adopted only for *fuel transfer*; inner tanks pumps can *feed the engine or transfer fuel* to the fuselage one. Fuselage central pumps only *feed the engine*.

For the transfer pumps, the distance between fuel collector location and the fuel destination are required, along with the fuel flow. The tool computed the pressure drops along the line.

For the engine (or APU) feed pumps, the distance between fuel collector location and the engine (or APU) is required. Also the fuel flow is an input value. Again pressure drops are computed.

Volume	Outer tanks	Inner tanks	Center tank	total
l	$880 * 2$	$6924 * 2$	8250	23858

Table 4.11: Tanks capacity

$$\dot{m}_{fuel} = 27000lbf * 0.34 = 9180lb/hr = 4163.978kg/h \tag{4.1}$$

in take-off condition.
FCU pressure

- min pressure 1.2 bar
- max pressure 2 bar.

	X(m)	Y(m)	Z(m)
Engine 1	12.65	-5.75	-0.9
Engine 2	12.65	5.75	-0.9
APU	35	0	0.5
Outer wing tank (right)	20	9.75	-1.5
Outer wing tank (left)	20	-9.75	-1.5
Inner Wing tank (right)	18	+4.5	-1.5
Inner wing tank (left)	18	-4.5	-1.5
Fuselage internal tank	15.65	0	-1.5

Table 4.12: Engines and tanks position

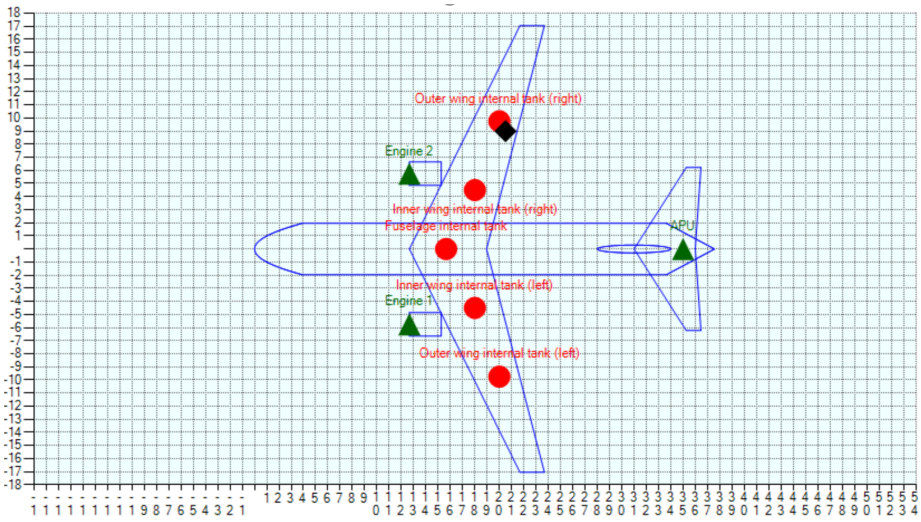

Figure 4.4: Scheme of main fuel system components

After the sizing step, it is necessary to define the pump.

The design choice to made, is explicable by using the following diagram (fig. 4.5), where the pressure produced by the pump is depicted in function of the fuel flow. ASTRID, then makes available a database of different fuel pumps, with some specifics. The choice should be of compromise between the requirements satisfaction and the weight (pumps cannot be oversized).

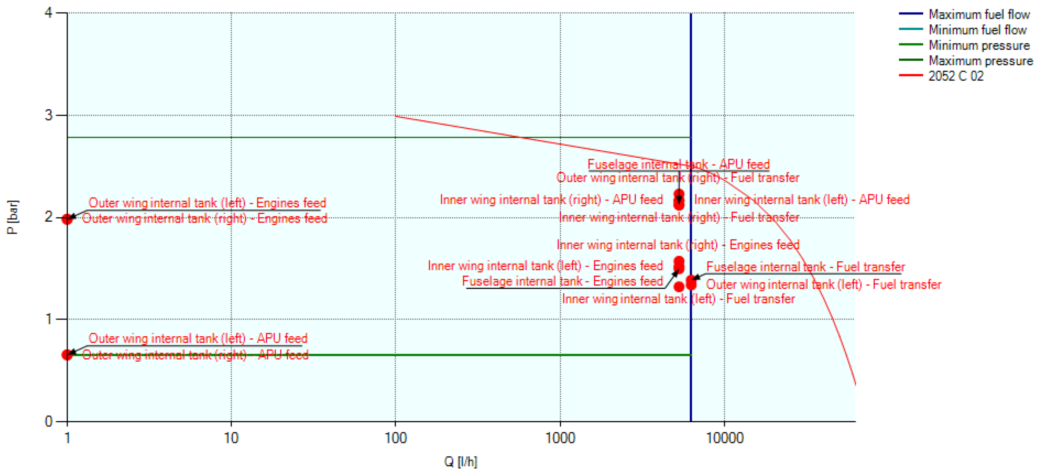

Figure 4.5: Fuel flow, pressure diagram and pump choice

Finally, the power budget is estimated. For every single phase are required which pumps are active, the SFC for single phase (just and approximation), thrust required, APU in function. For this preliminary stage, all pumps are considered active during all mission phases, at maximum fuel flow rate. However, the fuel system power, for the preliminary stage has been fixed at $8kW$ as a reference value. A more detailed analysis is provided in *Chapter 2, fuel system.*

4.2.5 ECS

For conventional and MEA 1 architecture are supplied by bleed air from engine compressors. Bleed temperature is 250 °C at 6 bar. For the ECS the following input data are required to define the Thermal Load

Minimum number of crew members	2
Maximum number of crew members	6
Maximum number of passengers	180
Fuselage wet surface [m^2]	372.9
Mach	0.8
Flight altitude [m]	10670
VIP aircraft	NO
Power of avionics [kW]	5.526
Heat transfer coefficient	2.5
Medium incident light transfert coefficient	0.7
Total trasparent area m^2	15
Heating T cab [°]	18
Heating T cab [K]	291.15
Cooling T cab [°]	25
Cooling T cab [K]	298.15
Maximum thermal load in heating condition [kW]	77.53
Maximum thermal load in cooling condition [kW]	-48.46

Table 4.13: Thermal load calculation

And then, the definition of the Cold Air Unit stage requires

Cau type (subfreezing or non-sbufreezing)	Subfreezing Cau
Cau type	Air cycle
Number of CAUs	2
Sufficient number of CAUs	1
CAU exit temperature [°C]	-22
CAU exit temperature [K]	251.15
Ticc [°C]	50
Ticc [K]	323.15
Ticf [°C]	-5.32
Ticf [K]	267.82
Perc recirculation	25
Fan power [kW]	18
Fan weight [kg]	1500
Percent of recirculation	50
Fan Voltage	115 V AC (400 Hz)

Table 4.14: Cold Air Unit estimation

Finally, the air flow required for the ECS is provided in table 4.17.
During the power budget, the ECS is considered always active, except during the take-off phase.

4.2.6 Anti Ice system

The first step is the definition

- protected surfaces (trough the extension and depth of the surface)
- technology required: aerothermal or electric.

For conventional and MEA1 architectures the aerothermal addresses to the engine air intake and the leading edge protection.

	area [m^2]	[m]	Type	Power [kW]	Air flow[kg/s]
Right engine air intake	1.5	5	Aero	15.96	0.063
Left engine air intake	1.5	5	Aero	15.96	0.063
Right wing leading edge	6	7.5	Aero	63.84	0.25
Left wing leading edge	6	7.5	Aero	63.84	0.25

Table 4.15: Aerothermal Anti Ice surfaces

Other smaller devices are Electrically supplied (the voltage is required).

User	Electric power [kW]	Electric voltage [V]
Windshield and cockpit windows	4.5	115 V AC (400 Hz)
Flight incidence angle gauges	1.5	115 V AC (400 Hz)
P. test connections flight gauges	1	115 V AC (400 Hz)
Waste-water drain mast	2	115 V AC (400 Hz)
Moving surfaces hinges	1.5	115 V AC (400 Hz)

Table 4.16: Electric Anti Ice surfaces

The outputs are the air flow required for each surface (in aerothermal) or the electric power.

Finally, the power budget requires to define

- if pneumatic and/or electric anti ice are active for the single phase;
- number of passenger on board;
- Cold Day, Hot day, ISA standard condition

Astrid esteems the bleed air required from ECS and ANTI ICE system for each segment. For the bleed less configuration all the surfaces are electrically supplied.

	ECS airflow	Anti-Ice airflow	Total Air flow
	[kg/s]	[kg/s]	[kg/s]
Taxi out	1.59	0.69	2.22
Take off(run)	0	0.69	0.69
Take off (manoeuvre)	0	0.69	0.68
Climb	1.59	0.69	2.22
Subsonic Cruise	1.59	0	1.59
Descent	1.59	0.69	2.22
Landing(manoeuvre)	1.59	0.69	2.22
Landing (run)	1.59	0.69	2.22
Taxi in	1.59	0.69	2.22

Table 4.17: Pneumatic system

For this architecture, the power budget gives the electric power which compressors need for anti-ice and environmental control function

	ECS[kW]	Anti ice [kW]
Taxi out	92.212	61.6
Take off(run)	0	61.6
Flps extension	0	61.6
Take off (manoeuvre)	0	61.6
Climb	138.58	61.6
Landing gear retraction	138.58	61.6
Flaps retraction	138.58	61.6
Subsonic Cruise	215.58	0
Descent	138.58	61.6
Flaps extension	138.58	61.6
Landing gear extension	138.58	61.6
Landing(manoeuvre)	92.21	61.6
Landing (run)	92.21	61.6
Spoiler up	92.21	61.6
Taxi in	92.21	61.6

Table 4.18: ECS and Anti-ice system power budget for MEA 2 and AEA configuration

4.2.7 Hydraulic system

The first step is the definition of the hydraulic system pressure (3000 psi for conventional and 5000 psi for MEA 2). Then, the power budget is loaded with all the utilities which require hydraulic power: FCS and LNDG. The hydraulic circuit are hence, defined. The A320 configuration has three continuously operating hydraulic systems with a 3000 psi pressure; each of them has its own hydraulic reservoir.

- Green system: the pump is driven by engine 1.
- Blue system: the pump is electric. (A pump driven by a RAT works in an emergency situation).
- Yellow system: the pump is driven by engine 2. An electric pump can also pressurize this circuit.

Each different circuit has been designed following the scheme in figure 4.6 for the FCS actuators.

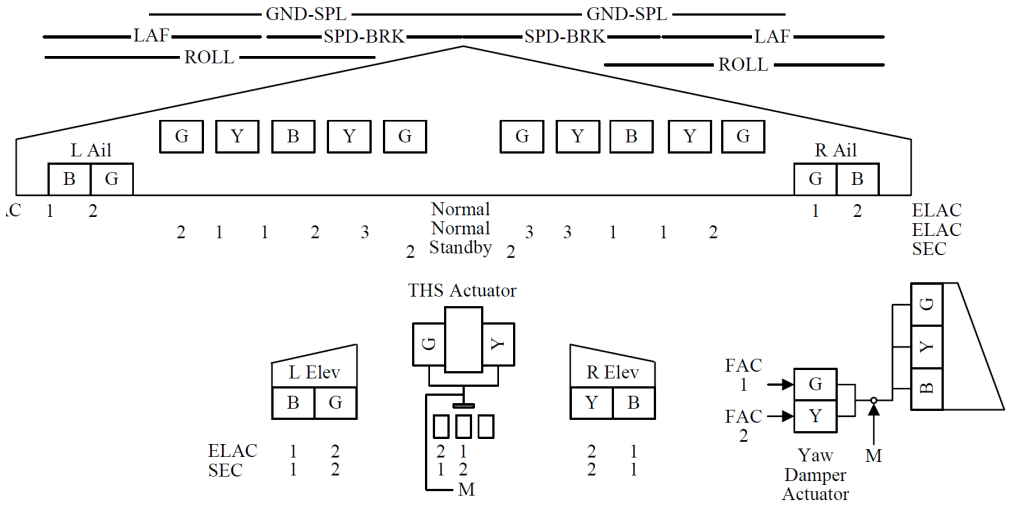

Figure 4.6: FCS divided for the three hydraulic systems [31]

While, for LNDG system actuators:

- braking is supplied by green and yellow system;
- steering is supplied by yellow system;
- extraction is supplied by green system.

From the power budget previously loaded, for every mission segment the tool provides the required oil flow.

Other inputs are

- overall efficiency (0.65 for engine driven; 0.8 for motor driven pumps)
- ratio between engine angular speed and the pump angular speed, only for engine driven pumps. Indeed, motor driven pumps are independent from the engine shaft speed.

	Ratio	Power[kW]
Taxi out	0.2	9.62
Take off(run)	0.95	9.62
Flaps extension	0.95	37.324
Take off (manoeuvre)	0.95	9.62
Climb	0.9	9.62
Landing gear retraction	0.9	14.67
Flaps retraction	0.9	37.32
Subsonic Cruise	0.5	9.04
Descent	0.6	9.04
Flaps extension	0.6	36.74
Landing gear extension	0.8	14.09
Landing(manoeuvre)	0.8	9.04
Landing (run)	0.8	31.42
Spoiler up	0.2	22.34
Taxi in	0.2	9.62

Table 4.19: Engine driven pumps (hydraulically supplied)

	Power[kW]
Taxi out	23.21
Take off(run)	23.21
Flaps extension	74.23
Take off (manoeuvre)	23.21
Climb	23.216
Landing gear retraction	33.73
Flaps retraction	74.23
Subsonic Cruise	22.01
Descent	22.01
Flaps extension	23.95
Landing gear extension	32.52
Landing(manoeuvre)	22.01
Landing (run)	76
Spoiler up	76
Taxi in	23.21

Table 4.20: Motor Driven pumps (electrically supplied)

4.2.8 Electric System

It is necessary to chose between a traditional or an innovative electric system architecture, the number of generators for each engine (1 for each engine), number of generator for the APU (1), APU on or off.

Once this boundary conditions are chosen, the mission profile is loaded and the tool computes all the electric utilities for every single mission segment.

Finally, other utilities are added.

	W		Phase
Power Distribution Unit	1000	28 V DC	Always
Elecric load management center	1200	28 V DC	Always
Miscellaneous	400	28 V DC	Always
Emercency lights	200	28 V DC	Taxi
Evacuation device	1000	28 V DC	Taxi
Light (External)	1000	28 V DC	Always
Cabin light	1500	115 V AC (400 Hz)	Always
Owens	12500	115 V AC (400 Hz)	Climb, cruise
Chillers	2600	115 V AC (400 Hz)	Climb, cruise
Coffee kettle	7800	115 V AC (400 Hz)	Climb, cruise
Lavatories	15000	115 V AC (400 Hz)	Climb, cruise
Cargo door actuators	2000	115 V DC	Taxi

Table 4.21: Other utilities introduced

When all the electric power budget is available, the generators power is esteemed.

Conventional		
Voltage	ARCH	POWER [kW]
115 V AC 400 Hz	IDG	73.2
Innovative		
VOLTAGE	ARCH	POWER [kW]
230 V AC VF	PMG	297

Table 4.22: Electric generators

4.3 Architectures definition

The architectures compared are the one adopted for the AGILE European Horizon 2020 project [10]

CONVENTIONAL. This is equipped with *hydraulically driven* FCS and landing gear actuators. The hydraulic system pressure is the standard 3000 psi.
The ECS and WIPS are supplied by pneumatic system (bleed air from engine compressor). Electric system is a traditional *115 V AC* and conversion to *28 V DC*. Power is extracted by the high pressure spool.

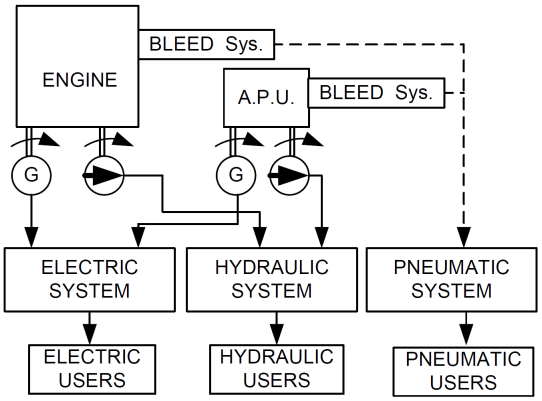

Figure 4.7: Conventional architecture.

MORE ELECTRIC 1. The hydraulic system is completely removed along with its distribution system. The traditional actuators are replaced with EMAs or EHAs (high voltage actuators).
Electro-Hydrostatic Actuators (EHAs) represent the replacement for the linear actuators; Electro-Mechanical Actuators (EMA) are the more-electric version of the screwjack actuator.
Electric system requires the generation in *235 V AC* and the further conversion in *270 V DC 115 V DC and 28 V DC*. At last, the generators have the function of electric starters (pneumatic turbines are removed.)

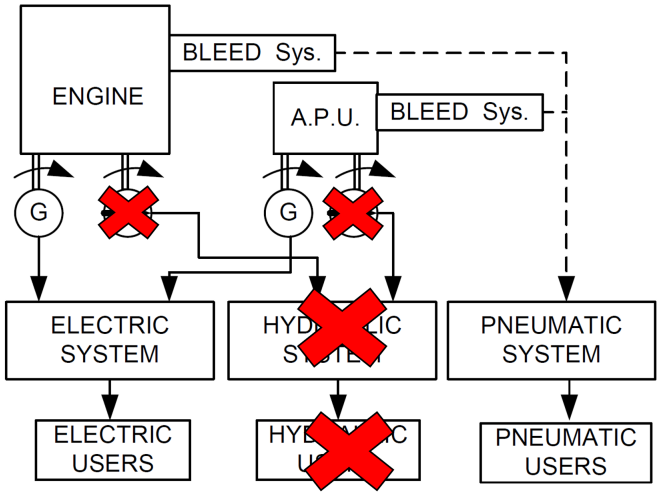

Figure 4.8: More electric 1 architecture.

MORE ELECTRIC 2. The More Electric 2 architecture is the so called "bleed less" configuration. The most innovative feature is the adoption of external compressor to feed

ECS and WIPS. The air bleeding and the pneumatic distribution are removed. The electric system required is the one of MEA 1. The second characteristic is the hydraulic pressure of 5000 psi. Hydraulic pumps are supplied by electric motors, thus the pumps efficiency is higher because it is not strictly related to engine speed.

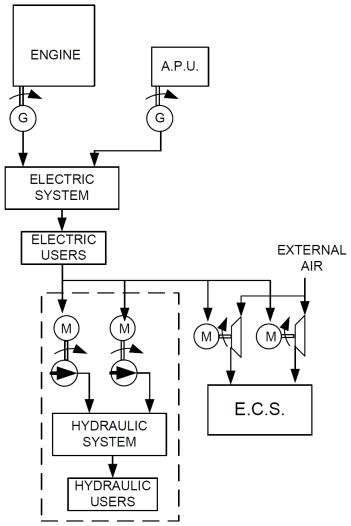

Figure 4.9: MEA 2 configuration

ALL ELECTRIC.

All electric architecture adopts the innovative features of MEA 1 and MEA 2, thus neither hydraulic nor pneumatic system are present.

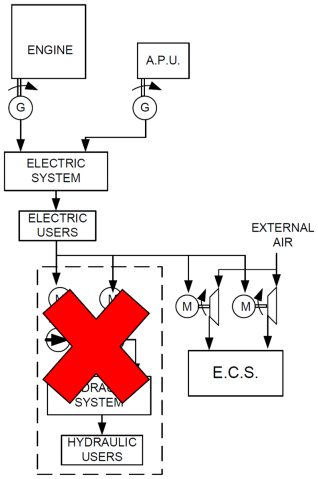

Figure 4.10: All electric architecture.

Electric System

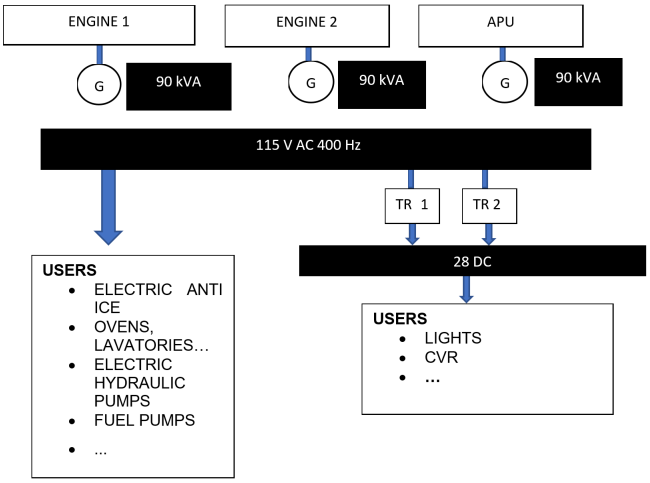

Figure 4.11: Electric generation and distribution system on board Conventional architecture

Primary electric generation is the 115 V AC (400 Hz), with the Integrated Drive Generator. The engine starter is pneumatic. A Transformer Rectifier Unit transforms into 28 DC voltage.

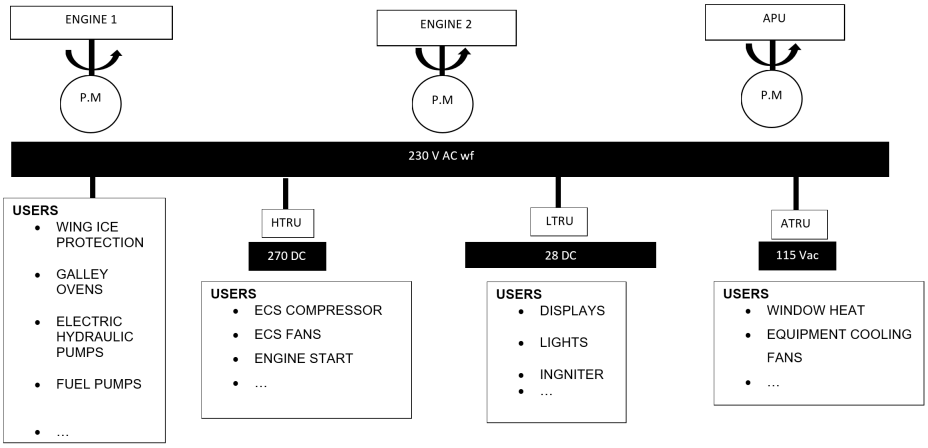

Figure 4.12: Electric generation and distribution system on board innovative architectures

Primary electric generation is 230 V AC VF, provided by Permanent Magnets Alternators. The engine starter is electric. High-Voltage Transformer rectifies into 270 V DC, Low-Voltage Transformer rectifies into 28 V DC, Auto-Transformer Rectifier transforms into 115 V AC.

4.3.1 Conventional architecture: outcomes

The conventional configuration represents the state of the art one, where the systems are pneumatically, hydraulically and electrically powered.
For this reason, the outcomes provided by *Astrid* are then modified with the *electric generator efficiencies* and *hydraulic system efficiency* [1] and finally grouped as

- Mechanical power for Electric System [kW];
- Mechanical power for Hydraulic System [kW];
- Bleed air off takes [kg/s].

The first values refers to the power required by all the systems so, they involve both engines. These have been useful to have a reference outputs of the average power involved. However, the SFC analysis is addressed to a single engine so, the previous values are then simply divided.

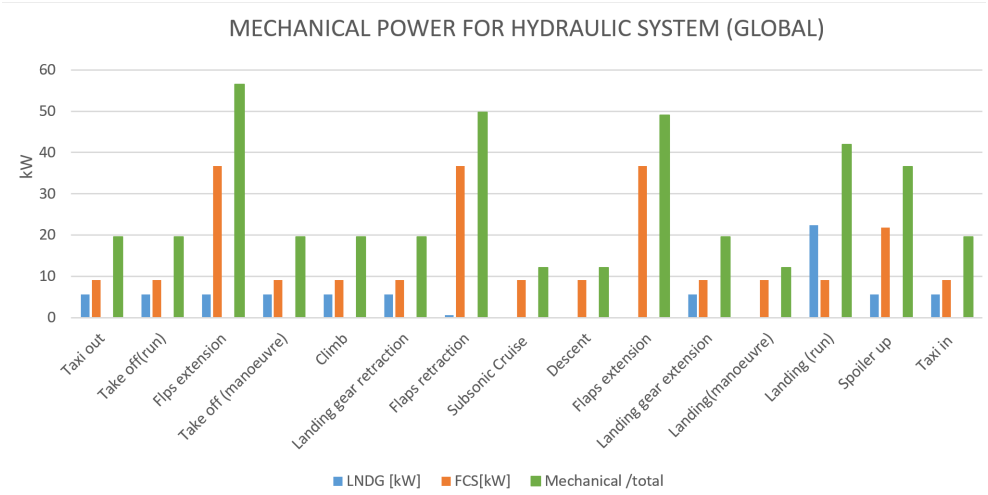

Figure 4.13: Mechanical power required by hydraulic system for 2 engines

The bar diagram provides the breakdown of the mechanical power which the flight control and landing gear systems require.

[1] Astrid outcomes do not consider the conversion efficiencies when dealing with generators and hydraulic pumps. The η applied are $\eta_{electric} = 95$ and $\eta_{hydralic} = 0.75$

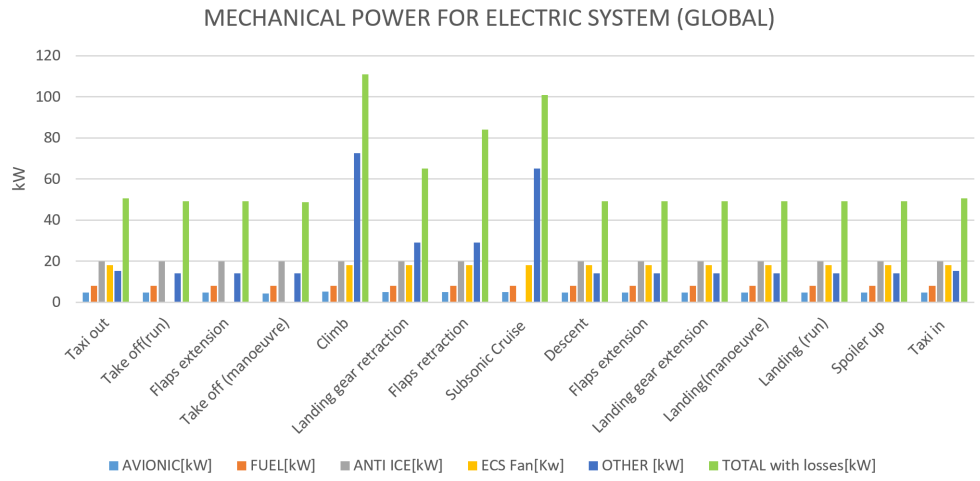

Figure 4.14: Mechanical power for electric system for 2 engines

In a traditional aircraft, most of electric power is required by IFE, galleys and lavatories, along with the ECS fans. On the other hand, avionic devices do not represent a great impact on the overall power budget. During climb and descent, when high lift surfaces and landing gear system are active, the hydraulic system generates an impulsive increment on the total mechanical power.

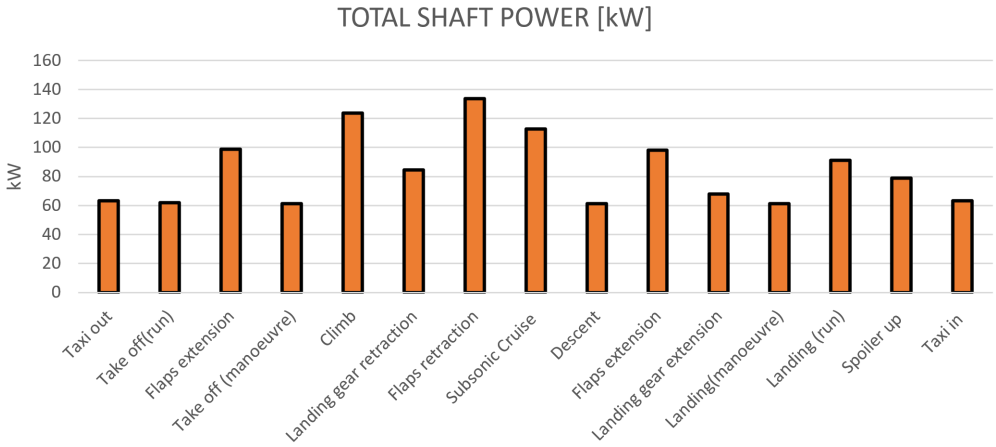

Figure 4.15: Total shaft power required for electric and hydraulic system

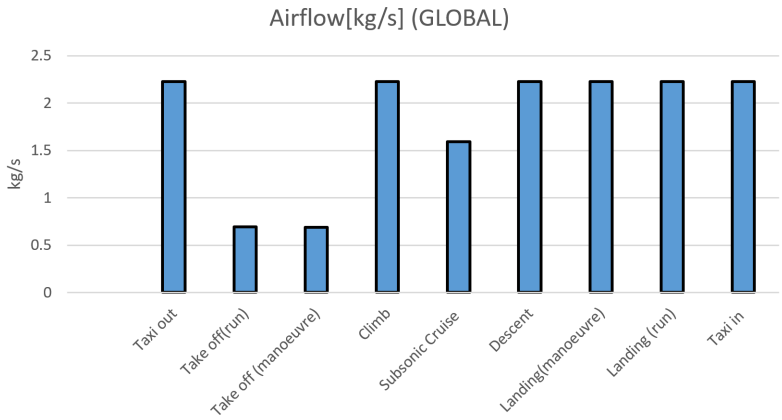

Figure 4.16: Air flow required

4.3.2 MEA 1: outcomes

This innovative configuration removes the adoption of the hydraulic distribution system.

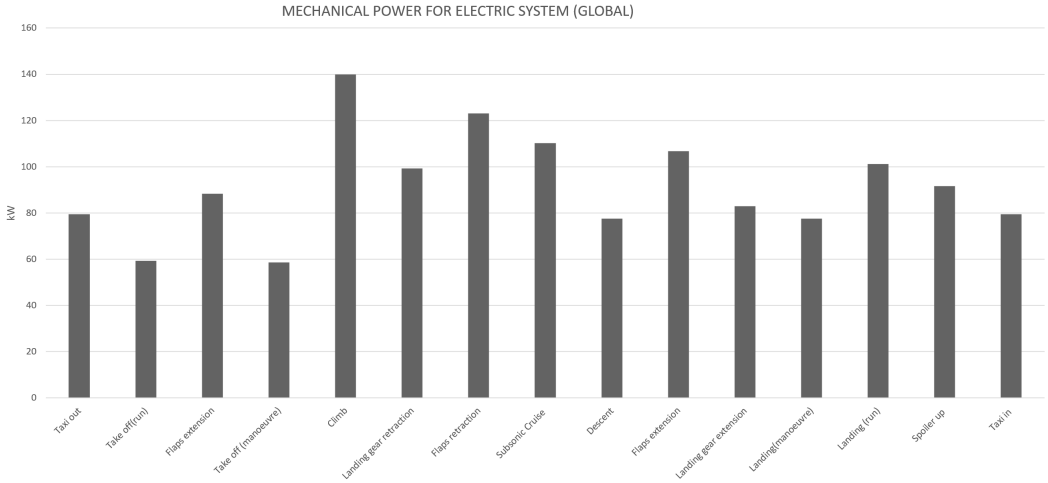

Figure 4.17: Total mechanical power for electric systems (MEA1)

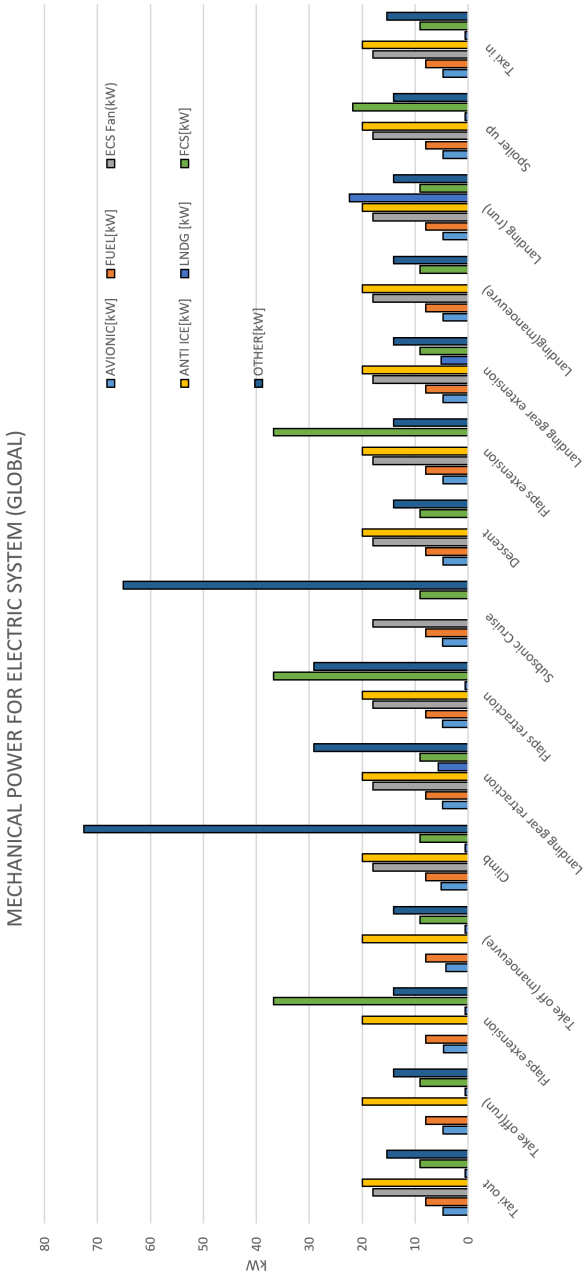

Figure 4.18: Mechanical power for electric systems: different utilities (MEA1)

The above figure underlines that an higher electrical power is required, if compared to the Conventional architecture. Indeed, the flight control and landing gear actuators are electrically supplied. The pneumatic system is retained in this configuration, thus the bleed air outcomes are expressed in 4.16.

4.3.3 MEA 2: outcomes

The MEA 2 configurations is bleed-less like; while hydraulic power is still necessary to feed the actuators. However, in figure 4.20 it clear that the hydraulic pumps are electrically supplied.

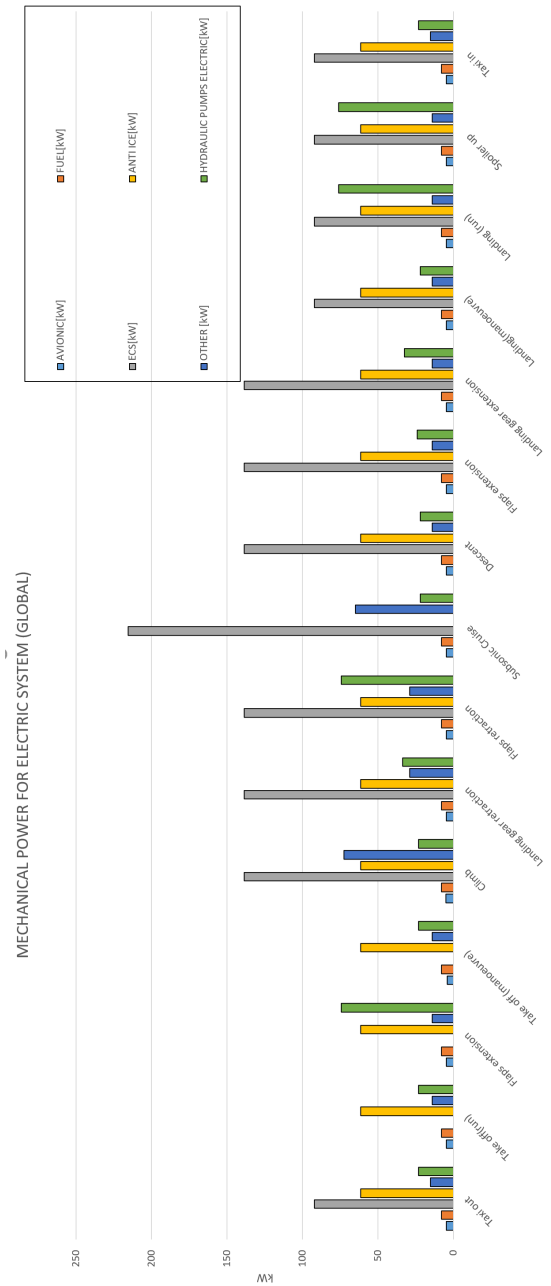

Figure 4.19: Mechanical power for for different utilities (MEA2)

The great increment in mechanical power for electric system is due to the installation of the external compressor for ECS and the electric WIPS.

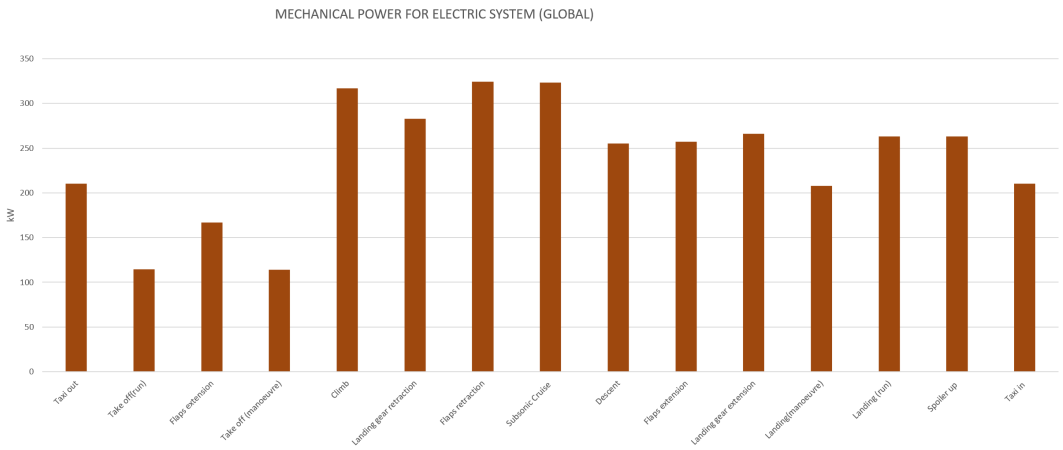

Figure 4.20: Total mechanical power for electric systems (MEA2)

For the MEA 2, a great contribution for the overall mechanical power is given by the ECS compressor and Electric anti-ice. Moreover, during climb and descent, the Flight control and Landing Gear systems have a great impact.

4.3.4 AEA: outcomes

The All Electric architecture, as previously explained, extracts only mechanical power and then adopts the generators in order to convert it all in electric power.
The following diagrams depicts the high amount of electric power which, for this architecture coincides with the total shaft power off-takes.

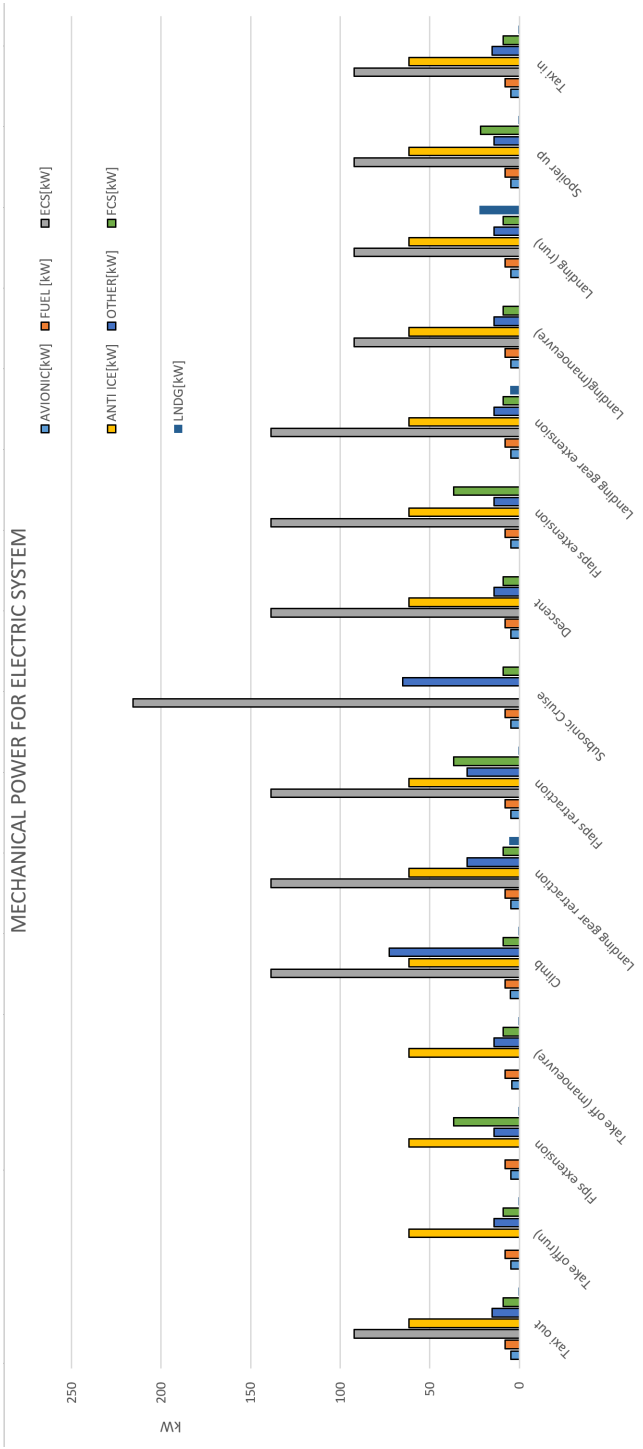

Figure 4.21: Mechanical power for different utilities (AEA)

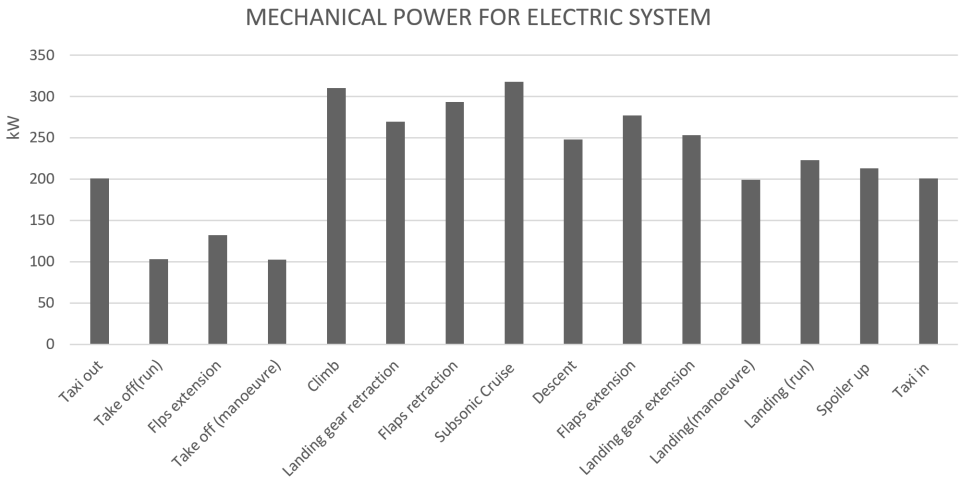

Figure 4.22: Total mechanical power for electric systems (AEA)

4.3.5 Architectures comparison for a single engine

The impact of the sub-systems integration on the engine refers to a single one; hence, the following tables and figures address to split outcomes.

Phase	**CONV**	**MEA1**	**MEA2**	**AEA**
	[kW]	[kW]	[kW]	[kW]
Taxi out	25.23	42.38	105.11	100.53
Take off(run)	24.56	32.26	57.19	51.45
Flaps extension	24.55	46.79	83.33	65.98
Take off (manoeuvre)	24.27	31.98	56.91	51.17
Climb	55.48	72.63	158.40	155.13
Landing gear retraction	32.52	49.67	141.38	134.82
Flaps retraction	41.97	61.57	162.14	146.71
Subsonic Cruise	50.37	55.12	161.72	158.85
Descent	24.60	38.80	127.64	123.95
Flaps extension	24.60	53.34	128.64	138.49
Landing gear extension	24.60	41.75	133.03	126.60
Landing(manoeuvre)	24.60	38.80	103.87	99.60
Landing (run)	24.60	50.55	131.55	111.35
Spoiler up	24.60	48.43	131.55	106.58
Taxi in	25.23	42.38	105.11	100.53

Table 4.23: Mechanical power for electric system

Phase	CONV	MEA1	MEA2	AEA
	[kW]	[kW]	[kW]	[kW]
Taxi out	9.78	0	0	0
Take off(run)	9.78	0	0	0
Flaps extension	28.25	0	0	0
Take off (manoeuvre)	9.78	0	0	0
Climb	9.78	0	0	0
Landing gear retraction	9.78	0	0	0
Flaps retraction	24.88	0	0	0
Subsonic Cruise	6.03	0	0	0
Descent	6.03	0	0	0
Flaps extension	24.50	0	0	0
Landing gear extension	9.78	0	0	0
Landing(manoeuvre)	6.03	0	0	0
Landing (run)	20.95	0	0	0
Spoiler up	18.26	0	0	0
Taxi in	9.78	0	0	0

Table 4.24: Mechanical power required by hydraulic system

Phase	CONV	MEA1	MEA2	AEA
Taxi out	1.11	1.11	0	0
Take off(run)	0.35	0.35	0	0
Take off (manoeuvre)	0.34	0.34	0	0
Climb	1.11	1.11	0	0
Subsonic Cruise	0.80	0.80	0	0
Descent	1.11	1.11	0	0
Landing(manoeuvre)	1.11	1.11	0	0
Landing (run)	1.11	1.11	0	0
Taxi in	1.11	1.11	0	0

Table 4.25: Bleed air flow required by the four architectures during the mission profile

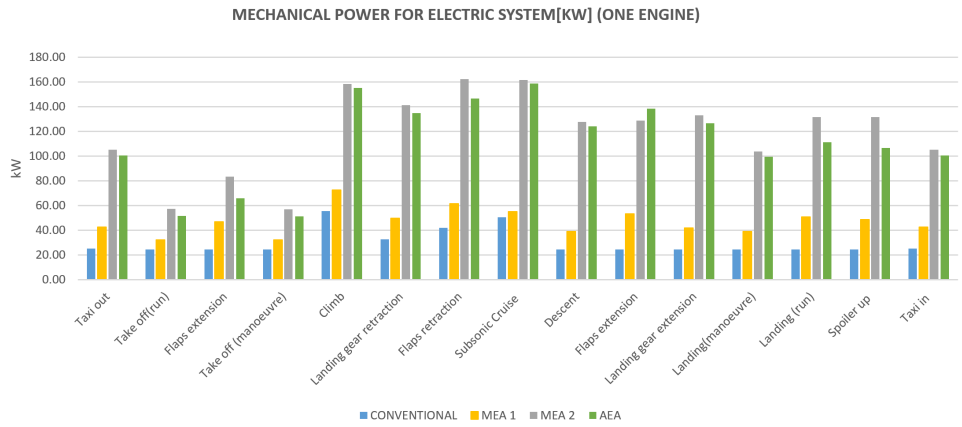

Figure 4.23: Mechanical power for electric systems and the four architectures

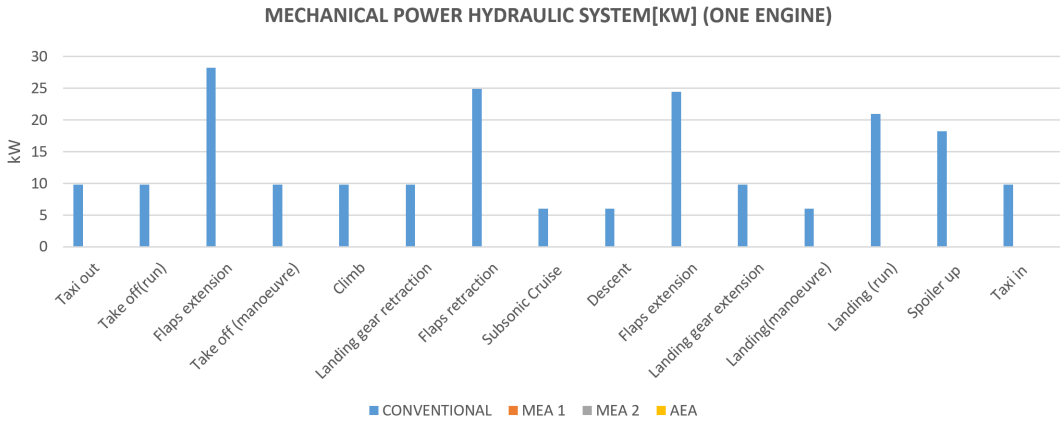

Figure 4.24: Mechanical power for hydraulic systems and the four architectures

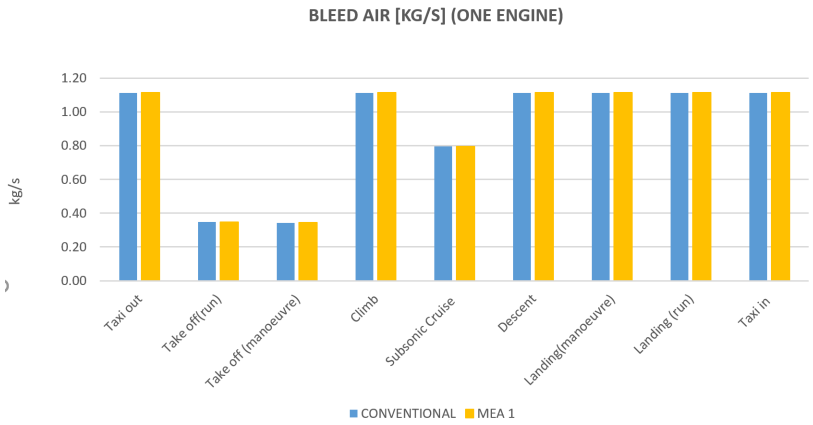

Figure 4.25: Bleed air required for the four architectures

The overall outcomes are presented in table 4.26

	CONV	**CONV**	**MEA 1**	**MEA1**	**MEA 2**	**AEA**
	[kW]	[kg/s]	[kW]	[kg/s]	[kW]	[kW]
Taxi	35.01	1.11	42.38	1.11	105.11	100.53
T.O	34.34	0.35	32.26	0.35	57.19	51.45
Flaps ext.	52.80	0.35	46.79	0.35	83.33	65.98
T.O. 2	34.06	0.35	31.98	0.35	56.91	51.17
Climb	65.26	1.11	72.63	1.11	158.40	155.13
LNDG retr.	42.30	1.11	49.67	1.11	141.38	134.82
Flaps retr.	66.85	1.11	61.57	1.11	162.14	146.71
Cruise	56.40	0.80	55.12	0.80	161.72	158.85
Descent	30.63	1.11	38.80	1.11	127.64	123.95
Flaps ext.	49.10	1.11	53.34	1.11	128.64	138.49
LNDG ext.	34.38	1.11	41.75	1.11	133.03	126.60
LNDG. 2	30.63	1.11	38.80	1.11	103.87	99.60
LNDG (run)	45.55	1.11	50.55	1.11	131.55	111.35
Spoiler up	42.86	1.11	48.43	1.11	131.55	106.58
Taxi	35.01	1.11	42.38	1.11	105.11	100.53

Table 4.26: Breakdown for shaft power off-takes and bleed air extraction

This final breakdown is of great interest for further considerations.

1. The most significant result is that conventional and MEA 1 architectures require both shaft power extraction and bleed air extraction. On the contrary, MEA 2 and AEA deal only with shaft power losses, whose values experiment a twofold increase.
2. The relative power peaks experimented by the conventional architecture are considerably lower for the bleed-less configurations. The amount of power for MEA2 and AEA is clearly much higher if compared with the first two. However, during all mission segments the aircraft does not undertake great fluctuations, except for the take off manoeuvre when the ECS system is off working.
   This has an important impact for the sizing phase: the conventional systems (e.g. hydraulic) are sized for one or two phases, while they are oversized (also for mass and volume) for the rest of the flight segments.
3. Engine driven pumps are less efficient than the motor driven ones. However for the MEA 2 architecture, when flaps are active, the electric power required is higher. These results could be misleading: the great difference is that for the Conventional architecture power extracted is immediately converted to hydraulic form, while, for the MEA 2 all shaft power is transferred to the electric distribution system, without the hydraulic conversion. Then, motor driven pumps adopt hydraulic power.
4. All Electric configuration requires less power than the MEA 2; this finds an explanation with the removal of hydraulic pumps. High voltage actuators represents a

great saving of power.

The previous results are shown in fig. 4.26.

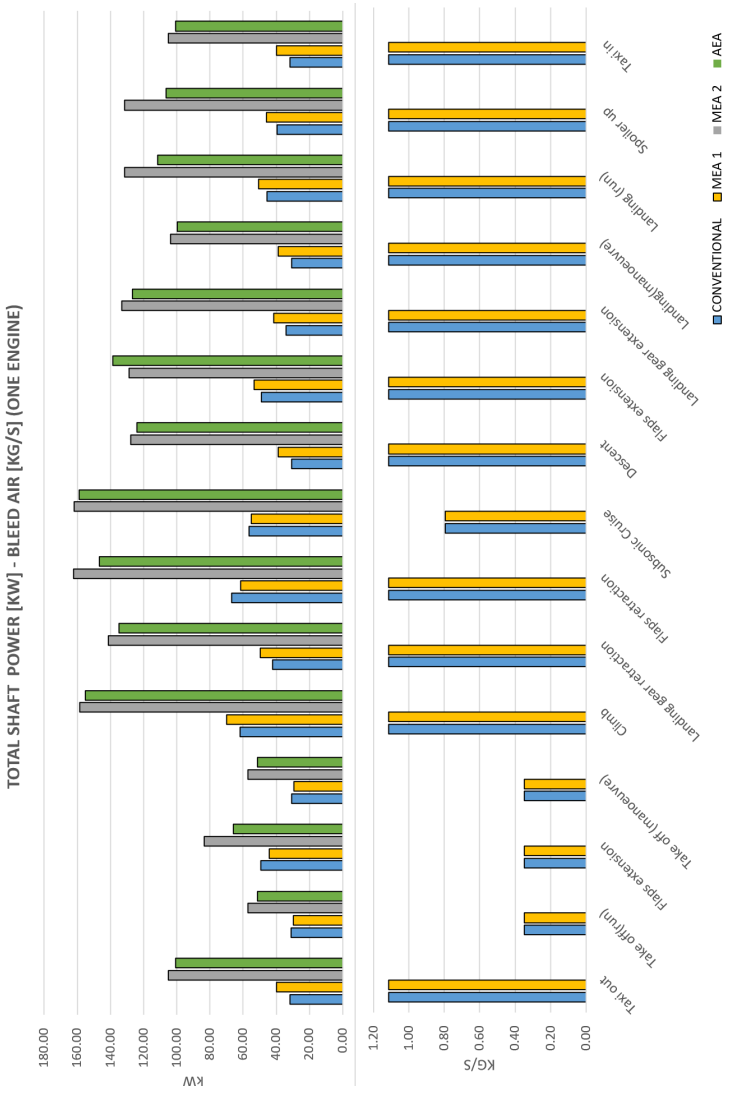

Figure 4.26: Breakdown diagram

Part II

SFC computation

This section aims to compute the increment on specific fuel consumption with respect to a clean engine, in *CRUISE CONDITION*.

4.4 Model 1

During the thesis, the results given by the TURBOMATCH study were applied to the CFM 56 B and V2500 engine.

The first step consists on the computation of the specific fuel consumption of a clean engine, in cruise condition using eq. 3.7 and 3.8

For the A320

BPR	5.7	Bypass ratio
$OAPR$	29.1	Overall pressure ratio
T_{TO}	$120[kN]$	Max take off thrust
T	$216[K]$	Cruise temperature
$\Delta p/p$	0.02	Inlet pressure loss
T_0	$288[K]$	Temperature at sea level std
γ	1.4	Gas adiabatic index
TET	$1453[K]$	Turbine inlet temp [1]
h	$11000[m]$	Cruise altitude
M	0.8	Mach cruise

Table 4.27: Input data

Actually the Mach number varies from $0 < Mach < 0.9$ with steps od 0.1 and the TET is $1000 < TET < 1600$ K.

As our firs interest in on **SFC is cruise conditions without any power-off takes**, the following results relates to that working point.

$$\boxed{SFC_{clean} = 14.81\,\text{g/kN} * \text{s}}$$

4.4.1 Kp

The TURBOMATCH simulation brought to the conclusion that the k_p factor is constant for a specific working point but not during the entire flight envelope. From real engines data, the following equation has been found, in order to relate k_p with the Mach number and the altitude [35]

$$k_p = 0.0057 + 4.60 * 10^{-8} * h - 0.0106 * M - 4.44 * 10^{-13} * h.^2 + 1.85 * 10^{-7} * M * h + 0.0049 * M^2 \tag{4.2}$$

Let Mach change from $0 < M < 0.9$ and the altitude $0 < h < 12000$ m and plot equation 4.2.

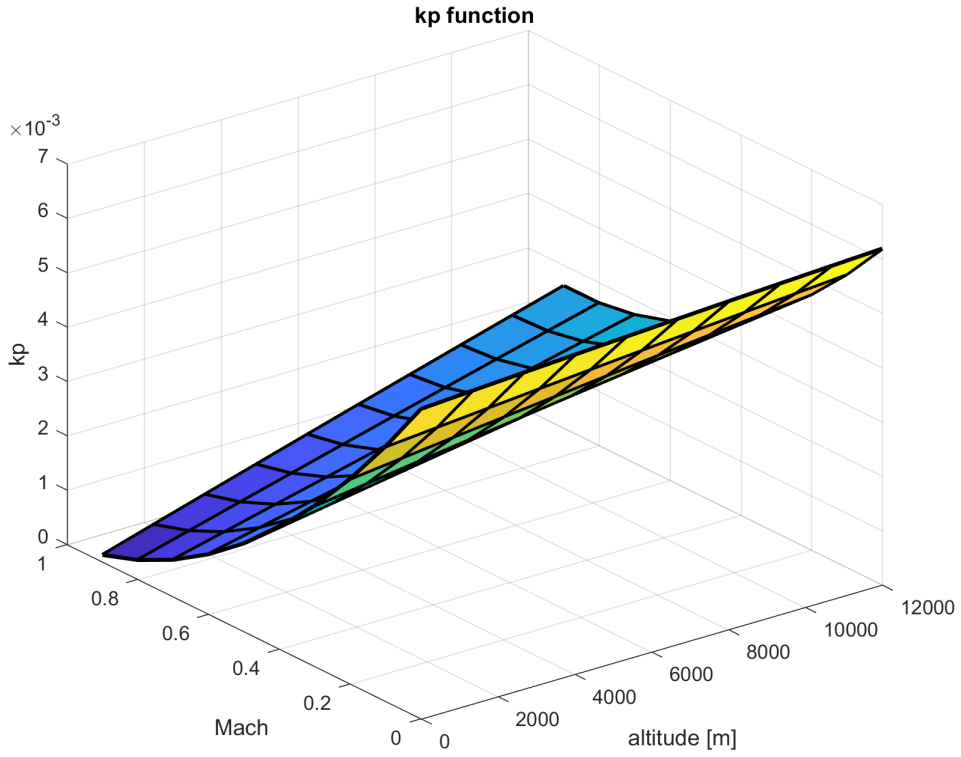

Figure 4.27: Shaft power factor against Mach number and flight altitude.

Figure 4.27 shows that kp decreases with Mach number and increases with altitude. In cruise condition at

- h=11000 m
- M=0.8

$$\boxed{k_p = 0.0024 N/W}$$

which is in line with the expected results.

Now, adopting 3.11, 3.10 and 3.12 it is possible to find the increment of specific fuel consumption and of the fuel flow due to the shaft power off takes.

The previous computational steps are done for the different architectures considered throughout the thesis. From the systems design, the amounts of shaft power extracted during cruise have been found and then

Architecture	Power$[kW]$	$\left(\frac{\Delta SFC}{SFC}\right)\%$
Conventional	56.4	0.62
MEA 1	55.12	0.61
MEA 2	161.72	1.79
AEA	158.85	1.75

Table 4.28: Shaft power off- takes for a single engine during cruise condition. Comparison between the four architectures. Percent increment of SFC due to power off-takes

In figure 4.28 the experimental data of power off-takes are compared with each other, following the model explained in this chapter.

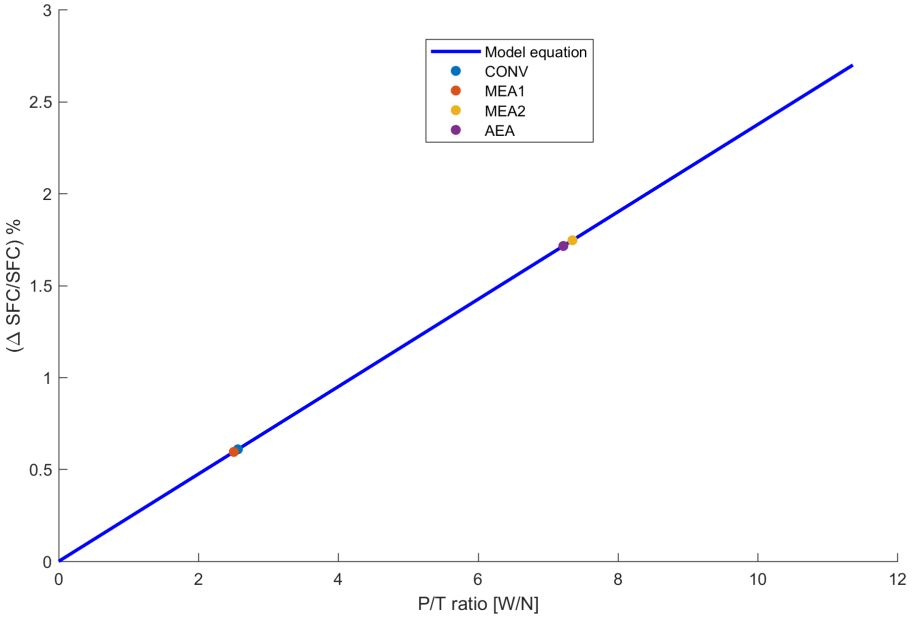

Figure 4.28: Percent increments of SFC adopting Scholz model

4.5 Model 2

According to [23] the computation of the detrimental effects attributed to the secondary power off-takes, begins estimating the efficiency changes.

The analysis is done for the design point of the engine, which means for fixed overall pressure ratio, fixed turbine inlet temperature and fixed components efficiencies.

TET[1]	$1453K$
$OAPR$	29.1
η_{fan}	0.9
η_{lpt}	0.86
η_{hpt}	0.88
η_{hpc}	0.86
$Thrust$	$22[kN]$
V_0	$233[m/s]$

Table 4.29: Input data for the analysis

4.5.1 Shaft Power off-takes

Then, the power produced by the core of a clean engine can be expressed by

$$P_{cp} = 7799\,\text{kW} \tag{4.3}$$

The power produced by the core after the extraction of the shaft power off-takes is given by 3.22. There is no need to obtain P_{shaft} from the thermodynamic analysis because the amount of power off takes are available from table 4.28.

	P^*
CONV.	77 421 kW
MEA 1	7744 kW
MEA 2	7637 kW
AEA	7640 kW

Table 4.30: Available core power after the shaft power extraction

[1]Computed with 3.8

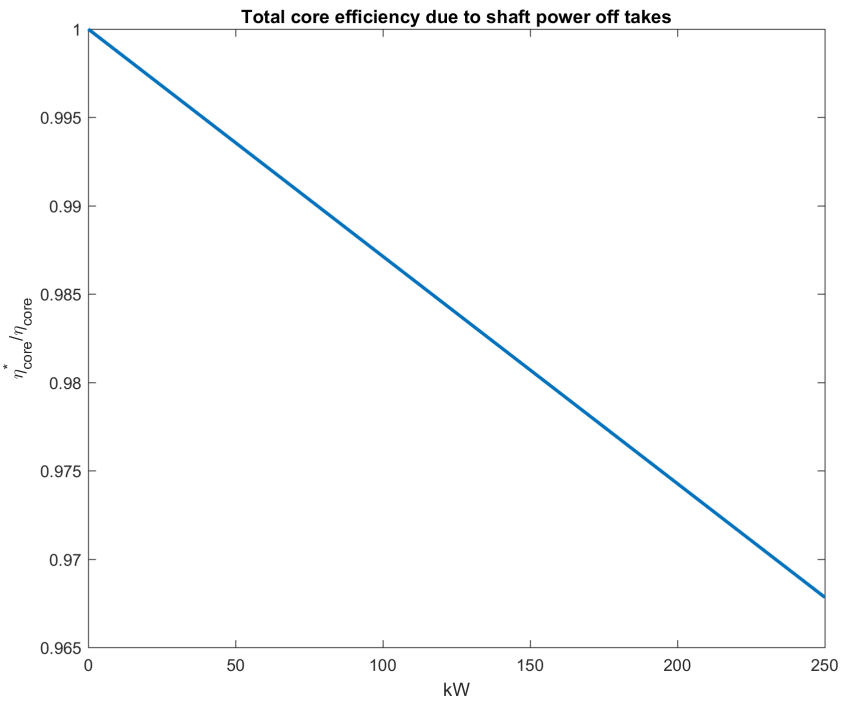

Figure 4.29: Total core efficiency decrease against power off takes, with everything else kept constant

4.5.2 Bleed air off takes

The core power after the extraction of the bleed air is expressed by

$$P^* = (1 - \beta)P_{cp} - \dot{m}_{bleed}\Delta_{hb} \tag{4.4}$$

where

- $\dot{m}_{bleed}$ represents the bleed air mass flow. During the study this parameter varies from $0 < \dot{m}_{bleed} < 1.5$ [kg/s], although in cruise condition it remains constant for a single architecture. From ASTRID outcome it has been found that, in cruise condition

$$\begin{array}{c|c} CONVENTIONAL & 0.8[kg/s] \\ MEA1 & 0.8[kg/s] \\ MEA2 & 0[kg/s] \\ AEA & 0[kg/s] \end{array}$$

- Δ_{hb} is the bleed-air enthalpy increase through the core [kJ/kg]. This is considered equal to 600 kJ/kg.

- β is the ratio between bleed air mass flow and core mass flow

The decrease of core efficiency due to the bleed off takes is expressed in the following figure

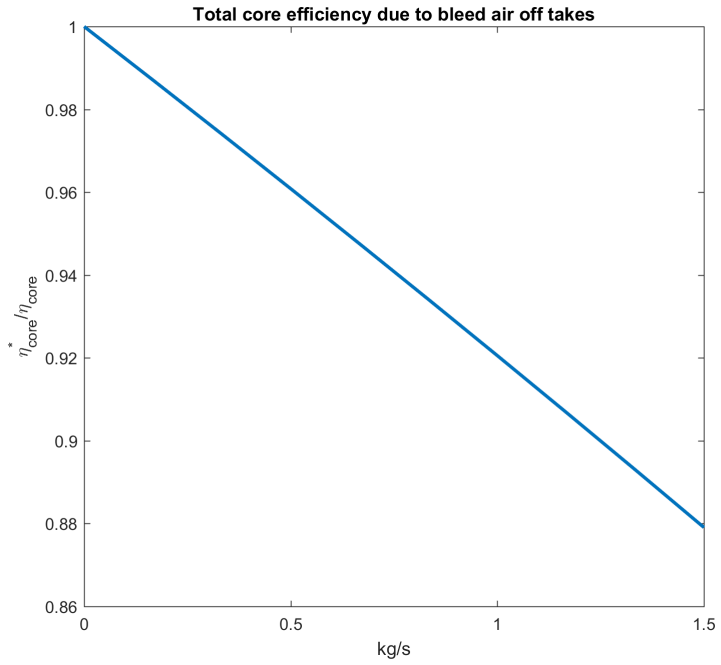

Figure 4.30: Total core efficiency decrease against bleed air off takes, with everything else kept constant

Finally, the SFC increment is calculated as 3.35.

Taking into account, the two contributes of the decrement on specific fuel consumption, given by the shaft power off-takes and the bleed air extraction, one can obtain the following curves. Figure 4.31 represents the influence of shaft power off-takes on SFC of a clean engine, which is driven by a linear relation.

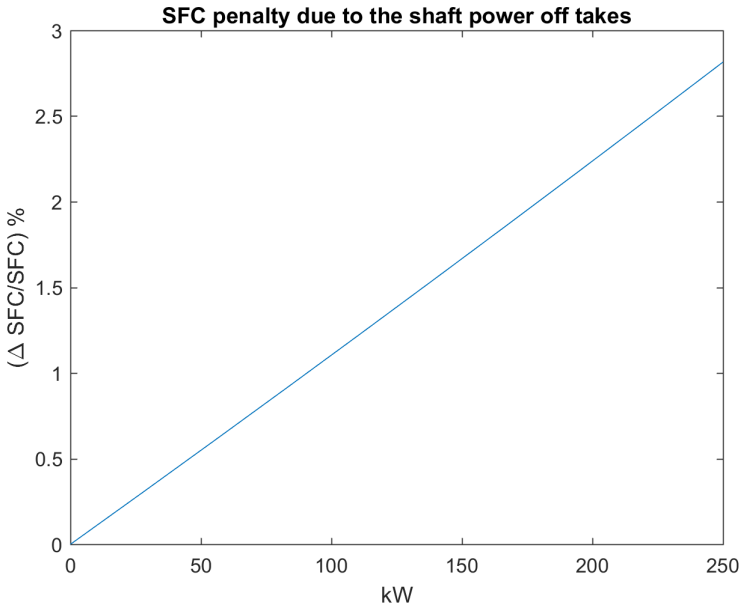

Figure 4.31: Influence of shaft power off takes on SFC, given by equations 3.35 and 3.26

In Figure 4.32 it can be observed how much the bleed air extraction impacts on the SFC: this time the relation is not linear.

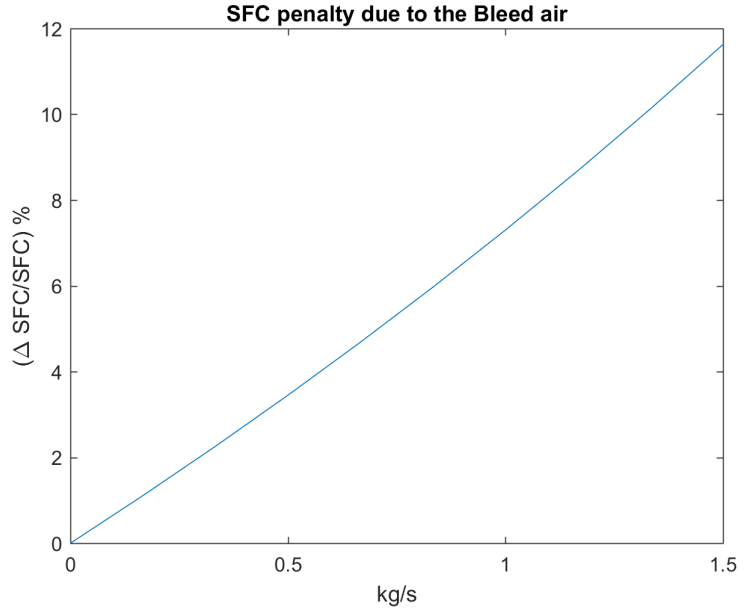

Figure 4.32: Influence bleed air off takes on SFC, given by equations 3.35 and 3.32

SFC varies almost linearly with bleed air extraction and shaft power off takes. However, bleeding pratictice has a most significant impact on the fuel consumption (as depicted in table 4.31)

Beginning from the power off takes given in table 4.28 the increment in SFC have been calculated for our case study.

	$\left(\frac{\Delta SFC}{SFC}\right)(shaft)\%$	$\left(\frac{\Delta SFC}{SFC}\right)(bleed)\%$	$\left(\frac{\Delta SFC}{SFC}\right)(TOT)\%$
CONV.	0.61	5.70	6.32
MEA 1	0.60	5.70	6.30
MEA 2	1.79	0	1.79
AEA	1.76	0	1.76

Table 4.31: Percentage increment of SFC with Giannakakis model

In order to compare the two mathematical models explained here, is necessary to express the ratio $Power/Thrust$ for both of them. This can be done with

$$\frac{P[W]}{Thrust(cruise)[N]} \tag{4.5}$$

obtaining the abscissa axes and in the ordinate axes there will be the SFC percent increment. Clearly, this is useful only for what concern the shaft power off takes, because Scholz model does not analyse the bleed.

Comparing the two algorithms, the outcomes are really close to each other for the P/T ratios considered throughout the thesis, representing the different architectures.

Architecture	Power$[kW]$	$P/T[W/N]$	$Giannakakis$	$Scholz$
Conventional	56.4	2.56	0.61	0.62
MEA 1	55.12	2.50	0.60	0.61
MEA 2	161.72	7.35	1.79	1.79
AEA	158.85	7.22	1.76	1.75

Table 4.32: Percentage of $\left(\frac{\Delta SFC}{SFC}\right)(shaft)\%$ for various power off takes to thrust ratio. Comparison between the models for a CFM 56

The diagram in figure 4.33 demonstrates that the two models give very similar results. in figure 4.34 the relative errors can be observed: the most relevant fact is that the error between the models increases as the ratio P/T increases: indeed, for conventional and MEA1 architectures the outcomes almost coincide, while for MEA2 and AEA, they begin to diverge. A closer look reveals Giannakakis model overestimates Scholz results.

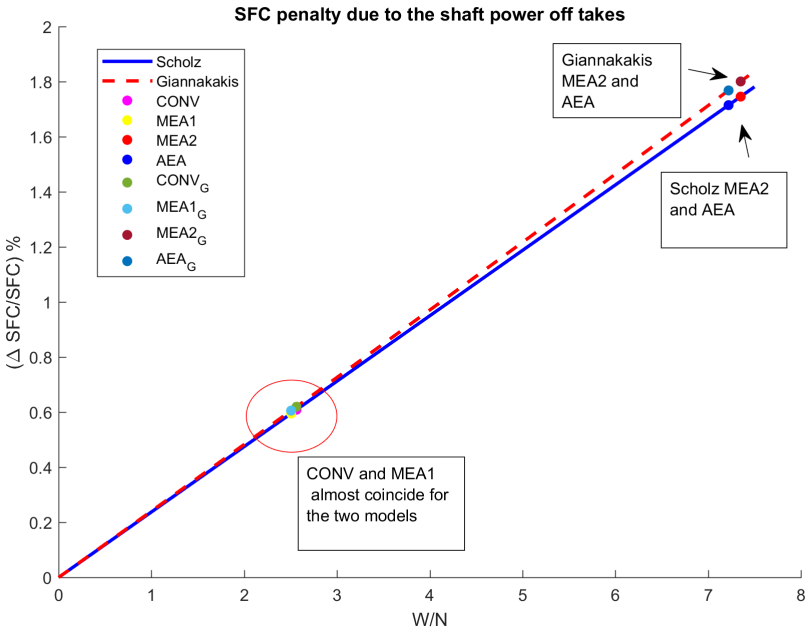

Figure 4.33: Comparison between the models

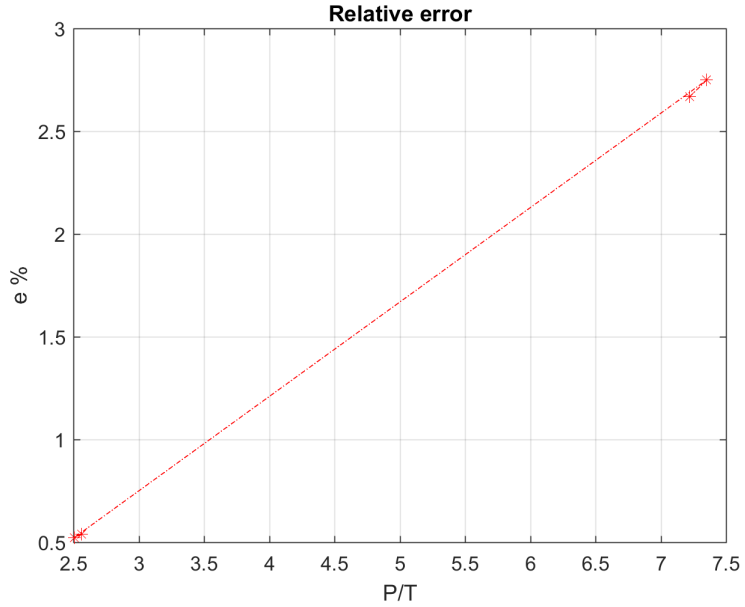

Figure 4.34: Error between experimental datas

However, as previously cited, the main disadvantage in Scholz approach is the absence of bleed air extraction. The other algorithm, instead, provides some formulas to estimate

the increment in SFC related to pneumatic extraction (see eq.4.4 and following) In the following table the final results are presented.

Architecture	$\left(\frac{\Delta SFC}{SFC}\right)\%$	$\left(\frac{\Delta SFC}{SFC}\right)\%$	$\left(\frac{\Delta SFC}{SFC}\right)\%$	$\left(\frac{\Delta SFC}{SFC}\right)\%$
	Shaft	Bleed	Tot Giann	Tot Scholz
Conventional	0.61	5.70	6.32	0.62
MEA 1	0.60	5.7	6.3153	0.61
MEA 2	1.80	0	1.8	1.79
AEA	1.76	0	1.76	1.79

Table 4.33: Breakdown table for SFC increments

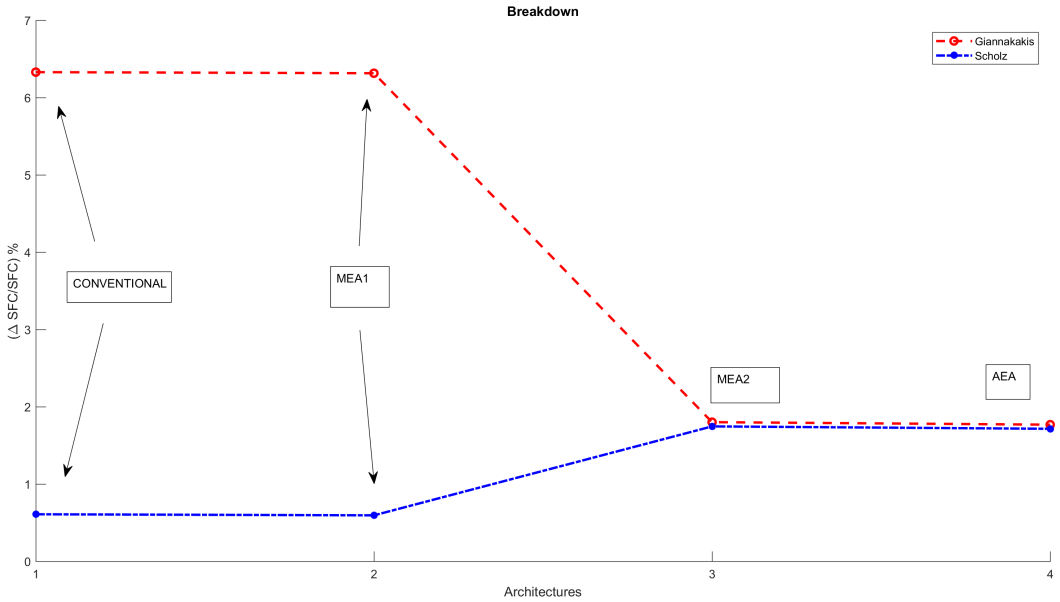

Figure 4.35: Breakdown table for SFC increments

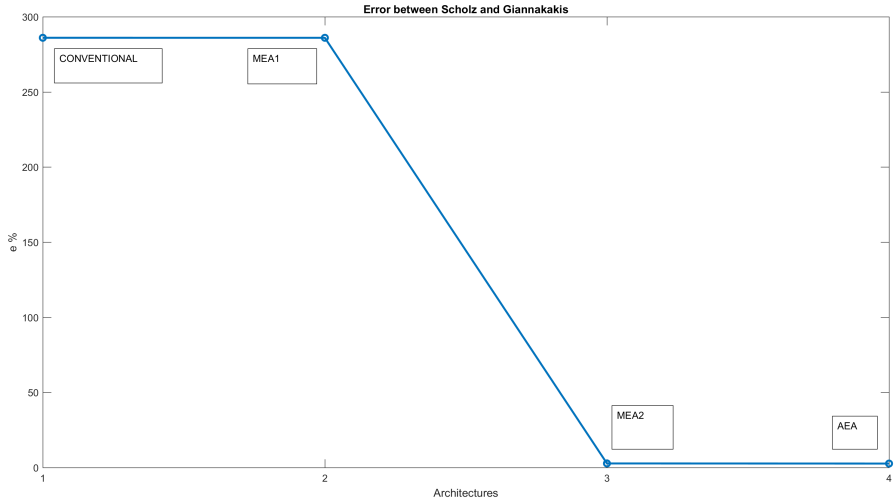

Figure 4.36: Percentage error between Scholz and Giannakakis model

4.6 Engine Deck 1

As previously said, the increment in SFC for the 3 different architectures are computed with the aid of two engine decks. The first one takes into account a smaller engine than a CFM 56 or a V2500. Indeed, the thrust considered is $T = 12000N$ against the $22000N$ of the one mounted on an A320. Another lack found during the comparison is ascribed to the range of power off-takes and bleed air off takes within the engine deck.

The engine deck varies from

Bleed [kg/s]	0	0.1	0.2	0.3	0.4	0.5	0.6
Power O.T. [kW]	0	20	40	60	80	100	

Table 4.34: Range of variables of the engine deck

On the other hand, the study for the A320 found by the system design give higher results for both power off-takes and shaft power off-takes.

CONV.	$0.8[kg/s]$
MEA1	$0.8[kg/s]$
MEA2	$0[kg/s]$
AEA	$0[kg/s]$

Table 4.35: Bleed

Architecture	Power$[kW]$
Conventional	56.4
MEA 1	55.12
MEA 2	161.72
AEA	158.85

Table 4.36: Power off takes

Table 4.37: Shaft power off- takes for a single engine during cruise condition. Comparison between the four architectures

These tables highlight that it is not allowed to compare the four architectures adopting this engine deck. Anyway, to compute a more proper analysis, a *scale factor* had been found.

The following consideration are drawn

- The thrust in cruise condition assumed throughout the work is $T = 22\,\text{kN}$, while the thrust given in the engine deck is $T = 12\,\text{kN}$. $\rightarrow$

$$\frac{12}{22} = 0.5455 \tag{4.6}$$

  is the ratio between the thrust of previous two cases. This scale factor is useful to compare two engine which, otherwise, could not match with each other.
- Applying the scale factor to the Power off takes an bleed of takes presented in tables 4.35 and 4.36 it is possible to find the equivalent values for a smaller engine, but still maintaining the relation. Indeed, the most important impact over the results is expressed by the ratio between the shaft power and the core power (which is function of the Thrust, by equation 3.25).
- The four points considered do not coincide with the 42 possible combinations of bleed air and shaft power off-takes. A Response Surface Methodolgy has been adopted.

4.6.1 Response Surface Methodology

The response model methodology is a statistic process which explores the relation between some independent variables and the response variables. The purpose of this model building methodology is to find an optimized response, which is a function of input variables.

The basic principle behind the RSM is the choice of some experiments: these are a series of tests, where an users changes the input variables in order to find the reason of the changes in output values.

Adopting the RSM to design optimization the computational cost addressed to analytic methods can be reduced.

In order to derive an approximation of the real relationship between the input and the output variables, al low order polynomial is adopted; once the response is derived, it is necessary to define the goodness of the model. If the output is not as accurate as it required, the iteration process restarts.

A really significant aspects of the RSM is the *design of experiments* (DoE), which represents the selection of the points where the response is, then, evaluated. This stage has a great impact on the response accuracy and on cost of its construction. Usually, the first step of the DoE is to find which variables have more influence on the output variables.

On our case study, the input variables are X is the series of bleed air extraction **[0 0.1 0.2 0.3 0.4 0.5 0.6]** [kg/s] which are repeated for 7 times, combined with the series of shaft power off takes **[0 20 40 60 70 80 100]** [kW].

While the output Y is the specific fuel consumption which will be function of both bleed and power off-takes, following a first-order model

$$Y = \beta_0 + \sum_{i=1}^{2} \beta_1 X_1 + \sum_{i=1}^{2} \beta_{11} X_2^2 \tag{4.7}$$

where Xi are the design variables (bleed and power)and β are the coefficients which compose the response within the range and between the design points.

Figure 4.37 represents the Matlab output which provide the behaviour of the Specific fuel consumption as a response of a bleed air change (left) and a shaft power extraction change(right). Trough this tool, the user can moves the input parameters and the values of SFC is computed as $y \pm \delta_y$ where δ_y is uncertainty in the mean value which depends on the global confidence level.

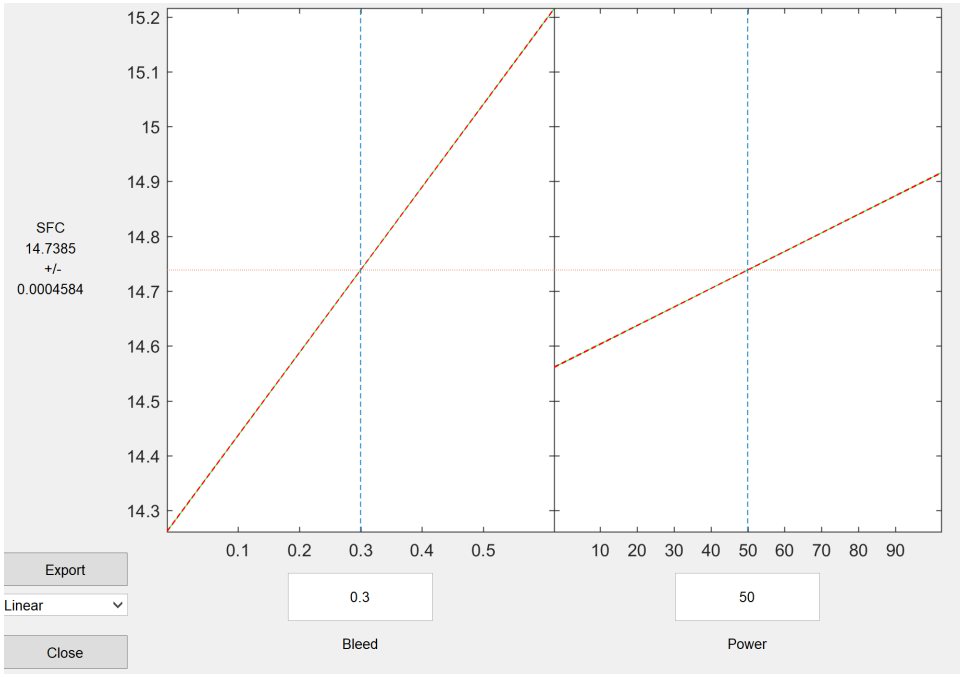

Figure 4.37: Response surface methodology

Finally the scale factor has been adopted to transforms the Power off-takes and this process gives

Architecture	Power$[kW]$	Scaled Power$[kW]$	SFC $[g/kNs]$	$\left(\frac{\Delta SFC}{SFC}\right)\%$
CONV.	56.4	30.76	14.87	5.36
MEA1	55.12	30.06	14.87	5.34
MEA2	131.72	88.21	14.41	2.06
AEA	158.85	86.65	14.4	2.02

Table 4.38: Increment of SFC found by the engine deck

where the values of $\left(\frac{\Delta SFC}{SFC}\right)\%$ are computed starting from the value of the clean engine SFC provided by the engine deck which is $SFC_{clean} = 14.12\,\mathrm{g/kNs}$.

	Power $[kW]$	Bleed $[kg/s]$	P/T ratio	Scholz $\left(\frac{\Delta SFC}{SFC}\right)\%$	Giannakakis $\left(\frac{\Delta SFC}{SFC}\right)\%$	Engine Deck $\left(\frac{\Delta SFC}{SFC}\right)\%$
CONV	56.4	0.8	2.56	0.62	6.32	5.36
MEA1	55.12	0.8	2.5	0.61	6.31	5.34
MEA2	161.72	0	7.35	1.79	1.80	2.064
AEA	158.85	0	7.22	1.75	1.76	2.02

Table 4.39: Increment of SFC: comparison

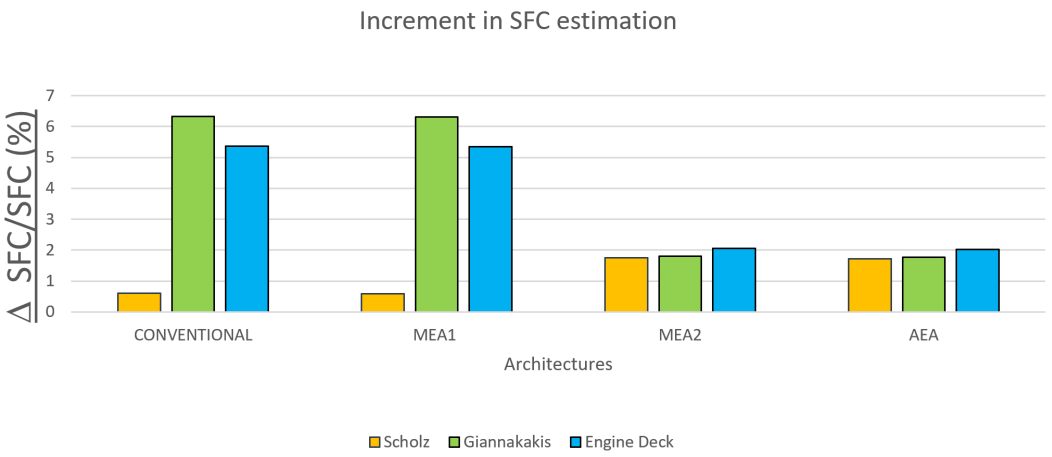

Figure 4.38: Bar diagram representing the complete outputs

4.7 DLR engine deck

As previously introduced, the engine deck provided by the *Deutsches Zentrum für Luft und Raumfahrt e.V. (DLR)*, Institute of Propulsion Technology, is related to the V2500 engine, which power the A320.

Anyway, in order to provide a more detailed comparison the model of Scholz and Giannakakis the following input data are adopted

1. flight altitude is $h = 10\,000\,\text{m}$;
2. $TET = 1363\,\text{K}$ [3] or $TET = 1512\,\text{K}$ if computed with 3.8 for Scholz model.
3. $BPR = 5.24$ [4], bypass ratio;
4. $OAPR = 24.6$ overall pressure ratio [5]

Architectures	Power kW	Bleed kg/s	SFC g/kNs	DLR Engine Deck $\left(\frac{\Delta SFC}{SFC}\right)\%$
CLEAN	0	0	16.44	–
CONVENTIONAL	56.4	0.8	17.35	5.5
MEA1	55.12	0.8	17.34	5.49
MEA2	161.72	0	16.73	1.73
AEA	158.85	0	16.72	1.7

Table 4.40: Increment of SFC provided by the engine deck from DLR

[3] TET found on the engine deck for the CLEAN ENGINE condition.

[4] The bypass ratio value remains fixed for the model 1 and 2. The value of 5.24 is the one provided by the engine deck for the clean engine

[5] The overall pressure ratio is fixed; as for BPR, the data is available from the engine deck.

The input data to compute the SFC with the aid of model 1 and 2 are the following

BPR	5.24	Bypass ratio
$OAPR$	24.2	Overall pressure ratio
T_{TO}	120$[kN]$	Max take off thrust
T	216$[K]$	Cruise temperature
$\Delta p/p$	0.02	Inlet pressure loss
T_0	288$[K]$	Temperature at sea level std
γ	1.4	Gas adiabatic index
TET	1512$[K]$	Turbine inlet temp
h	10000$[m]$	Cruise altitude
M	0.8	Mach cruise

Table 4.41: Input data

The SFC for an engine with the previous characteristics and no bleed or power extraction is computed with 3.7

$$\downarrow$$

$$\boxed{SFC_{clean} = 16.73\,\text{g/kNs}}$$

Architectures	Power kW	Bleed kg/s	Scholz g/kNs)	Giannakakis g/kNs	En. Deck g/kNs	DLR En. Deck g/kNs
CLEAN	0	0	16.73	16.44	14.81	16.44
CONV	56.4	0.8	16.72	17.39	14.90	17.35
MEA1	55.12	0.8	16.82	17.44	14.90	17.34
MEA2	161.72	0	17.008	16.72	14.41	16.73
AEA	158.85	0	17.003	16.71	14.40	16.72

Table 4.42: SFC consumption relative to the four architectures computed with different analysis.

	Power kW	Bleed kg/s	Scholz $\left(\frac{\Delta SFC}{SFC}\right)\%$	Giannakakis $\left(\frac{\Delta SFC}{SFC}\right)\%$	En.Deck $\left(\frac{\Delta SFC}{SFC}\right)\%$	DLR En.Deck $\left(\frac{\Delta SFC}{SFC}\right)\%$
CONV	56.4	0.8	0.57	5.83	5.36	5.5
MEA1	55.12	0.8	0.56	5.82	5.34	5.49
MEA2	161.72	0	1.65	1.65	2.06	1.73
AEA	158.85	0	1.62	1.62	2.02	1.7

Table 4.43: SFC increment with respect to the clean engine condition relative to the four architectures computed with different analysis.

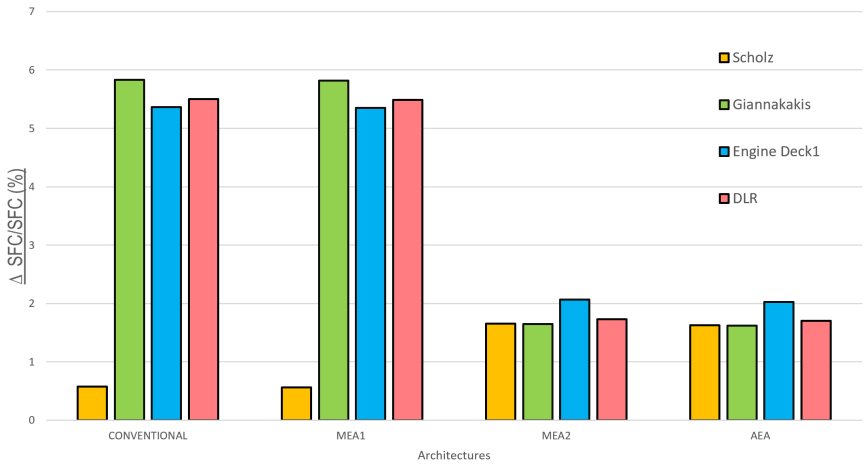

Figure 4.39: Increment in SFC

Architecture	Scholz Relative Error %	Giannakakis Relative Error %
CLEAN	1.76	0
CONV	-3.00	+0.27
MEA1	-2.96	+0.63
MEA2	+1.66	-0.023
AEA	+1.69	-0.053

Table 4.44: Percentage relative error computed with respect to the DLR results of SFC

4.8 Numerical comparison

1. The outputs provided by the engine deck from DLR are considered as the most accurate between the four models: the in-house performance tool **GTlab** is a sophisticated instrument, which takes into account the thermodynamic impact of the off-takes.
   Figure 4.45 underlines some of the outputs provided by the engine deck.

		Clean	CONV	MEA1	MEA2	AEA
Shaft power	[W]	0	56400	55120	161720	158850
Bleed air	[kg/s]	0	0.8	0.8	0	0
Altitude	[m]	10000	10000	10000	10000	10000
Mach		0.8	0.8	0.8	0.8	0.8
Thrust	[N]	22000	22000	22000	22000	22000
Fuel flow	[kg/s]	0.36	0.38	0.38	0.37	0.37
Δ fuel flow	[kg/s]		0.02	0.02	0.01	0.01
SFC	[g/kNs]	16.45	17.35	17.35	16.73	16.73
Δ SFC			0.91	0.90	0.29	0.28
$\left(\frac{\Delta SFC}{SFC}\right)\%$			5.51	5.49	1.74	1.71
TET	[K]	1368.46	1422.28	1422.14	1385.94	1385.62
BPR		5.24	5.22	5.22	5.29	5.29
OAPR		24.64	24.24	24.24	24.52	24.52

Table 4.45: Engine Deck Output

2. From what concerns the other engine deck (in column 6 of table 4.42) the results are underestimated for the conventional and MEA1 architectures; an opposite trend is found for the other two architectures.
   The reason of this discrepancy is to be ascribed to two main reasons
   - Table 4.42 highlights the difference between this engine and all the other taken into account: the thrust and flight mach number are smaller. The TET for a clean engine and the BPR are not known but it is reasonable to think that they have a great impact on the simulation output, given that these parameters cannot be changed as input values.
   - The ratio between the Power extracted and the thrust is maintained, along with bleed air off takes through the scale factor. However, the Surface Response Methodology does not assure an accurate prediction of the results, especially for high amounts of power required without any bleed off takes.
   - although engine characteristics are different from the reference ones, the results still express the same trend. Bleed less configurations represent a good solution to decrease the specific fuel consumption.
3. Giannakakis equations and Scholz model are in good agreement with each other. Actually, the SFC of a clean engine is not the one found by the engine deck (table 4.42) with a discrepancy of 1.76%.
   However, Giannakakis model does not base the study on the computation of SFC for a clean engine thus it provides the increment on SFC for a certain design parameters. For this reason, assuming that the SFC of the clean engine is known from the DLR engine table(4.42), the outcomes are extremely accurate.
4. Scholz method does not take into account the bleed air off takes, which represents

the great inefficiency of the model. Clearly for the first two architectures, the results provided by Scholz cannot be considered. Another limit of Scholz model addresses to kp evaluation which is strictly related to cruise condition. Indeed, kp varies with Mach and flight altitude as expressed in eq. 4.2; however, this formula is found from a series of a database engine data which refers to a $T/T_0 \simeq 0.18 - 0.2$. The value of phase thrust and take off thrust addresses to a typical cruise condition. Hence Scholz approach is not really reliable for other mission segments.
The logical process followed by Scholz relies on the computation of SFC without any extraction, hence this approach addresses to the relative error for a specific engine. If a different engine is considered, the computational step need to start from the SFC of a clean engine, which, again is an error source. Scholz method adopts eq.3.7 to compute the clean engine SFC and eq. 3.8 to find the TET, which are incongruous with the reference values. This is one of the model limit and reason of the discrepancy in clean engine SFC.
Observing table 4.43 the outcomes can be commented as follow

- Scholz model is still completely incorrect when bleed air extraction is considered;
- MEA2 and AEA results are almost as accurate as Giannakakis equations.

Giannakakis model represents the most useful resource for the estimation of the increment in SFC although it should be optimized.

Table 4.44 contains very interesting results: the $\Delta SFC/SFC\%$ is overestimated for those configurations which deal with bleed air off-takes. The error is $+0.27\%$ and $+0.63\%$ for conventional and MEA1 respectively.

From equations 3.30 and 3.31 some other observation can be depicted

- Δ_{hb} which is considered 600 kJ/kg; it is a reference value [23] but an enthalpy increase of 570 kJ/kg brings to a an increment of 5.57 and 5.56 respectively for conventional and MEA1.
  With this new value on the increment of the air enthalpy, the error would be -0.032% and -0.09%. Hence, the enthalpy increment has great influence on the SFC computation.

  Eequation 3.32 expresses the strictly relation between the decrease in core efficiency and the bleed enthalpy increase:

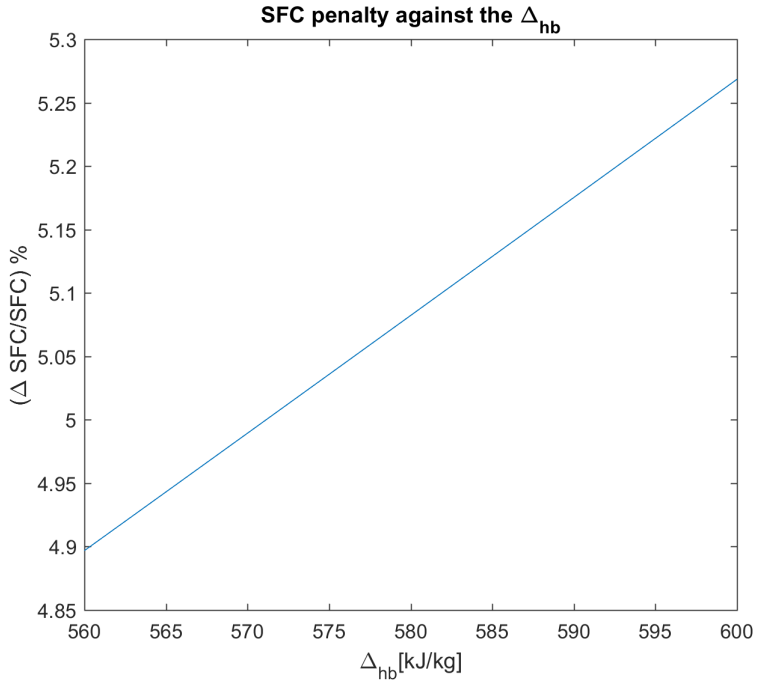

Figure 4.40: SFC increment with bleed air enthalpy

$\Delta_{hb}[kJ/kg]$	600	595	590	585	580	575	570	565	560
$\left(\frac{\Delta SFC}{SFC}\right)\%$	5.27	5.22	5.18	5.13	5.08	5.04	4.99	4.94	4.90

Table 4.46: SFC increment with bleed air enthalpy: numerical values

This analysis is made with constant BPR, ST V_0, β and TET, with no other extraction. Enthalpy varies as $600\,\text{kJ/kg} < \Delta_{hb} < 560\,\text{kJ/kg}$. The increment in Specific Fuel is around 0.05% every 5 kJ/kg. This means that an accurate values of this parameter need to be chosen from the engine deck. More test with different engines should be done in order to find an optimization of Giannakakis like model.

- The air inlet flow along with the specific thrust need to be taken into account with more accuracy, to provide greater precision thus the engine geometry is starting point for a good outputs.
- The components efficiencies are fixed throughout the study; however, they should be known for the specific engine model.
- For further investigation on this topic the most interesting approach is to adopt an engine deck (the one provided by *Deutsches Zentrum für Luft und Raumfahrt e.V. (DLR)*, Institute of Propulsion Technology, if available) in order to run more experiments, taking into account different engine model.

  Moreover, as the Giannakakis model relates to a point where TET, OAPR and η

are constant, with the aid of an engine deck, the input value of TET and efficiencies could be more accurate; if more data are available, the relation between the SFC increment, BPR and TET will be closer to real outputs.

- Another issue addresses to the installation penalties which are completely neglected along the study.

4.9 Impact of different architectures: comments

Table 4.44 underlines that the conventional and MEA 1 architechtures are less efficient than the two other bleed-less configuration. The SFC increment ascribed to secondary power systems is around 5 % for a traditional configuration and it is in line with what expected. This value decrese to less than 2 % when dealing with a bleed-less architecture.

A remarkable comparison is presented in table 4.47; while the previous results concern to the increment of SFC on the SFC of a clean engine, this comparison underlines the difference between Innovative and Conventional architectures.

	Power kW	Bleed kg/s	Scholz $\left(\frac{\Delta SFC}{SFC}\right)$ %	Giannakakis $\left(\frac{\Delta SFC}{SFC}\right)$ %	DLR En.Deck $\left(\frac{\Delta SFC}{SFC}\right)$ %
CONV.	56.4	0.8	-	-	-
MEA1	55.12	0.8	-0.01	-0.01	-0.01
MEA2	161.72	0	1.07	-4.18	-3.77
AEA	158.85	0	1.04	-4.21	-3.8

Table 4.47: Difference between the SFC consumption of the innovative architectures against the conventional one.

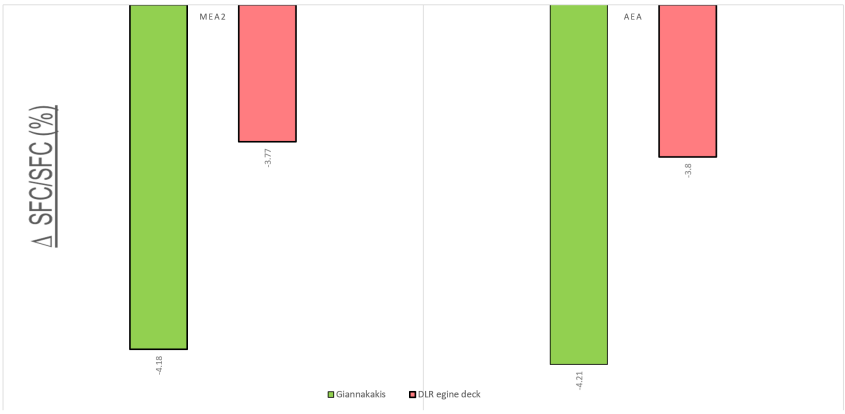

Figure 4.41: $\left(\frac{\Delta SFC}{SFC}\right)$ % saving for MEA2 and AEA architectures respect to a conventional architecture (DLR and Giannakakis results)

	Power ratio	Bleed ratio	$\left(\frac{\Delta SFC}{SFC}\right)\%$ power	$\left(\frac{\Delta SFC}{SFC}\right)\%$ bleed	Decrement power	Decrement bleed
CONV			-	-		
MEA1	0.97	1	0.55	5.26	-0.03	0
MEA2	2.86	0	1.65	0	1.06	-5.26
AEA	2.81	0	1.62	0	1.03	-5.26

Table 4.48: Comparison with conventional architecture for Giannakakis model

Table 4.48 represents a breakdown for Giannakakis model which is really useful to compare bleeding and power extraction contributes. The bleeding practice is far more inefficient in terms of SFC. Even if the electric power required in MEA 2 architecture is almost three times the power of the conventional, this parameter has less influence on the SFC.

The engine deck from DLR is, again, assumed to be the most accurate between the three models. Scholz model is incorrect because the conventional architecture SFC estimation is wrong. The examination of the results brings to the following considerations

1. all the innovative architectures produces the saving in fuel consumption; the MEA1 is less efficient between the three considered with a decrease in SFC of only a -0.001%. This saving ascribes to the innovative high voltages actuators, with the removal of hydraulic power. However, a great benefit of the EMAs and EHAs adopted is not considered: the weight saving.
2. Model 2 and DLR engine deck actually describes the same trend, despite the discrepancy due to the computational errors (already investigated in section *Numerical comparison*.
3. As expected, the bleed less configuration affects the SFC in a positive direction, producing a save in the fuel consumption of 3.77% (referring to DLR engine deck). This is mainly due to the removal of bleed air extraction.
4. AEA architectures is the one which brings the highest advantage: this ascribes to both the removal of bleed air and the hydraulic distribution systems.

The power values required for the architectures describe the electrification trend in aviation. The outcomes for every single system are more accurate for the conventional architecture, for which reference values are available. Otherwise, the innovative architectures design introduces some inaccuracies due to the modern components installed (e.g the generators, the variable frequency fuel pumps *Chapter II*) whose study could be interesting for a detailed analysis. During the thesis, indeed, the focus has been on the average amount of power which an A320 like aircraft requires, if equipped with an unconventional architecture but not all the modern technologies adopted have been investigated.

The study has brought really promising outcomes for what concerns the benefits of

the modern architectures on the specific fuel consumption. More detailed results will be achieved when

- masses
- volumes
- weights

will be taken into account.

However More Electric components adopted for the innovative configurations already equip (or will soon do) the aircraft next generation (e.g. EMAs and EHAs, variable frequency generator, the high level of digital data available and electronic devices). Thus, it is reasonable that, in the near future, new devices will be very efficient: this issue requires a more accurate investigation.

During the thesis, the study on variable frequency boost pump highlights that MEAs undertake a smarter adoption of electric power.

For a typical civil aircraft, during cruise condition fuel consumptions are the highest, hence this phase has been chosen for the study. However, other shorter mission segments generates impulsive and transitional inefficiencies, which could be interesting to investigate.

The other main interesting consideration is about the engine design: throughout the thesis, the engine airframe and outline have remained fixed. On the other hand, a deep concern relies on new Engine configurations along with new system architectures. If bleed air extraction is removed the complex ducting system is withdrawn as well as the preecoler; while the higher power levels need greater generators.

The thermodynamic cycle will be slightly different from the actual one; this, indeed, represents a very curious topic to be studied.

Conclusions

The integration between aircraft engine and on-board system has been investigate throughout the thesis.
One conventional and three innovative architectures of a commercial aviation aircraft have been designed. During the first stage of the work the amount of electric, hydraulic and pneumatic power required for each system has been found with the aid of *Astrid*. The results are in line with what expected from the theory: the bleed air extraction will decrease or will be completely retained for the innovative configuration, given that the trend in aviation is to reduce the power distribution forms. In the other hand, for an All Electric Aircraft, the extracted shaft power increases threefold if compared to the conventional configuration. Thus, different and more efficient electric generation systems are necessary to satisfy these high power requirements.
Moreover, the design of fuel system provides an interesting result: for the case study vehicle, the adoption of variable frequency boost pumps permit the saving of electric power required, especially during cruise condition, where the fixed frequency pumps are usually oversized.
The analysis over the Specific Fuel Consumption has led to different conclusions. All the non propulsive extractions have detrimental effect on the engine SFC. All four different approaches adopted for te SFC computations are in good agreement with the previous statement.
Another relevant issue relates to the different contribution of shaft power and bleed extraction over the overall SFC increment. The most reliable outputs are provided by the DLR engine deck, thus these have been used a reference values. The first analytical model adopted (Scholz) gives accurate results when power extraction is considered but it does not consider the bleed air extraction. It can be only reliable in cruise condition. Giannakakis's equations gives very promising results: this is based on a thermodynamic analysis. Moreover it is independent from the clean engine SFC computation and it provides directly the percent increment over it. However, the SFC increment is strictly dependent on the air bleed enthalpy which is an input for Giannakakis model and for the case study, it is higher than the real one. Beginning from this consideration and relying on the contribution of an engine deck, an optimization process could be introduced. The second engine deck refers to a smaller engine than the one of other three models. A

Surface Response Methodology has been used to find proportional values of Shaft power and bleed air extraction: the outcomes proved again a diminishing SFC for bleed-less architecture.
All four models (except for Scholz) prove that the bleeding practice has a greater impact on the fuel consumption then the shaft power. The conventional and More Electric 1 architectures overcomes an $0.8kg/s$ of bleed extraction producing 5.5% increment of SFC. On the other hand, the other two bleed less architectures required three times the electric power but the SFC increment is around 1.7%.
The All Electric configuration is the most efficient one in terms of Specific Fuel Consumption: this means that the removal of bleeding and hydraulic system is really promising for future vehicle. Only power and bleed extraction are taken into account during the study, thus more accurate outputs will be achieved with the introduction of mass, weight and volumes when the systems are designed.
Another significant future investigation could deal with the re-design of the engine for different configurations in order to define even better solutions to adopt.

Bibliography

[1] Tech. rep. 787 No-Bleed Systems: Saving Fuel and Enhancing Operational Efficiencies, available as http://www.boeing.com/commercial/787.

[2] Tech. rep. Eaton Comportation Main Gear Fuel Pumps, Also Available as http://www.eaton.com/Eaton/ProductsServices/Aerospace/Fuel/PCT_247879.

[3] Tech. rep. A380 briefing for pilots, Also available as http://www.smartcockpit.com/plane/AIRBUS/A380.html.

[4] Tech. rep. Engine Specifications, Also available as http://www.jet-engine.net/civtfspec.html.

[5] Tech. rep. Fuel boost pumps, also available as http://www.eaton.com/Eaton/ProductsServices/Aerospace/Fuel/PCT_247872.

[6] Tech. rep. Code of Federal Regulation, available as https://www.ecfr.gov/.

[7] Tech. rep. System Applications for Aerospace Products , ITT engineered for life , available as https://www.ittaerospace.com.

[8] Tech. rep. A320 FLIGHT CREW OPERATING MANUAL, available as http://www.smartcockpit.com/plane/AIRBUS/A320.html.

[9] Tech. rep. A340 FLIGHT CREW OPERATING MANUAL, available as http://www.smartcockpit.com/plane/AIRBUS/A340.html.

[10] Tech. rep. AGILE project website, https://www.agile-project.eu/.

[11] Tech. rep. Lufthansa Technik, also available as https://www.lufthansa-technik.com/cabin-air-circulation.

[12] Tech. rep. Safran Ventilation Systems, available as https://www.safran-ventilation-systems.com/safran-ventilation-systems-inventing-tomorrows-solutions.

[13] Tech. rep. Aircraft Characteristics Airport and Maintenance Planning, available as http://www.airbus.com/aircraft/support-services/airport-operations-and-technical-data/aircraft-characteristics.html.

[14] Consortium POA. 2003. "AIAA 100 years of powered flight http://www.poaproject.com." In: (Aug 2008.).

[15] "Airbus, Technical Report RP0304267, . Aircraft power consumption - top level estimation of the impact of more electric power systems". In: ().

[16] Ilan Berlowitz. "All/more electric aircraft engine & airframe systems implementation". In: *9th Israeli Symposium on Jet and Gas Turbines*. 2010.

[17] Luca Boggero et al. "On-Board Systems Preliminary Sizing in an Overall Aircraft Design Environment". In: *17th AIAA Aviation Technology, Integration, and Operations Conference*. 2017, p. 3065.

[18] Imon Chakraborty. "Subsystem architecture sizing and analysis for aircraft conceptual design". PhD thesis. Georgia Institute of Technology, 2015.

[19] James S Cloyd. "Status of the United States Air Force's more electric aircraft initiative". In: *IEEE Aerospace and Electronic Systems Magazine* 13.4 (1998), pp. 17–22.

[20] Michael J Cronin. "'All Electric vs Conventional Aircraft: The Production/Operational Aspects". In: *J. Aircr* 20 (1983).

[21] M. Davies. *Standard Handbook For Aeronautical And Astronautical Engineers*. McGraw-Hill Professional Publishing.

[22] Andrew J Fleming. "Energy optimized aircraft and equipment systems". In: *Aerospace America* 50.11 (2012), pp. 71–71.

[23] Panagiotis Giannakakis, Panagiotis Laskaridis, and Pericles Pilidis. "Effects of offtakes for aircraft secondary-power systems on jet engine efficiency". In: *Journal of Propulsion and Power* 27.5 (2011), pp. 1024–1031.

[24] Susan Hanke. "A model-based methodology for integrated preliminary sizing and analysis of aircraft power system architectures". PhD thesis. Toulouse, INSA, 2008.

[25] Steffen HERRMANN. *Untersuchung des Einflusses der Motorenzahl auf die Wirtschaftlichkeit eines Verkehrsflugzeuges unter Berücksichtigung eines optimalen Bypassverhältnisses*. Berlin, Technical University, Institute for Aerospace Sciences, Department of Aircraft and Lightweight Design, Thesis, 2010.

[26] Paul Jackson. "All The World's Aircraft 2004-2005". In: *Jane's All the World's Aircraft* 95 (2004).

[27] T Jomier. "More Open Electric Technologies (MOET)". In: *Airbus Operations SAS and MOET Consortium Partners Rept. FP6-030861* (2009).

[28] RI Jones. "The more electric aircraft—assessing the benefits". In: *Proceedings of the Institution of Mechanical Engineers, Part G: Journal of Aerospace Engineering* 216.5 (2002), pp. 259–269.

[29] Yi-Guang Li et al. "Multiple-point adaptive performance simulation tuned to aero-engine test-bed data". In: *Journal of Propulsion and Power* 25.3 (2009), pp. 635–641.

[30] WL Macmillan. "Development of a modular-type computer program for the calculation of gas turbine off-design performance". In: (1974).

[31] I. Moir and A. Seabridge. *Aircraft Systems: Mechanical, Electrical and Avionics Subsystems Integration*. Aerospace Series. Wiley, 2008. ISBN: 9780470770948. URL: https://books.google.it/books?id=2PBa68zWggEC.

[32] Metin F Ozcan et al. "Gas Turbine Transient Response to Subsystem Architecture Secondary Power Off-Takes". In: *52nd AIAA/SAE/ASEE Joint Propulsion Conference*. 2016, p. 4639.

[33] N Peacock. "Engine design and systems integration for propfan and high bypass turbofan engines". In: *23rd Joint Propulsion Conference*. 1987, p. 1730.

[34] JA Rosero et al. "Moving towards a more electric aircraft". In: *IEEE Aerospace and Electronic Systems Magazine* 22.3 (2007), pp. 3–9.

[35] Dieter Scholz et al. "Fuel consumption due to shaft power off-takes from the engine". In: *4th International Workshop on Aircraft System Technologies (AST 2013), 23-24 April 2013, Hamburg, Germany*. Shaker Verlag. 2013, pp. 169–179.

[36] RR SECUNDE, RP MACOSKO, and DS REPAS. "Integrated engine-generator concept for aircraft electric secondary power(Design and characteristics of integrated engine-generator system for installation on aircraft turbojet and turbofan engines)". In: (1972).

[37] Egbert Torenbeek. *Synthesis of subsonic airplane design: an introduction to the preliminary design of subsonic general aviation and transport aircraft, with emphasis on layout, aerodynamic design, propulsion and performance*. Springer Science & Business Media, 2013.

[38] Dominique Van Den Bossche. "The A380 flight control electrohydrostatic actuators, achievements and lessons learnt". In: *25th international congress of the aeronautical sciences*. 2006, pp. 1–8.

[39] Patrick W Wheeler et al. "An overview of the more electrical aircraft". In: *Proceedings of the Institution of Mechanical Engineers, Part G: Journal of Aerospace Engineering* 227.4 (2013), pp. 578–585.